

**I. LEWIS BASE-CATALYZED ALDOL REACTION IN THE TOTAL SYNTHESIS OF
ERYTHRONOLIDE B
II. EFFORTS TOWARDS THE TOTAL SYNTHESIS OF AMPHIDINOLIDE H**

by

Dezhi Fu

Bachelor of Science, Lanzhou University, 2002
Master of Science, Brown University, 2006

Submitted to the Graduate Faculty of
Arts and Sciences in partial fulfillment
of the requirements for the degree of
Doctor of Philosophy

University of Pittsburgh

2011

UNIVERSITY OF PITTSBURGH
FACULTY OF ARTS AND SCIENCES

This dissertation was presented

by

Dezhi Fu

It was defended on

April 8, 2011

and approved by

Theodore Cohen, Professor, Department of Chemistry

Craig S. Wilcox, Professor, Department of Chemistry

Billy W. Day, Professor, Department of Pharmaceutical Sciences

Dissertation Advisor: Scott G. Nelson, Professor, Department of Chemistry

Copyright © by Dezhi Fu

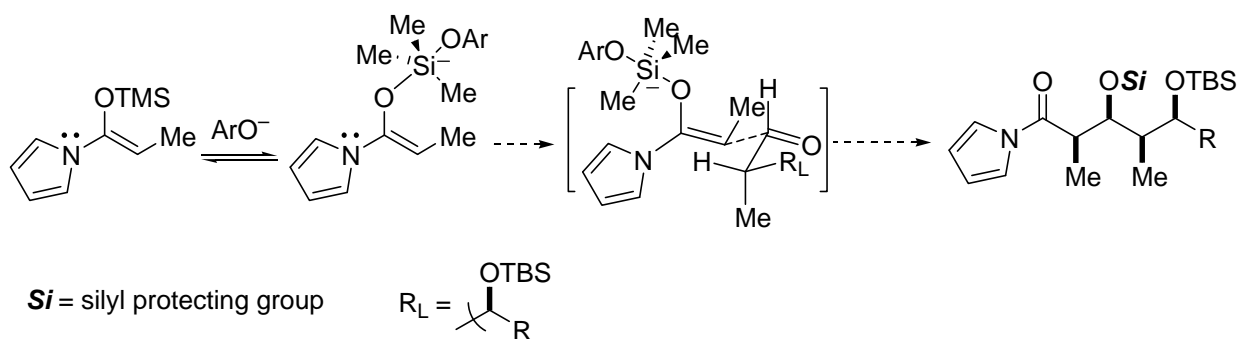
2011

**I. LEWIS BASE-CATALYZED ALDOL REACTION IN THE TOTAL SYNTHESIS
OF ERYTHRONOLIDE B**
II. EFFORTS TOWARDS THE TOTAL SYNTHESIS OF AMPHIDINOLIDE H

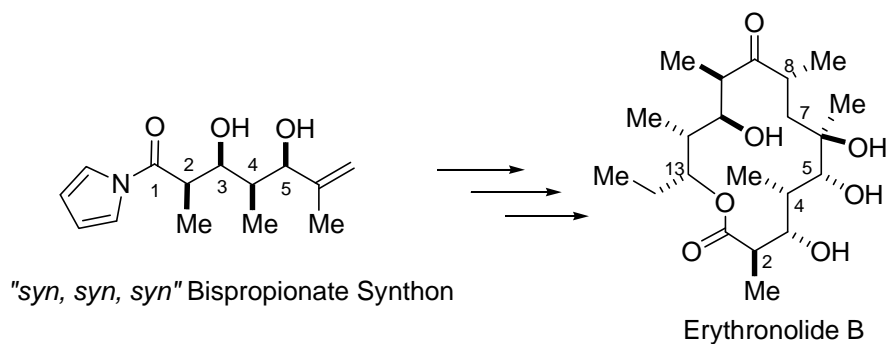
Dezhi Fu, PhD

University of Pittsburgh, 2011

Lewis base (trimethylsilylquinine and trimethylsilylquinidine) catalyzed acyl halide-aldehyde cyclocondensation (AAC) reactions have been developed to prepare synthetically important bispropionate units previously by the Nelson group. A new Lewis base-catalyzed diastereoselective Mukaiyama aldol reaction has extended this bispropionate unit preparation methodology to all-*syn* bispropionates which widely occurred in polypropionate natural products. By using phenoxides as Lewis base catalysts, enol silanes were activated and underwent a Felkin attack on an aldehyde through an antiperiplanar transition state to generate all-*syn* bispropionate product in high yields and excellent diastereoselectivities.



All-*syn* bispropionate prepared from the Lewis base-catalyzed diastereoselective Mukaiyama aldol reaction has been utilized in natural product synthesis of erythronolide B establishing “*syn, syn, syn*” stereochemical relationships from C₂-C₅.



Studies towards the total synthesis of the cytotoxic marine macrolide amphidinolide H (**89**) have been disclosed. By exploiting AAC methodology, several key stereochemical relationships present in major fragments **198** and **199** were established. A highly enantioselective synthesis of methyl ketone **200** was realized from commercially available (*S*)-(-)-glycidol. Iodide **198** was coupled with boronic ester **199** via an efficient Suzuki reaction to form a C₇-C₂₀ fragment.

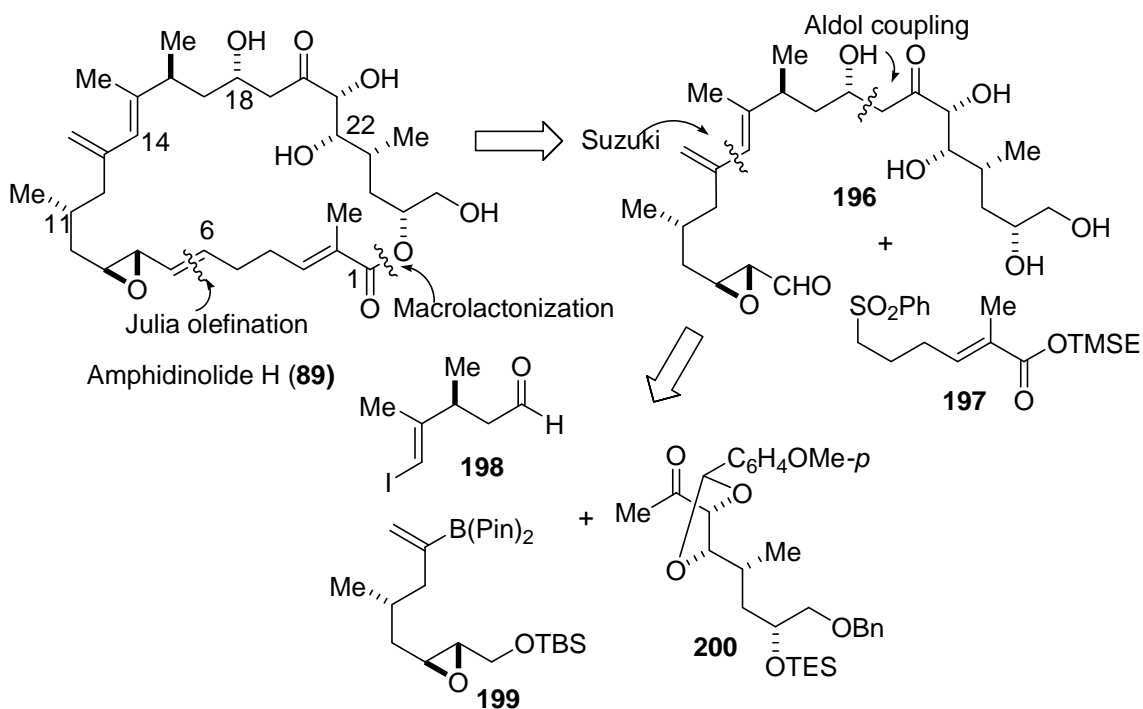


TABLE OF CONTENTS

1.0	LEWIS BASE-CATALYZED DIASTEREOSELECTIVE MUKAIYAMA ALDOL REACTION FOR ALL-SYN BISPROPIONATE UNITS	1
1.1	INTRODUCTION	1
1.1.1	Aldol Reaction.....	1
1.1.2	Synthesis of Polyketide and Polypropionate Units	3
1.1.3	Lewis Base-Catalyzed Mukaiyama Aldol Reaction.....	8
1.2	LEWIS BASE-CATALYZED DIASTEREOSELECTIVE MUKAIYAMA ALDOL REACTION FOR ALL-SYN BISPROPIONATE UNITS	13
1.2.1	Bispropionate Units in the Total Synthesis of Erythronolide B	13
1.2.2	Design of Enol Silane for Mukaiyama Aldol Reaction.....	15
1.2.3	BF₃-Mediated Mukaiyama Aldol Reaction	17
1.2.4	Lewis Base-Catalyzed Mukaiyama Aldol Reaction.....	20
1.3	CONCLUSION	36
1.4	EXPERIMENTALS	38
2.0	EFFORTS TOWARDS THE TOTAL SYNTHESIS OF AMPHIDINOLIDE H	54
2.1	INTRODUCTION	54
2.1.1	The Amphidinolides	54
2.1.1.1	Isolation.....	54

2.1.1.2	Structural Features and Biological Activity	55
2.1.2	Previous Approaches to the Total Synthesis of Amphidinolide H1	57
2.1.3	Application of AAC Reaction Technology in the Total Synthesis of Amphidinolide H1	66
2.2	EFFORTS TOWARDS THE TOTAL SYNTHESIS OF AMPHIDINOLIDE H 69	
2.2.1	The Retrosynthesis of Amphidinolide H1	69
2.2.2	The First Generation of Synthesis of the C ₁₄ -C ₂₆ Fragment	70
2.2.2.1	Model Study for preparing Fragment C ₁₄ -C ₂₆	70
2.2.2.2	Synthesis of the C ₁₄ -C ₂₁ Fragment 148.....	72
2.2.2.3	Synthesis of the C ₂₂ -C ₂₆ Model Fragment.....	74
2.2.2.4	Model Study of Aldol Coupling of C ₁₄ -C ₂₁ Fragment With C ₂₂ -C ₂₆ 76	
2.2.3	The Second Generation of Synthesis of the C ₁₄ -C ₂₆ Fragment	77
2.2.3.1	The Retrosynthesis of the C ₁₄ -C ₂₆ Fragment.....	77
2.2.3.2	The Synthesis of Fragment 168.....	78
2.2.3.3	The Synthesis of Fragment 169.....	80
2.2.3.4	Dithiane Addition Trials.....	85
2.2.4	Revised Synthesis of Amphidinolide H1	87
2.2.4.1	The Revised Retrosynthesis of Amphidinolide H1.....	87
2.2.4.2	Synthesis of the C ₇ -C ₁₃ Fragment 199 ¹⁰⁰	88
2.2.4.3	Synthesis of the C ₁₄ -C ₁₈ Fragment 211.....	90
2.2.4.4	Synthesis of the C ₁₉ -C ₂₆ Fragment 200.....	92
2.2.4.5	Fragments Coupling.....	93
2.3	CONCLUSIONS.....	95

2.4 EXPERIMENTALS	96
APPENDIX.....	112
BIBLIOGRAPHY.....	161

LIST OF TABLES

Table 1. Initial trial of Lewis base for Mukaiyama aldol reaction.....	22
Table 2. Screen of counter ions of the Lewis base for Mukaiyama aldol reaction.....	23
Table 3. Lithium phenoxide-catalyzed Mukaiyama aldol reaction	25
Table 4. Screen of substituents on phenoxide.....	27
Table 5. Solvents screened for tetrabutylammonium phenoxide-catalyzed Mukaiyama aldol reaction.....	29
Table 6. Temperature screen of tetrabutylammonium phenoxide-catalyzed Mukaiyama aldol reaction.....	30
Table 7. Comparison of Lewis base-catalyzed Mukaiyama aldol reaction and Lewis acid-mediated Mukaiyama aldol reaction for all- <i>syn</i> bispropionate synthesis	32
Table 8. Comparison of enol silanes for electronic properties	34
Table 9. Enol silane comparisons	35
Table 10. Scope of enol silanes.....	36
Table 11. Crystal data and structure refinement for 84	113
Table 12. Atomic coordinates (x 10 ⁴) and equivalent isotropic displacement parameters (Å ² x 10 ³) for 81	114
Table 13. Bond lengths [Å] and angles [°] for 84	115
Table 14. Anisotropic displacement parameters (Å ² x 10 ³) for 84	119

Table 15. Hydrogen coordinates ($\times 10^4$) and isotropic displacement parameters ($\text{\AA}^2 \times 10^3$) for 84	120
Table 16. Crystal data and structure refinement for 68	121
Table 17. Atomic coordinates ($\times 10^4$) and equivalent isotropic displacement parameters ($\text{\AA}^2 \times 10^3$) for 68	123
Table 18. lengths [\AA] and angles [$^\circ$] for 68	124
Table 19. Anisotropic displacement parameters ($\text{\AA}^2 \times 10^3$) for 68	128
Table 20. Hydrogen coordinates ($\times 10^4$) and isotropic displacement parameters ($\text{\AA}^2 \times 10^3$) for 68	129
Table 21. Crystal data and structure refinement for 81	130
Table 22. Atomic coordinates ($\times 10^4$) and equivalent isotropic displacement parameters ($\text{\AA}^2 \times 10^3$) for 81	132
Table 23. Bond lengths [\AA] and angles [$^\circ$] for 81	133
Table 24. Anisotropic displacement parameters ($\text{\AA}^2 \times 10^3$) for 81	137
Table 25. Hydrogen coordinates ($\times 10^4$) and isotropic displacement parameters ($\text{\AA}^2 \times 10^3$) for 81	138
Table 26. Crystal data and structure refinement for 78	139
Table 27. Atomic coordinates ($\times 10^4$) and equivalent isotropic displacement parameters ($\text{\AA}^2 \times 10^3$) for 78	141
Table 28. Bond lengths [\AA] and angles [$^\circ$] for 78	143
Table 29. Anisotropic displacement parameters ($\text{\AA}^2 \times 10^3$) for 78	150

Table 30. Hydrogen coordinates ($\times 10^4$) and isotropic displacement parameters ($\text{\AA}^2 \times 10^{-3}$) for 78	152
Table 31. Crystal data and structure refinement for 188	154
Table 32. Atomic coordinates ($\times 10^4$) and equivalent isotropic displacement parameters ($\text{\AA}^2 \times 10^3$) for 188	156
Table 33. Bond lengths [\AA] and angles [$^\circ$] for 188	157
Table 34. Aisotropic displacement parameters ($\text{\AA}^2 \times 10^3$) for 188	159
Table 35. Hydrogen coordinates ($\times 10^4$) and isotropic displacement parameters ($\text{\AA}^2 \times 10^{-3}$) for 188	160

LIST OF FIGURES

Figure 1. Zimmerman-Traxler model	2
Figure 2. Open transition state model for Lewis acid mediated Mukaiyama aldol reaction	3
Figure 3. Examples of Lewis base-catalyzed Mukaiyama aldol reactions	9
Figure 4. Proposed catalytic cycle of AcOLi-catalyzed aldol reaction in DMF	10
Figure 5. Erythronolide A and B.....	13
Figure 6. X-ray crystal structure 68 generated with ORTEP 3 v2 and visualized with POV-Ray® software.....	19
Figure 7. X-ray crystal structure of 81	26
Figure 8. The proposed transition state for 79	26
Figure 9. X-ray crystal structure of 78	31
Figure 10. X-ray crystal structure of 84	33
Figure 11. Amphidinolide H and G family	55
Figure 12. X-ray Crystal structure of amphidinolide H1	56
Figure 13. Chakraborty's approach to the synthesis of fragments of amphidinolide H1	58
Figure 14. Kalesse's approach to the synthesis of fragments of amphidinolide H2	59
Figure 15. Murga's approach to amphidinolide H1 fragments.....	60
Figure 16. Crews's approach to amphidinolide H1 fragments	61
Figure 17. Zhao's approach to amphidinolide H1 fragments.	62

Figure 18. Fürstner's total synthesis of amphidinolide H1	64
Figure 19. Our approach to the synthesis of amphidinolide B1	65
Figure 20. Accessible structural motifs from enantioenriched β -lactones.....	68
Figure 21. Retrosynthetic analysis of amphidinolide H1.....	70
Figure 22. Copper-catalyzed asymmetric O-H bond insertion reaction	72
Figure 23. Retrosynthesis of top fragment 166	78
Figure 24. Retrosynthesis of right fragment 169	81
Figure 25. Synthesis of 187 and structure verification	83
Figure 26. Dithiane addition strategy in amphidinolide B synthesis	86
Figure 27. Dithiane coupling for making C ₁₄ -C ₂₆ fragment	87
Figure 28. Revised retrosynthesis of amphidinolide H1.....	88

LIST OF SCHEMES

Scheme 1. Iterative AAC application to polypropionate units	5
Scheme 2. Evans strategy of preparing all- <i>syn</i> bispropionate units	6
Scheme 3. Crimmins auxiliary controlled all- <i>syn</i> bispropionates	6
Scheme 4. Lewis acid-mediated Mukaiyama aldol reaction to prepare an all- <i>syn</i> bispropionate ..	7
Scheme 5. BF ₃ -mediated Mukaiyama aldol reaction to prepare an all- <i>syn</i> bispropionate	7
Scheme 6. TBAF-catalyzed Mukaiyama aldol reaction	8
Scheme 7. Mukaiyama aldol reaction example	11
Scheme 8. Retrosynthesis of erythronolide B.....	14
Scheme 9. Reduction of acyl pyrrole by catalytic hydrogenation	16
Scheme 10. Design of a new enol silane for Mukaiyama aldol reaction.....	17
Scheme 11. BF ₃ -mediated Mukaiyama aldol reaction.....	18
Scheme 12. BF ₃ -mediated Mukaiyama aldol reaction trial	20
Scheme 13. The control experiment for Lewis base screen.....	22
Scheme 14. Two versions of β-lacton formation reactions.....	67
Scheme 15. Plan to set up upper fragment.....	71
Scheme 16. Synthesis of the C ₁₄ -C ₂₁ subunit 70	74
Scheme 17. Synthesis of the C ₂₂ -C ₂₆ model fragment.....	76
Scheme 18. Aldol coupling for making C ₁₄ -C ₂₆ fragment.....	77

Scheme 19. Synthesis of fragment 79	80
Scheme 20. Synthesis of 186	82
Scheme 21. Completion of fragment 169	85
Scheme 22. Synthesis of the C ₇ -C ₁₃ fragment 199	90
Scheme 23. Synthesis of the C ₁₄ -C ₁₈ fragment 211	91
Scheme 24. Synthesis of the C ₁₄ -C ₁₈ fragment 198	92
Scheme 25. An alternative synthesis of intermediate 214	92
Scheme 26. Synthesis of the C ₁₉ -C ₂₆ fragment 200	93
Scheme 27. Fragments coupling	94

LIST OF ABBREVIATIONS

AAC	Acyl halide-aldehyde cyclocondensation
APCI	Atmospheric-pressure chemical ionization
aq.	aqueous
Bn	Benzyl
CSO	Camphorsulfonyl oxaziridine
DIBAL	Diisopropylaluminum hydride
DMAP	4-Dimethylaminopyridine
DMF	<i>N,N</i> -Dimethylformamide
DMSO	Dimethyl sulfoxide
DDQ	2,3-Dichloro-5,6-Dicyanobenzoquinone
De	Diastereomeric excess
Dppf	1,1'-Bis(diphenylphosphino)ferrocene
Dr	Diastereomer ratio
Ee	Enantiomeric excess
EI	Electron Ionization
Equiv.	Equivalent
ESI	Electrospray ionization
EtOAc	Ethyl acetate

GC	Gas chromatography
HPLC	High pressure liquid chromatography
HRMS	High resolution mass spectrum
LDA	Lithium diisopropylamide
MOM	Methoxymethyl
MsCl	Methanesulfonyl chloride
KHMDS	Potassium bis(trimethylsilyl)amide
PMB	p-Methoxybenzyl
RCM	Ring-closing metathesis
TBAF	Tetrabutylammonium fluoride
TBS	tert-Butyldimethylsilyl
TBSCl	tert-Butyldimethylsilyl chloride
TEA	Triethylamine
TES	Triethylsilyl
TESCl	Triethylsilyl chloride
Tf	Trifluoromethanesulfonyl
TFA	Trifluoroacetic acid
Tf ₂ O	Trifluoromethanesulfonic anhydride
THF	Tetrahydrofuran
TIPS	Triisopropylsilyl
TLC	Thin-layer chromatography
TMS	Trimethylsilyl
TMSCl	Chlorotrimethylsilane

TMS <i>Qd</i>	Trimethylsilylquinidine
TMS <i>Qn</i>	Trimethylsilylquinine
Ts	Tosyl

ACKNOWLEDGEMENT

I would like to thank my advisor, Professor Scott G. Nelson, for providing me with the opportunity to work on the challenging and rewarding projects. It has been Dr. Nelson's scientific insight that has guided my research projects enabled my success. I truly appreciate the time and effort that you have devoted to helping me to become a better chemist.

I would like to thank Professors Theodore Cohen, Craig S. Wilcox and Billy W. Day for the guidance they gave me as my committee members, and thank Professor Cohen again for serving as my proposal mentor.

To the past and present members of the Nelson group, I wish to thank all of you for your friendship and for your help during my time at Pittsburgh. I would especially like to thank Binita Chandra whose work has directly enabled the successful completion of erythronolide B.

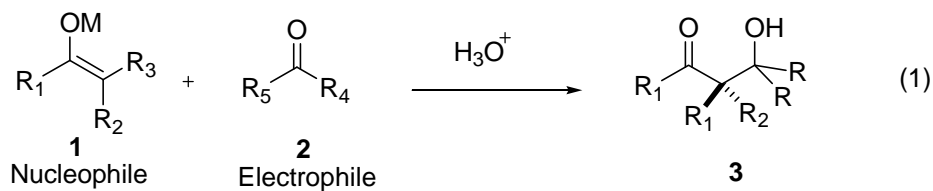
I would like to thank my wife, Na Ji, for her constant support over the past years. I am eternally indebted to her for taking full responsibility of family and business. Finally I would like to thank my parents for their encouragement and support during the past few years and throughout whole life

1.0 LEWIS BASE-CATALYZED DIASTEREOSELECTIVE MUKAIYAMA ALDOL REACTION FOR ALL-SYN BISPROPIONATE UNITS

1.1 INTRODUCTION

1.1.1 Aldol Reaction

The aldol reaction is one of the most important reactions for stereoselectively constructing carbon-carbon bonds.¹ This reaction typically involves the addition of an enolate (**1**, nucleophile) to an aldehyde or ketone (**2**, electrophile) (eq 1)² to afford β -hydroxy carbonyl compound **3**. The β -hydroxy carbonyl motif is a widely occurring subunit in polypropionates, polyketides natural products and various pharmaceutical agents.³ Since the resulting β -hydroxy carbonyl compound **3** has newly formed stereocenters, the control of the stereochemical outcome of this reaction becomes very important and challenging. Highly enantio- and diastereoselective aldol reactions continue to be an active area of research.^{4,5}



In order to achieve a highly enantio- and diastereoselective aldol reaction, many transition state models have been proposed to predict and explain the overall stereoselectivities of the aldol product. In 1957, Zimmerman and Traxler proposed that some aldol reactions proceed through a six-membered closed transition state, in a chair conformation.⁶ This became known as the Zimmerman-Traxler model. This model demonstrated that *E*-enolates gave rise to *anti* products; whereas *Z*-enolates gave rise to *syn* products (Figure 1). Other than closed transition state models, open transition state models have also been proposed to explain the stereochemistry in Lewis acid-mediated Mukaiyama aldol reactions (Figure 2)⁵. Transition states **B**, **C**, and **F** are not favored due to steric and dipolar interactions, but transition states **A**, **D** and **E** are close in energy. When substituent R_3 is small and R_2 is bulky, the transition state **D** is favored giving the *syn*-diastereomer as the major product. In some cases, the stereochemical outcome of the aldol reaction is unpredictable. Fortunately, the Zimmerman-Traxler model and open transition state models are effective and widely used to explain and predict the stereochemistry of aldol products.

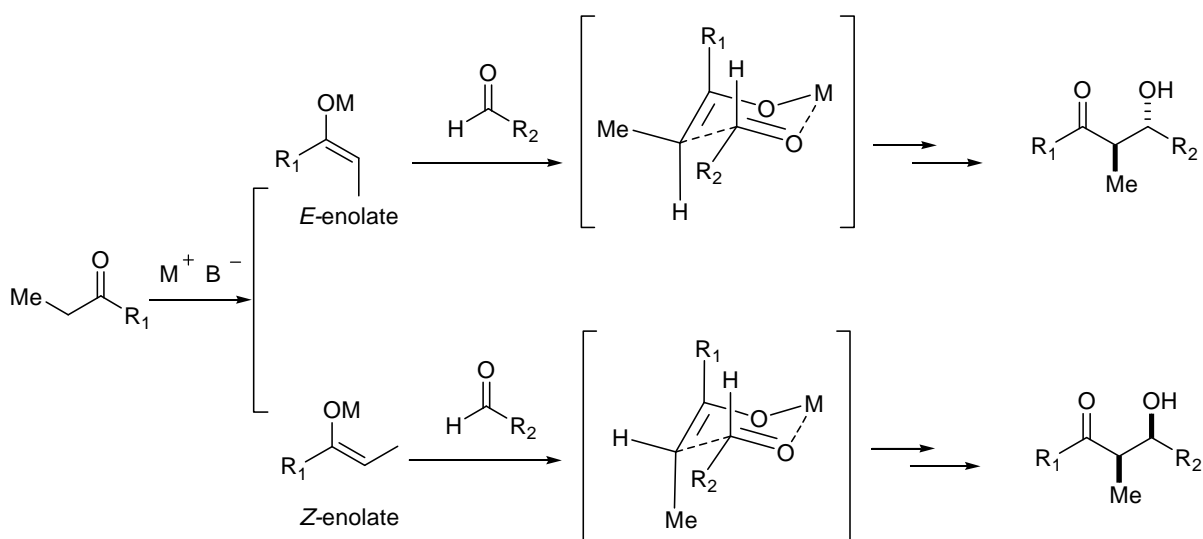


Figure 1. Zimmerman-Traxler model

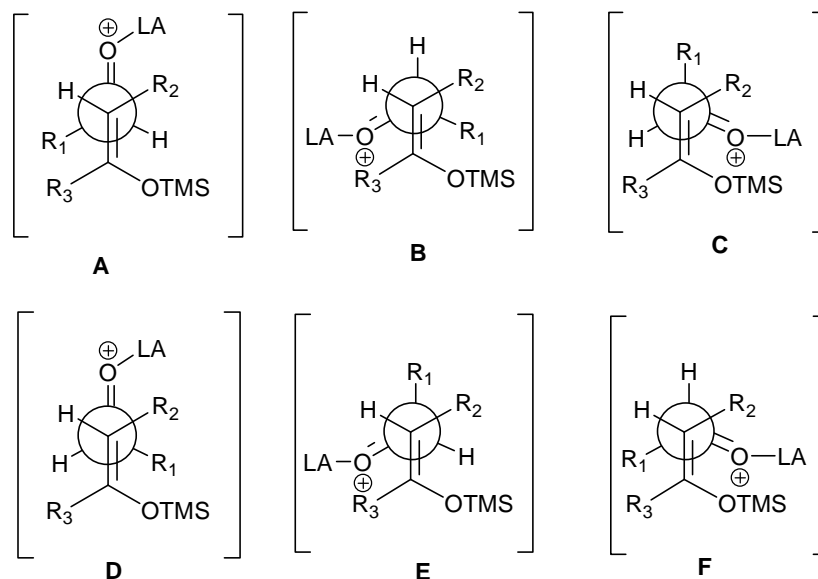


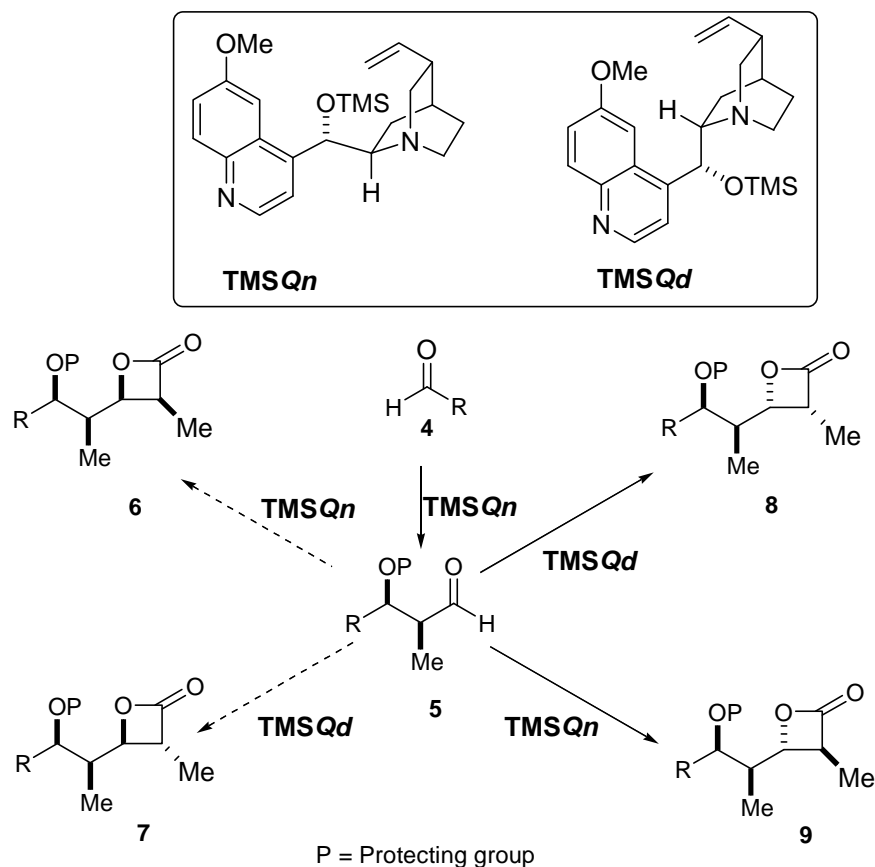
Figure 2. Open transition state model for Lewis acid mediated Mukaiyama aldol reaction

1.1.2 Synthesis of Polyketide and Polypropionate Units

The aldol reaction has frequently been used to construct polyketides and polypropionates.³ To address these types of natural products, synthetic chemists have been challenged to develop methods to iteratively assemble repeating acetate or propionated units stereospecifically.⁷⁻⁹ Frequently, auxiliary-controlled aldol reactions have proven to be a reliable method to install repeating polypropionate units.¹⁰⁻¹² Auxiliaries are not atom economical, however, and can add many extra steps along with expensive chiral reagents. Catalytic aldol reactions have always been the goal of many scientists, including our group. Though many catalytic asymmetric aldol reactions have been successfully developed to form a single propionate unit,⁴ few examples have been used to set repeating networks of acetates or propionates.

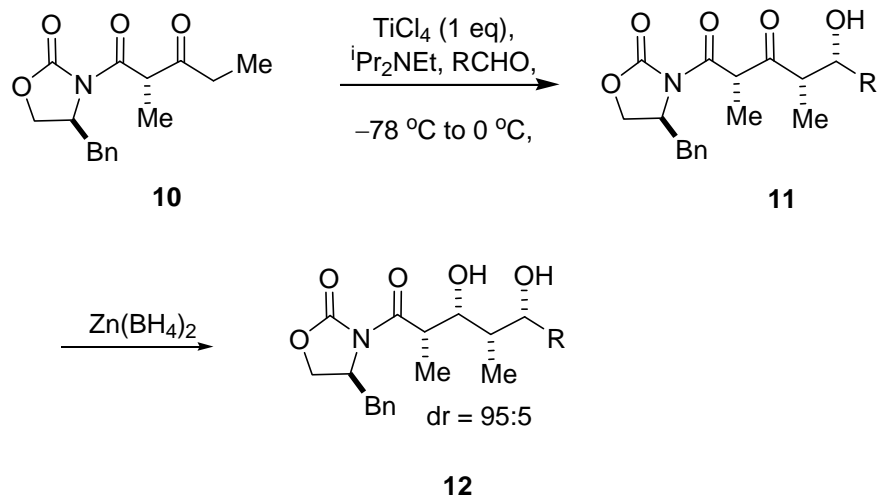
The acyl halide-aldehyde cyclocondensation (AAC) reaction recently developed in the Nelson group has consistently demonstrated the reliable construction of bispropionate units (Scheme 1).¹³ Thus far, *syn, anti, syn*-bispropionate precursor **8** and *syn, anti, anti*-bispropionate precursor **9** have been prepared by AAC chemistry starting from *syn*-aldehyde **5**. The *syn*-aldehyde **5** can be prepared from simple aldehyde **4** by 1st generation AAC chemistry.¹⁴ Unfortunately, aldol precursors **6** and **7** cannot be made by AAC chemistry, due to the chirality mismatch between catalyst and substrates. There is, however, a need for these all-*syn* bispropionate units. One such natural product containing this pattern of repeating units is erythronolide B.

Scheme 1. Iterative AAC application to polypropionate units



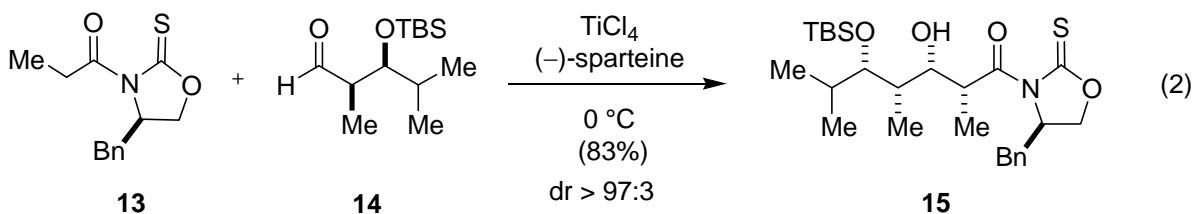
Although all-*syn* polypropionate units are not currently available via AAC chemistry, two ways to prepare all-*syn* aldol products are commonly used. First is the auxiliary-controlled aldol reaction, the second is a Lewis acid-mediated Mukaiyama aldol reaction. In 1990, the Evans group developed a two-step protocol to make all-*syn* bispropionates (Scheme 2).¹¹ The titanium (IV) *Z*-enolate of the β -keto imide **10** undergoes a diastereoselective aldol reaction to afford the hydroxy β -keto imide **11**. Compound **11** is then stereoselectively reduced with $\text{Zn}(\text{BH}_4)_2$ to provide the *syn*-diol carboximides **12**, thus establishing the all-*syn* bispropionate synthon.

Scheme 2. Evans strategy of preparing all-*syn* bispropionate units



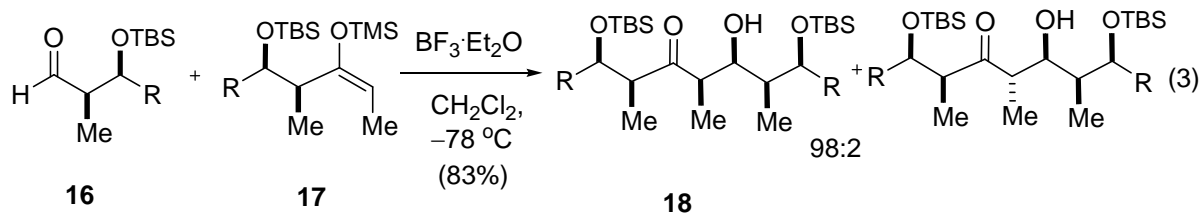
Another single step protocol has been developed in Crimmins group (Scheme 3, eq 2).¹⁰ With titanium tetrachloride and 2.5 equiv. of (–)-sparteine as the base, *N*-methyl-2-pyrrolidinone **13** reacts with aldehyde **14** to provide all-*syn* bispropionate **15** with 97:3 diastereoselectivity.

Scheme 3. Crimmins auxiliary controlled all-*syn* bispropionates



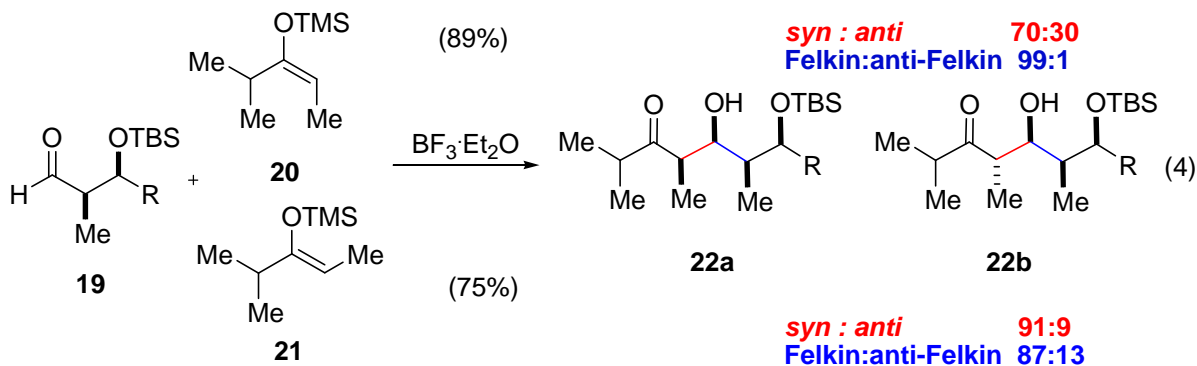
The Evans group also used a Lewis acid-mediated Mukaiyama aldol reaction to prepare an all-*syn* bispropionate (Scheme 4).¹⁵ This method displayed excellent Felkin control through an open transition state. When the chiral enol silane **17** was sterically matched with the chiral aldehyde **16**, excellent diastereoselectivity was observed (98:2).

Scheme 4. Lewis acid-mediated Mukaiyama aldol reaction to prepare an all-*syn* bispropionate



The achiral enol silane in eq 4 (Scheme 5) provided, however, only moderate selectivity.^{15,16} Generally, the methods mentioned above provide some solutions concerning the construction of all-*syn* bispropionate units. Unfortunately, most of those reactions employed stoichiometric chiral auxiliary coupled with harsh Lewis acids. Also, the auxiliary-controlled aldol reaction involved multiple steps to install, recycle and remove the chiral auxiliary. Poor diastereoselectivities have been obtained for achiral enolates. Thus, our goal is to find a mild and catalytic method to perform these reactions without using any harsh stoichiometric Lewis acids or a lengthy, stepwise process. A solution to this problem would be to employ a Lewis base-catalyzed Mukaiyama aldol reaction to synthesize the all-*syn* bispropionates catalytically and stereospecifically.

Scheme 5. BF₃-mediated Mukaiyama aldol reaction to prepare an all-*syn* bispropionate

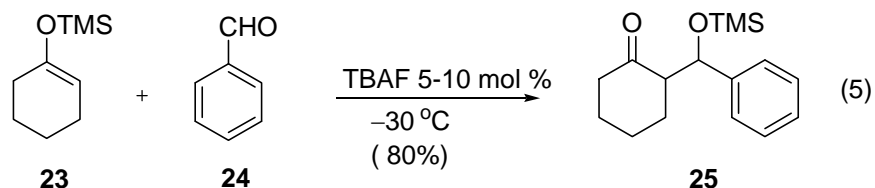


syn and *anti* relationship refers to the relative stereochemistry along the red bond.
 Felkin and anti-Felkin relationship refers to the relative stereochemistry along the blue bond.

1.1.3 Lewis Base-Catalyzed Mukaiyama Aldol Reaction

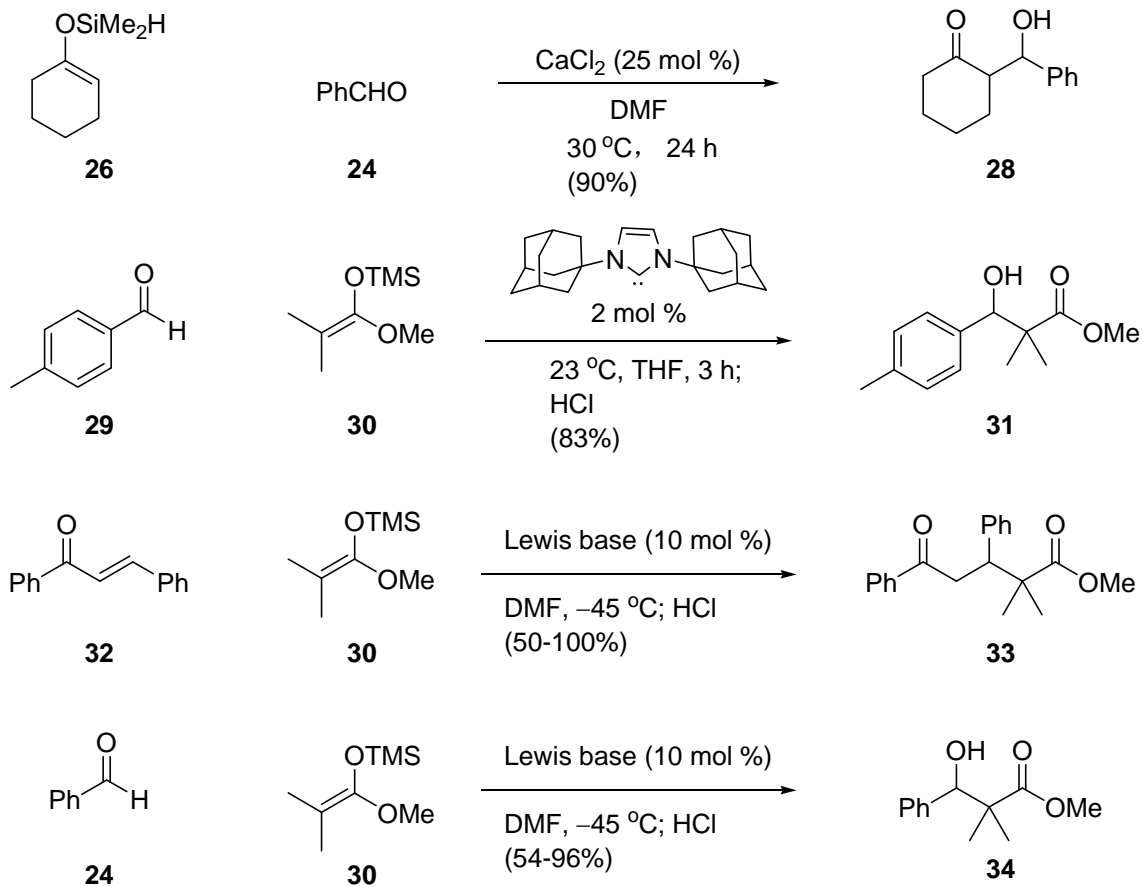
The Lewis base-catalyzed Mukaiyama aldol reaction is an underappreciated topic compared to the Lewis acid-mediated Mukaiyama aldol reaction.¹ One of the earliest examples was a tetrabutylammonium fluoride (TBAF) catalyzed Mukaiyama aldol reaction demonstrated in the Noyori group in 1977 (Scheme 6, eq 5).¹⁷ With a catalytic amount (5-10 mol %) of TBAF, the enol trimethylsilyl ether **23** reacted with an equivalent of benzaldehyde **24** in THF smoothly at low temperatures, providing the aldol silyl ether **25** in an 80% yield.

Scheme 6. TBAF-catalyzed Mukaiyama aldol reaction



New methods of silyl activation with Lewis base catalyst by formation of hypervalent silicon intermediates were also extensively studied in the Demark⁶, Hasimori¹⁸ and Mukaiyama¹⁹ labs. Many Lewis bases have been used to activate various silyl enol ethers, such as CaCl_2 ,¹⁸ carbenes,²⁰ lithium acetate, and lithium phenoxide (Figure 3).^{21,22}

Based on these examples, Lewis base-catalyzed Mukaiyama aldol reactions have only been used to provide racemic aldol products. There is much room to improve on the aforementioned chemistry and provide specific products, namely all-*syn* bispropionate type compounds.



Lewis base = AcOLi, PhCOOLi, PhOLi

Figure 3. Examples of Lewis base-catalyzed Mukaiyama aldol reactions

In order to understand the mechanism of Lewis base-catalyzed Mukaiyama aldol reaction, a catalytic cycle has been proposed involving a hypervalent silicate intermediate.^{21,23} The open transition state model has been used to explain the stereochemistry of Lewis base-catalyzed Mukaiyama aldol reactions. This transition state model will be the foundation of the design of our experiments.

As shown in Figure 4, a polar solvent and base catalyst coordinates to silicon and forms the hexacoordinated hypervalent silicate **37**. This high energy intermediate **37** nucleophilically attacks the aldehyde to form lithium aldolate **39**, which reacts with trimethyl silyl acetate **38** to give O-silyl **40** and regenerate lithium acetate. The open transition state **41** is also proposed to explain the *syn* steric outcome. To avoid unfavorable interaction between

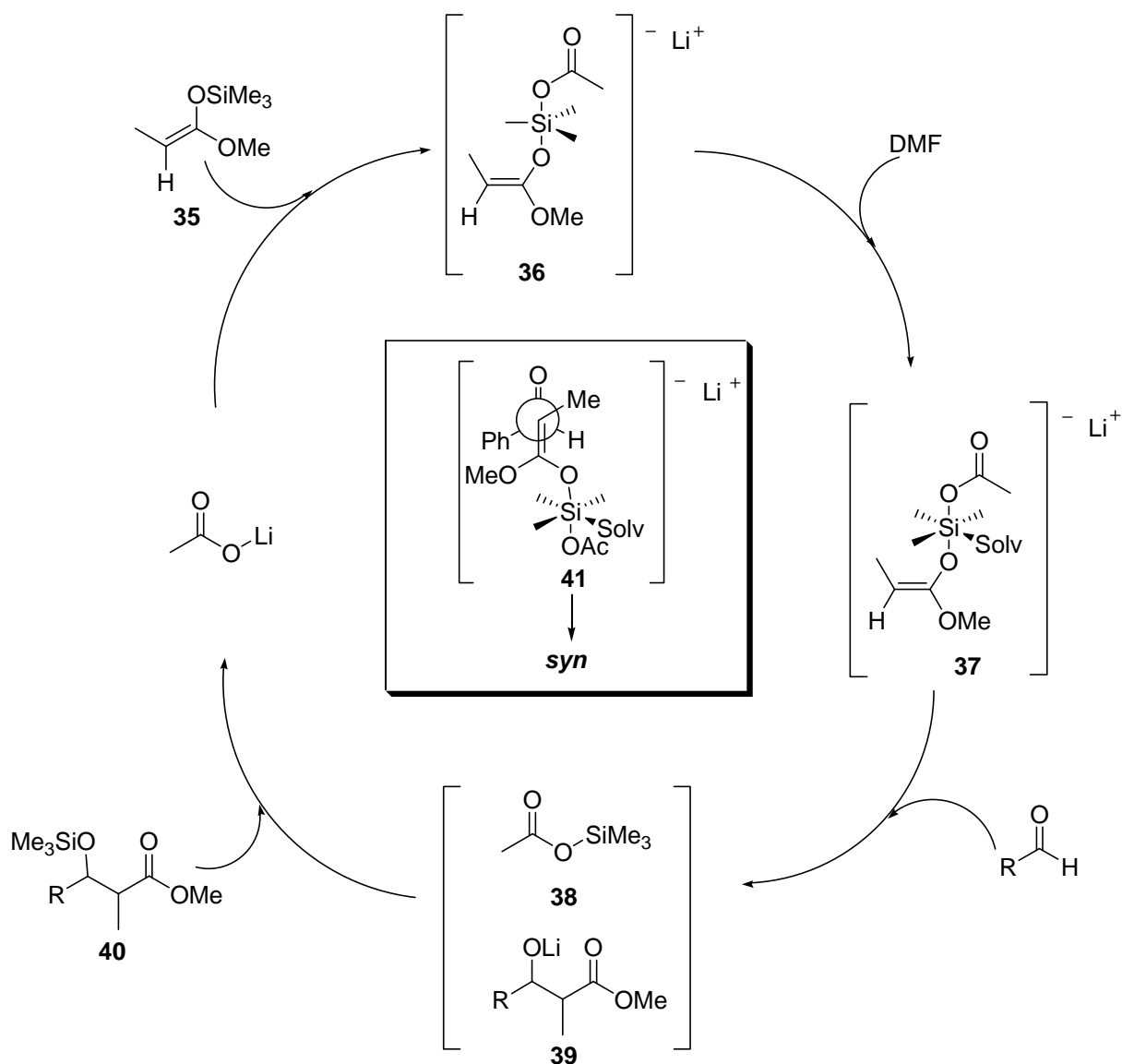


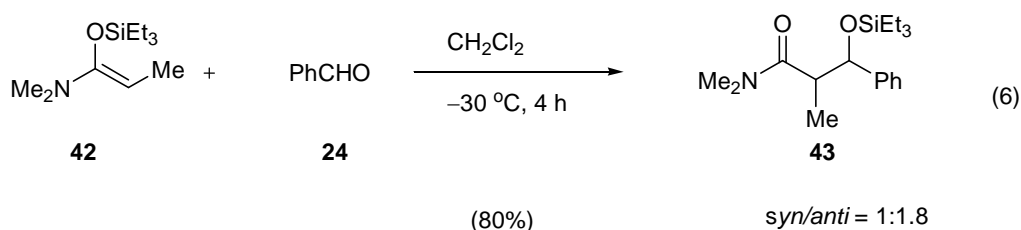
Figure 4. Proposed catalytic cycle of AcOLi-catalyzed aldol reaction in DMF

silyl acetate **38** to give O-silyl **40** and regenerate lithium acetate. The open transition state **41** is also proposed to explain the *syn* steric outcome. To avoid unfavorable interaction between

phenyl and methyl groups, they chose to be oriented in an *anti* position to one another. For the same reason, the phenyl group is proposed to be away from bulky hypervalent silyl group.²¹ The *Z*-enolate will be a good enolate to satisfy this steric demand. Based on the catalytic cycle and the transition state of the Lewis base-catalyzed Mukaiyama aldol reaction, the *syn*-aldol is formed preferentially from the *Z*-enolate.

The reactivity of the enol silane also plays an important role in any Mukaiyama aldol reaction. The Lewis base can only activate the enol silane component, however, the Lewis acid-mediated aldol reaction can activate the aldehyde part. Electron rich enol silanes typically exhibit high reactivities. With the amide derived enol silane **42**, the aldol reaction proceeds automatically without any catalyst (eq 6).²⁴ It has also been established that non-catalyzed aldol reactions using silyl ketene acetals proceed at the high temperatures,²⁵ and in H₂O,²⁶ DMSO, DMF and DME.²⁷ Based on the research stated above, solvent polarity, electron dense enol silanes and high temperature have a dramatic impact in reactivity.

Scheme 7. Mukaiyama aldol reaction example



The catalytic asymmetric approach to all possible polypropionates is always desired in the organic synthesis. Based on the previous research of AAC chemistry in our group, we have obtained a reliable strategy to iteratively prepare many stereochemistry patterns of

bispropionated units (Scheme 1).¹³ As a complement to AAC chemistry, we are trying to develop a new method to set up the all-*syn* bispropionate unit in a catalytic and diastereoselective fashion. As a solution, we examined Lewis base-catalyzed Mukaiyama aldol reactions and tried to find suitable conditions to prepare all-*syn* bispropionate units and furnished an all-*syn* moieties in the total synthesis of erythronolide B.

1.2 LEWIS BASE-CATALYZED DIASTEREOSELECTIVE MUKAIYAMA ALDOL REACTION FOR ALL-SYN BISPROPIONATE UNITS

1.2.1 Bispropionate Units in the Total Synthesis of Erythronolide B

The erythromycins A and B, isolated from *Saccharopolyspora erythraea*, are 14-membered macrolide antibiotics and owe their potent antibiotic activity to the efficient inhibition of ribosomal-dependent protein biosynthesis.²⁸ Their therapeutic value and densely functionalized architecture have made these macrolides an attractive target for synthesis. Over the last few decades, many total syntheses have been reported for the erythromycins themselves as well as a number of their aglycon derivatives including erythronolide A (**44**)^{29,30} and B (**45**)³¹⁻³³ (Figure 5). To date three total syntheses of erythronolide B have been reported, the first of which was completed by Corey in 1978,³¹ later Kochetkov (1987)³² and finally Mulzer (1991).³³

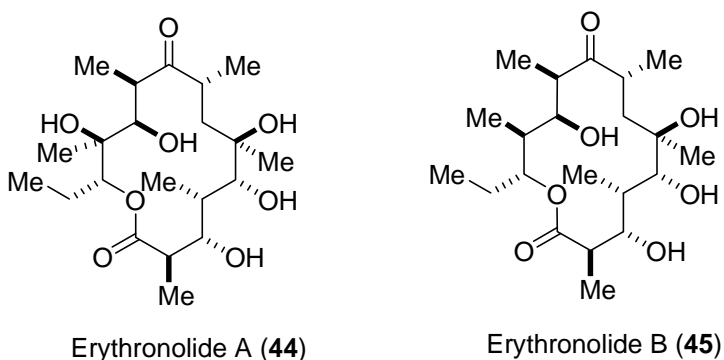
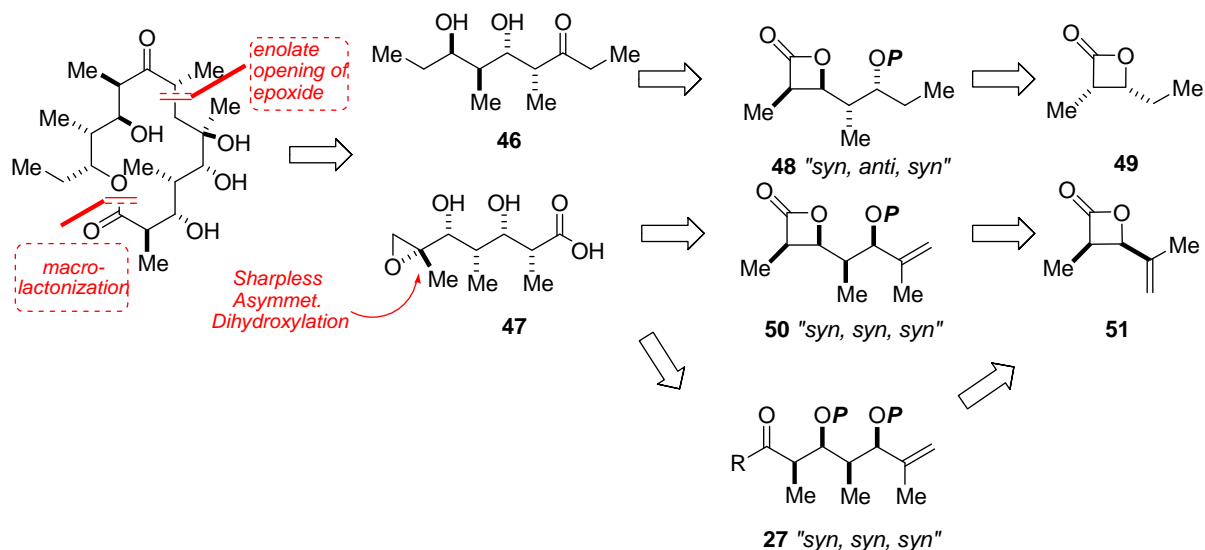


Figure 5. Erythronolide A and B

Scheme 8. Retrosynthesis of erythronolide B



As shown in Scheme 8, erythronolide B contains two key bispropionate units. One is *syn, anti, syn* configuration and the other is the *syn, syn, syn* configuration. Based on the AAC chemistry developed in our group (Scheme 8), a bispropionate unit can be synthesized by two consecutive AAC reactions. Based on previous research in our group, the *syn, syn, syn* bispropionate **50** cannot be synthesized by AAC chemistry due to the stereochemistry mismatch between chiral substrates and chiral ligands. In order to perform a highly stereoselective and catalytic synthesis of erythronolide B, we were driven to develop a new method to effectively generate the *syn, syn, syn* bispropionate unit **27**. The Mukaiyama aldol reaction has been established as an efficient way to provide *syn* aldol products, however we employed the Lewis base-catalyzed and Lewis acid-mediated Mukaiyama aldol reaction to

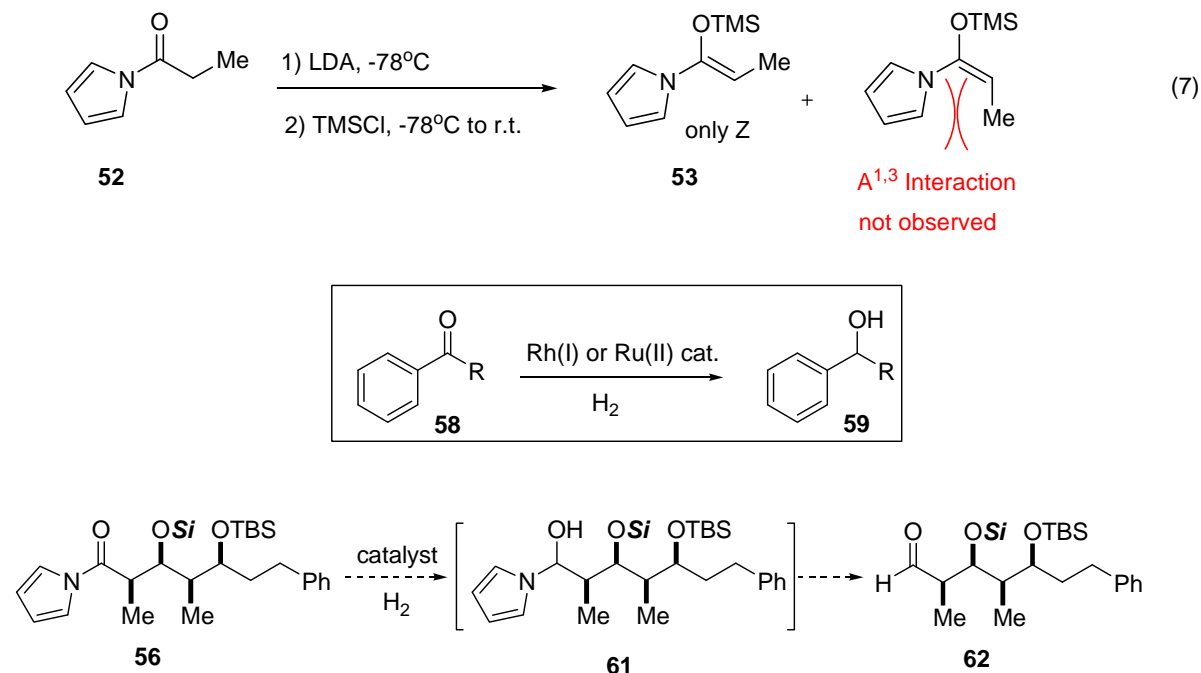
efficiently and diastereoselectively provide *syn, syn, syn* bispropionate units of the type exemplified by **27**.

1.2.2 Design of Enol Silane for Mukaiyama Aldol Reaction

In order to design an enol silane for a diastereoselective Mukaiyama aldol reaction, several requirements needed to be satisfied. First, a highly reactive enol silane was needed. Second, the *E, Z* selectivity of the enol silane should be easily controlled. Third, the product needed to be easily converted to the aldehyde for subsequent rounds of aldol reactions. Enol silanes could be generated from a variety of carbonyl groups, such as ketones, aldehydes, esters, thioesters and amides. Enol silanes derived from these carbonyl compounds have very different electronic properties. Among these enosilanes, amide derived enol silanes should have the highest nucleophilicity, because the amide nitrogen is a good electron donating group. Acyl pyrrole was a good candidate to enhance the nucleophilicity of enol silanes, because the lone pair on the pyrrole nitrogen increases the electron density of enol silane. Furthermore, our goal was to find an enol silane which was not only very reactive but also demonstrated a good *Z* selectivity. The *Z* enol silane is preferred due to its tendency to provide *syn* aldol products.¹⁵ In order to get only the *Z* isomer, we used propionyl pyrrole **52** to generate enol silane **53** (eq 7). Due to A^{1,3} interactions, the *E* isomer experiences repulsion between the methyl and pyrrole group. The *Z* isomer was the only isomer obtained from the reaction of **52** with LDA and TMSCl (eq 7). Considering the aromaticity of acyl pyrrole **52**, acyl pyrrole might show a similar reactivity with aryl ketone to give hydroxyl functionality (Scheme 9). Based on this assumption, the acyl pyrrole derived all-*syn* bispropionate **56** can be reduced by catalytic hydrogenation to aldehyde **62** which can be used for further aldol reactions. Thus, the acyl pyrrole derived enol

silane **53** could satisfy all three requirements for our Lewis base-catalyzed Mukaiyama aldol reaction.

Scheme 9. Reduction of acyl pyrrole by catalytic hydrogenation

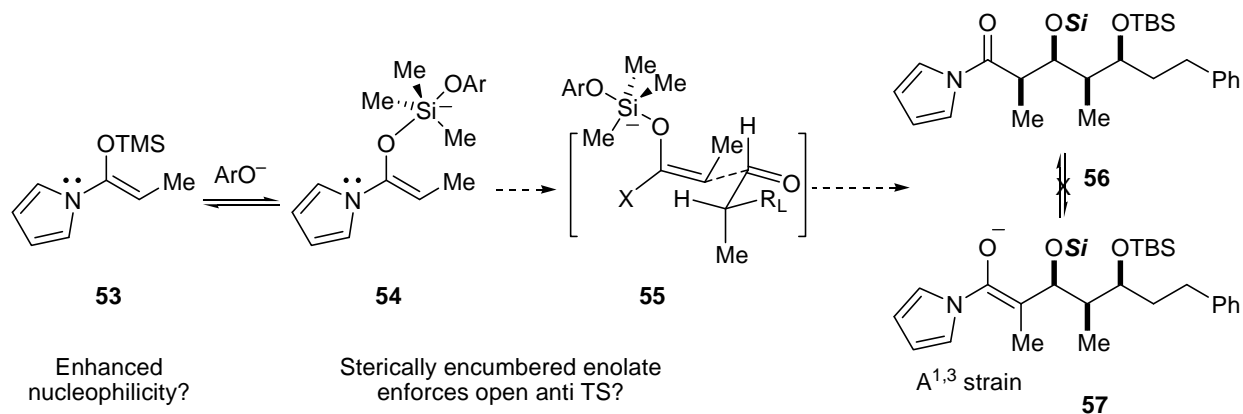


Si = TBS, TBDPS, etc.

Based on the recent research in the Mukaiyama group, a Lewis base catalyst could attack a silyl group to form a hypervalent silane **54** (Scheme 10)²¹. The activated enol silane **54** bearing higher electron density would undergo a Felkin attack to an aldehyde through antiperiplanar transition state **55**. As shown in transition state **55**, because of the bulky silyl group, the methyl group would be oriented away from the alkyl group of aldehyde and the flat pyrrole group would be oriented towards alkyl side of aldehyde, *Z* enol silane would match the steric requirement of the transition state.³⁴ This is our reasoning behind using *Z* enol silanes to produce all-*syn* bispropionate units. The resulting acyl pyrrole **56** could also inhibit α -

deprotonation, due to the $A^{1,3}$ interactions between pyrrole and methyl in the corresponding enolate form **57**. Once compound **56** is formed in Scheme 10, it would be stable to basic reaction conditions reducing the chance of epimerization of α -methyl group.

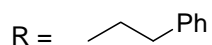
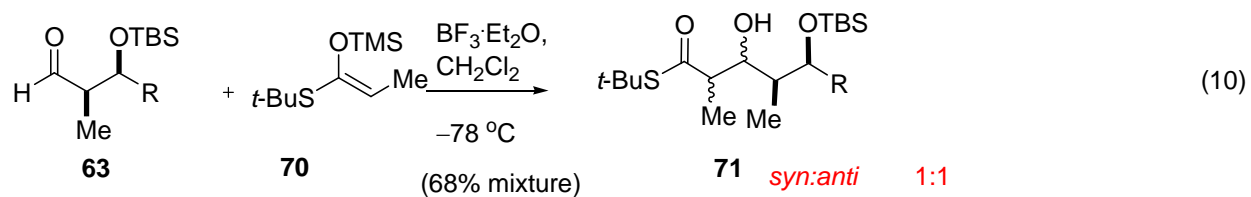
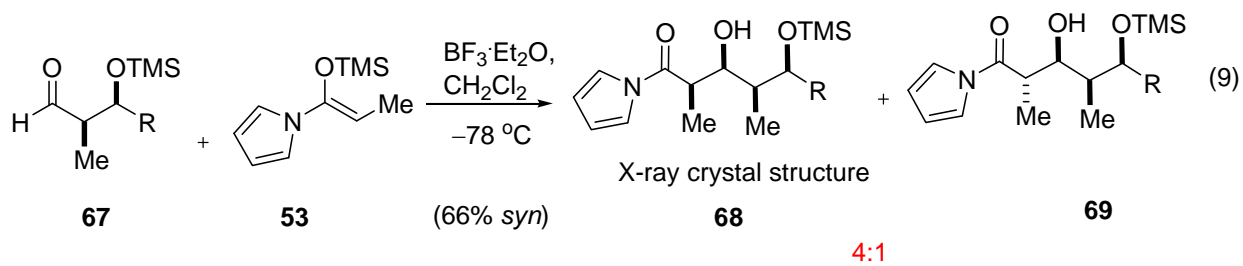
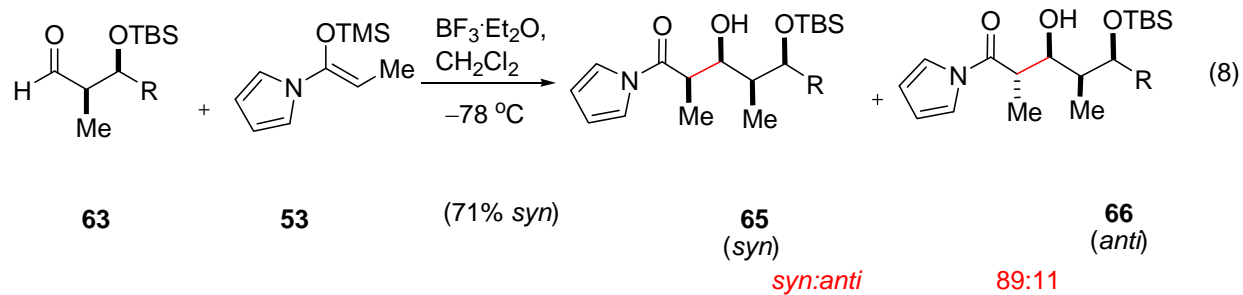
Scheme 10. Design of a new enol silane for Mukaiyama aldol reaction

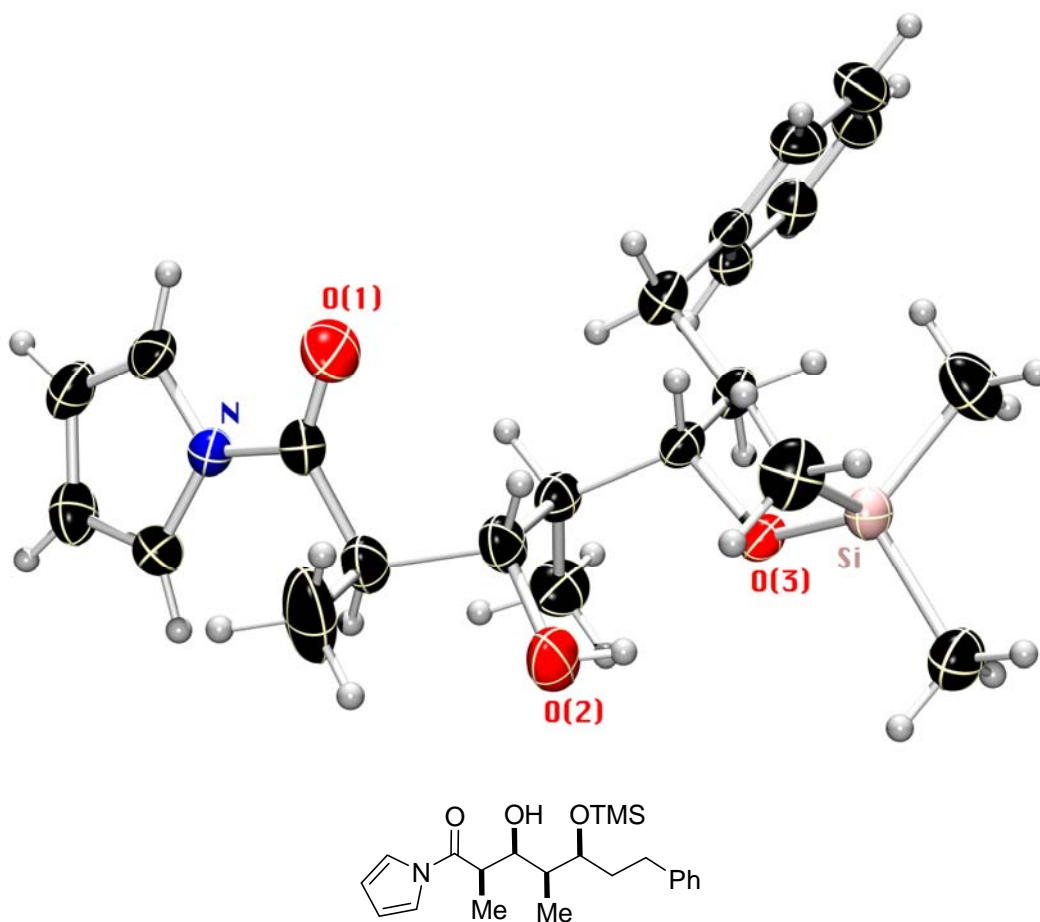


1.2.3 BF_3 -Mediated Mukaiyama Aldol Reaction

Our research started with the BF_3 -mediated Mukaiyama aldol reaction, because the all-*syn* product **65** could be easily prepared with moderate diastereoselectivity (Scheme 11).³⁴ The *syn* aldehyde **63** and **67** reacted with enol silane **53** at -78 °C to afford a 71% yield of the all-*syn* product **65** with a 80:20 diastereomeric ratio (eq 8). This result demonstrated excellent Felkin selectivity, which suggested an open transition state pathway. The X-ray crystal structure of **68** was obtained verifying the all-*syn* configuration (Figure 6).

Scheme 11. BF₃-mediated Mukaiyama aldol reaction





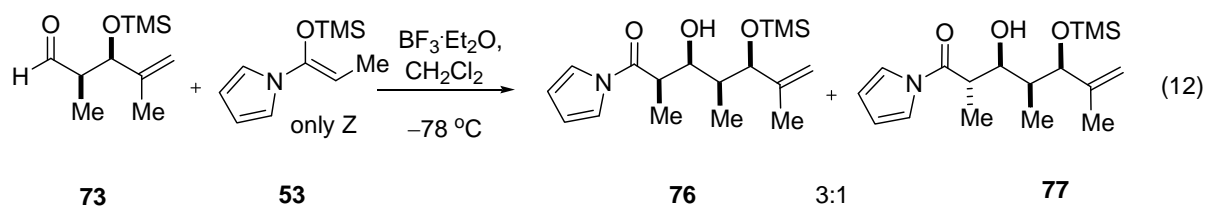
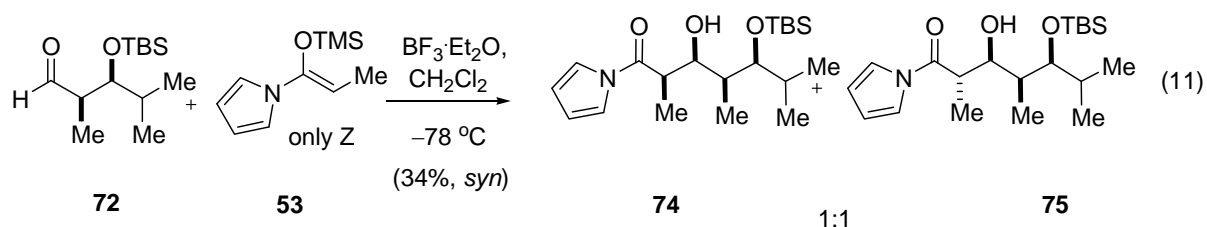
68

Figure 6. X-ray crystal structure **68** generated with ORTEP 3 v2 and visualized with POV-Ray® software.

As a comparison, the reaction of enol silane **70** with the same aldehyde **63** was examined (Scheme 12, eq 10). Unfortunately, two diastereomers were observed in a 1:1 ratio, based on ^1H NMR. Acyl pyrrole derived Mukaiyama aldol **53** demonstrated better selectivity than the thioester derived enol silane **70**. However, when aldehyde **72** was used, diastereoselectivity was not observed (1:1 ratio). Aldehyde **73**, our target substrate for the total synthesis of

erythronolide B gave a moderate 3:1 diastereoselectivity (eq 12). These results have shown that selectivity with BF_3 -mediated Mukaiyama aldol reaction was very poor and not very useful in the total synthesis of erythronolide B. Also, these results promoted the exploration to find an alternate and efficient method to improve the selectivity of this reaction.

Scheme 12. BF_3 -mediated Mukaiyama aldol reaction trial

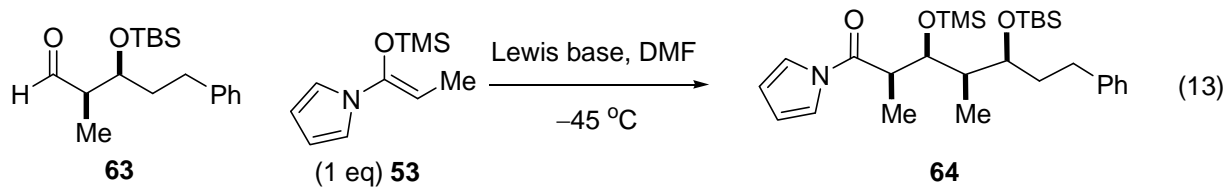


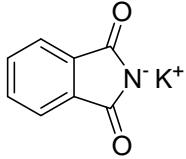
1.2.4 Lewis Base-Catalyzed Mukaiyama Aldol Reaction

Based on the reaction design (Scheme 10), a Lewis base-catalyzed Mukaiyama aldol reaction should demonstrate predominantly *syn* selectivity. However, a diastereoselective Lewis base-catalyzed Mukaiyama aldol reaction has not been explored up to this point, especially diastereoselectively constructing bispropionate units. We tried to investigate the Lewis base-catalyzed Mukaiyama aldol reaction and find if there is any all-*syn* stereochemistry preference to

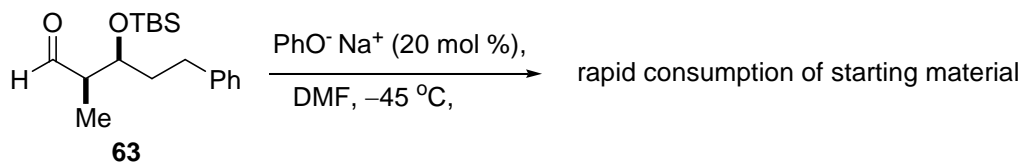
fit our designed model (Scheme 10). Based on the recent research in the Mukaiyama group, lithium amide, lithium acetate and lithium phenoxide were good base catalysts for Mukaiyama aldol and Michael reactions.²¹ So our first trials targeted these Lewis bases. The initial test reactions employed enol silane **53** as the nucleophile and *syn* aldehyde **63** in DMF at $-45\text{ }^{\circ}\text{C}$, which is the same condition as used in the Mukaiyama group.²¹ Lewis base (10 mol %) was then added under a N_2 atmosphere at $-45\text{ }^{\circ}\text{C}$ (eq 13, Table 1). Table 1 showed most catalysts gave a small amount of product. Different solvents and temperatures were screened to improve the yield, but no improvement was observed. It was determined via a control experiment (Scheme 13) that the base catalyst decomposed the aldehyde **63**. When 10 mol % of NaOPh was mixed with aldehyde **63** at $-45\text{ }^{\circ}\text{C}$ in DMF, aldehyde **63** disappeared in 5 min. It meant that there was a competing side reaction, enolization, between aldehyde **63** and Lewis base catalyst. This reactivity pattern was also observed by Mukaiyama that aliphatic aldehydes gave low yields with Lewis base as catalyst.²²

Table 1. Initial trial of Lewis base for Mukaiyama aldol reaction



entry	Lewis base	% yield
1	$\text{PhO}^- \text{Na}^+$	32%
2	$\text{PhO}^- \text{Li}^+$	28%
3	$\text{AcCO}_2^- \text{Li}^+$	23%
4		trace

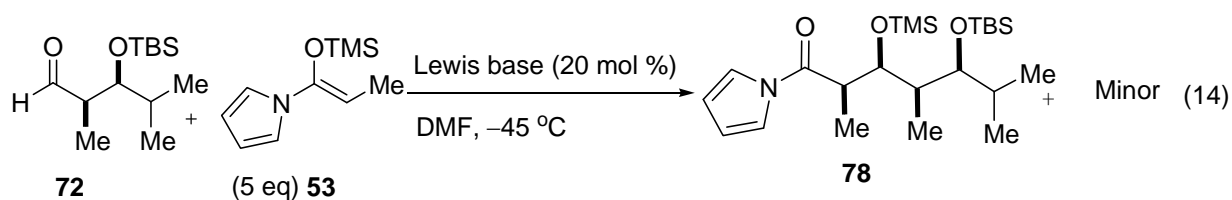
Scheme 13. The control experiment for Lewis base screen.



In order to address the side-reaction of eq 13, 5 equiv. of enol silane were used to accelerate the reaction between aldehyde and enol silane. Fortunately, the yield was improved dramatically to 70%, and the diastereoselectivity was improved to 5:1 as measured by ^1H NMR. However, aldehyde **72** (entry1, Table 2) just gave a poor selectivity 60:40. Since previous BF_3 -

mediated Mukaiyama aldol reactions also gave poor selectivity (eq 11), these results indicated that aldehyde **72** could be a difficult substrate for good selectivity. We began with aldehyde **72** to optimize our catalysts and conditions. For the systematic investigation of the Lewis base-catalyzed Mukaiyama aldol reaction, several factors needed to be addressed, such as the counter ions of the Lewis base, substitutions on the phenoxide, solvent and temperature.

Table 2. Screen of counter ions of the Lewis base for Mukaiyama aldol reaction



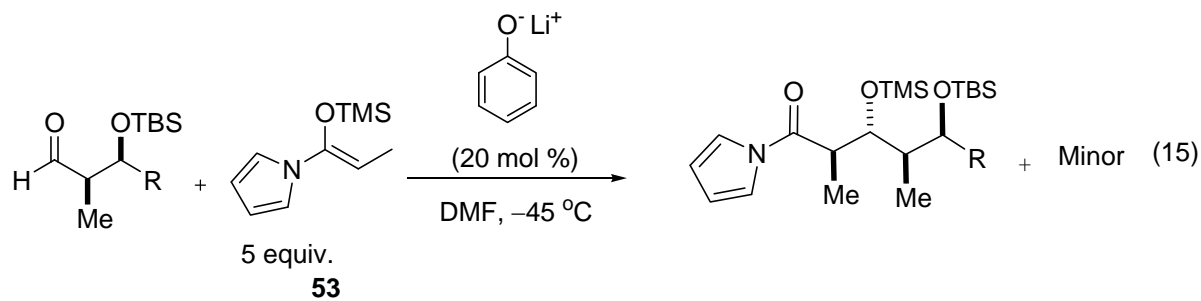
entry	Lewis base	% yield, 78 : Minor
1		73%, 60:40
2		80%, 91:9
3		trace
4		56%, 83:17

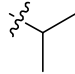
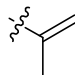
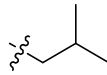
Reaction scheme showing the Mukaiyama aldol reaction of aldehyde **72** with enone **53** (5 eq) using a Lewis base (20 mol %) in DMF at $-45\text{ }^{\circ}\text{C}$. The reaction yields product **78** and a minor product (14%).

Reaction scheme showing the Mukaiyama aldol reaction of aldehyde **72** with enone **53** (5 eq) using a Lewis base (20 mol %) in DMF at $-45\text{ }^{\circ}\text{C}$. The reaction yields product **79** and a minor product (14%).

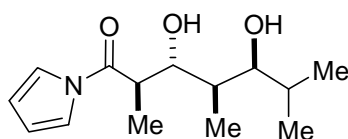
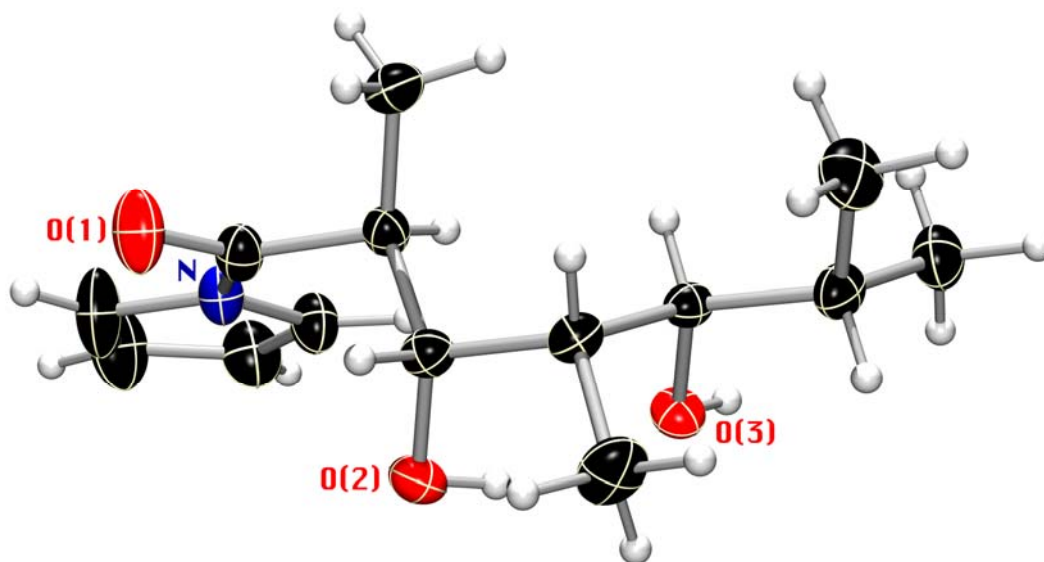
At first, a standard condition was chosen to perform the catalyst screen: one equivalent of aldehyde and 5 equiv. of enol silane were mixed in DMF at $-45\text{ }^{\circ}\text{C}$, followed by 20 mol % of Lewis base catalyst. Lithium, sodium, potassium, lanthanum and tetrabutylammonium phenoxides were tested under these conditions. The lanthanum phenoxide gave just trace amount of aldol product (Table 2, entry 3). In Table 2, most results indicated that the all-*syn* product was the major product except with the lithium phenoxide-catalyzed reaction. However, tetrabutylammonium phenoxide showed some improvements in diastereoselectivity over the sodium phenoxide-catalyzed reaction (Table 2, entry 4). Attention was therefore focused on tetrabutylammonium phenoxide and changed other variables to further optimize the reaction.

Surprisingly, lithium phenoxide-catalyzed the reaction quickly and smoothly with good selectivity and excellent yield (Table 2, entry 2). However, the product was not our desired stereoisomer. After compound **79** was deprotected with HF, the stereochemistry of compound **79** was confirmed via X-ray crystallographic analysis of diol **81** (Figure 7). Unfortunately, as substitutions changed, the diastereoselectivity and yield dropped (Table 3).

Table 3. Lithium phenoxide-catalyzed Mukaiyama aldol reaction

entry	Aldehyde	% yield, diastereomeric ratio ^a
1	R =  72	85%, 85:8:6
2	R =  73	62%, 80:10:8
3	R =  82	58%, 70:30

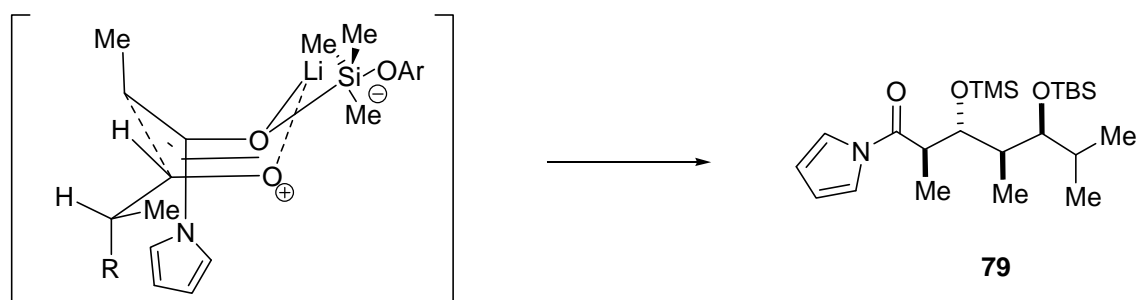
^a Monitored by gas chromatography.



81

Figure 7. X-ray crystal structure of **81**.

Generated with ORTEP 3 v2 and visualized with POV-Ray® software.

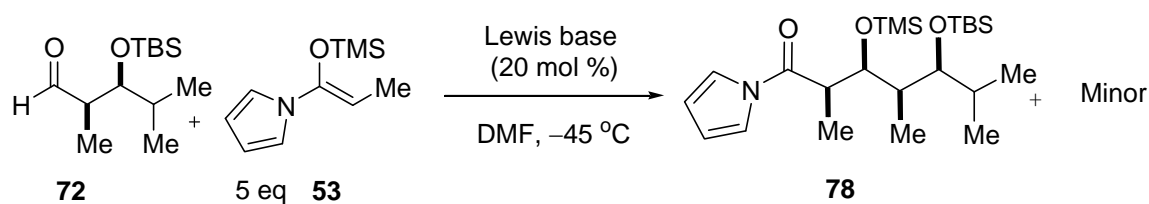


79

Figure 8. The proposed transition state for **79**

The transition state of this *anti, anti, syn*-product **81** continued to be elusive. It was not the anticipated open transition state typical for a Mukaiyama aldol reaction or the Zimmerman-Traxler model, since the Felkin product was not observed. A boat transition state could explain the stereochemistry of **79** (Figure 8).

Table 4. Screen of substituents on phenoxide

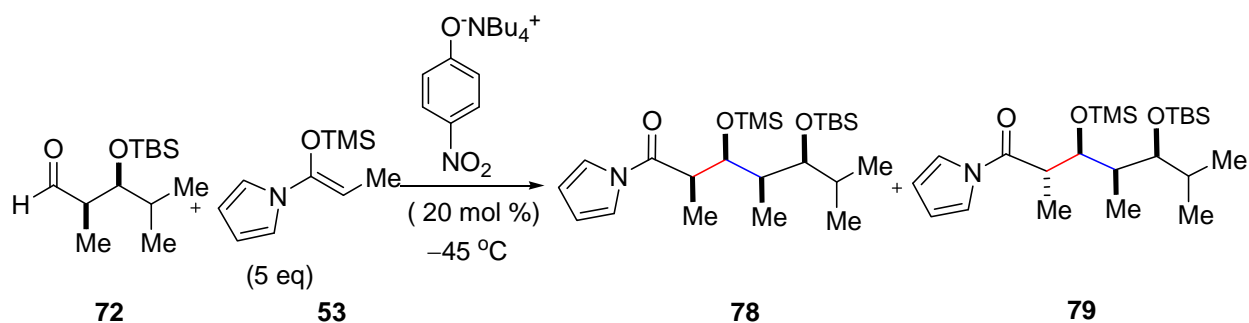


entry	Lewis base	% yield, 78 : Minor
1		56%, 80:20
2		54%, 83:17
3		57%, 83:17
4		57%, 80:20

The substitutions on the phenoxides in Table 4 would impact on the electronic properties of the phenoxide which would then effect the electron properties of silyl activation. Several substituents have been screened (Table 4), but they all demonstrated similar reactivities and selectivities. One observation was that the weakest base, *p*-nitro phenoxide did retard the reaction rate. This result provided a potential way to modulate reactivity, potentially minimizing undesired side reactions.

A variety of polar and non-polar solvents was screened and is listed in Table 5. Since polar solvents have been shown to accelerate Mukaiyama aldol reactions²⁷ and help solvate phenoxides, polar solvents were the first solvents tested. Methylene chloride gave a poor yield. DME demonstrated excellent *syn/anti* selectivity, but Felkin/anti-Felkin selectivity was only about 4:1. Acetonitrile gave a moderate selectivity for both *syn/anti* and Felkin/anti-Felkin product. Solubility problems with tetrabutylammonium *p*-nitro phenoxide in toluene prevented this base from interacting sufficiently with the substrate to provide any appreciable amount of product. Diglyme is structurally similar to DME and demonstrated similar selectivity. Most polar solvents didn't have low melting points, THF was chosen as a suitable solvent for further temperature investigation. It seems that acyclic and cyclic ethers helped the *syn/anti* selectivity. However, since THF has demonstrated potential to be a suitable solvent to get further improvement of the reaction, no further experiments to investigate the solvent effect to this reaction was performed.

Table 5. Solvents screened for tetrabutylammonium phenoxide-catalyzed Mukaiyama aldol reaction



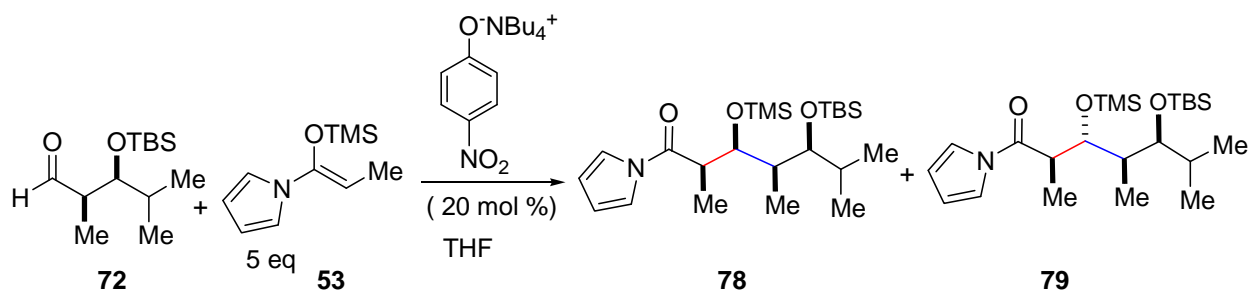
entry	solvent	yield,	<i>syn:anti</i>	Felkin: anti-Felkin
1	CH ₂ Cl ₂	31%,	88:12	75:25
2	THF	39%,	87:13	75:25
3	DMF	57%,	87:13	85:15
4	DME	57%,	>99:1	80:20
5	CH ₃ CN	46%,	86:14	87:13
6	Toluene	trace		
7	Diglyme	41%,	97:3	83:17

syn and anti relationship refers to the relative stereochemistry along the red bond.
Felkin and anti-Felkin relationship refers to the relative stereochemistry along the blue bond.

Attention was next turned to screening of different temperature ranges (Table 6). The best result was obtained at $-70\text{ }^{\circ}\text{C}$. Both yield and selectivity were improved to an acceptable

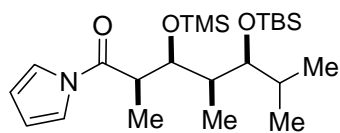
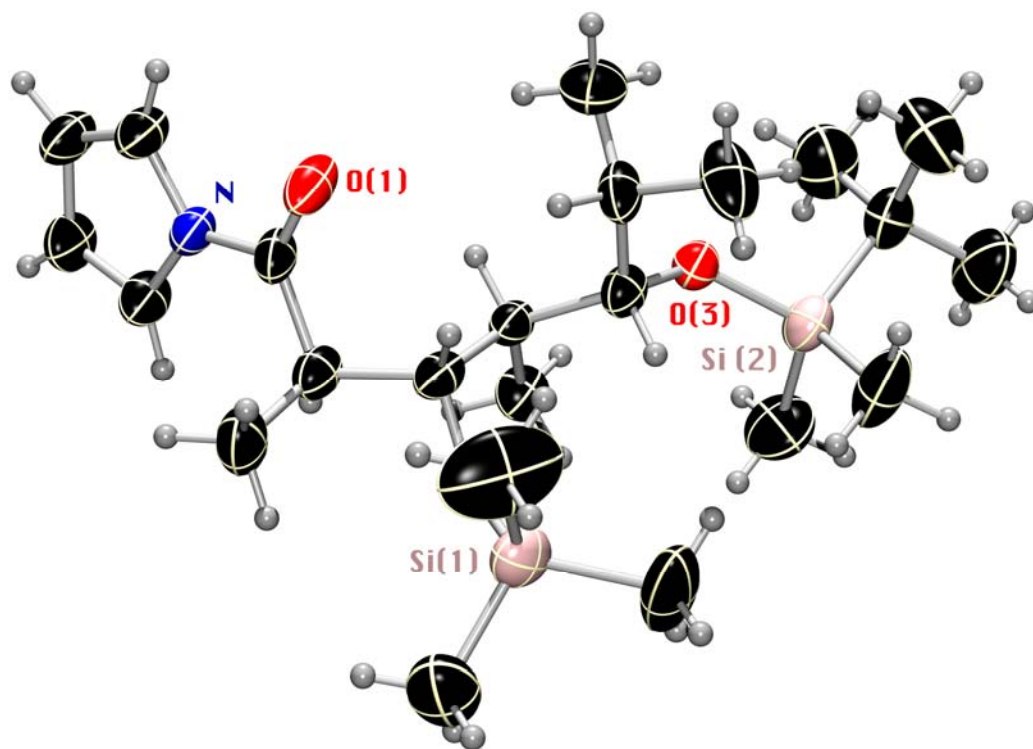
level to give 62%, 90:10 dr (entry 2, Table 6). The reaction rate was slowed down dramatically at $-90\text{ }^{\circ}\text{C}$. In entry 3, at $-90\text{ }^{\circ}\text{C}$ the crude ^1H NMR showed a very clean reaction after 30 min. Only product and starting materials was observed without any noticeable side product. However, low yield was obtained due to short reaction time (30 min). However, full conversion and a better yield were obtained if the reaction mixture was stirred for 6 hours (entry 4, Table 6). The absolute stereochemistry of compound **78** was confirmed by X-ray crystal analysis of **78** (Figure 9).

Table 6. Temperature screen of tetrabutylammonium phenoxide-catalyzed Mukaiyama aldol reaction



entry	Temperature	yield,	<i>syn:anti</i>	Felkin: anti-Felkin
1	$-45\text{ }^{\circ}\text{C}$	39%	87:13	75: 25
2	$-70\text{ }^{\circ}\text{C}$	62%	99:1	90:10
3	$-90\text{ }^{\circ}\text{C}$	15% ^a	>99:1	90:10
4	$-90\text{ }^{\circ}\text{C}$	67%	>99:1	90:10

^a: Reaction was quenched too early.



78

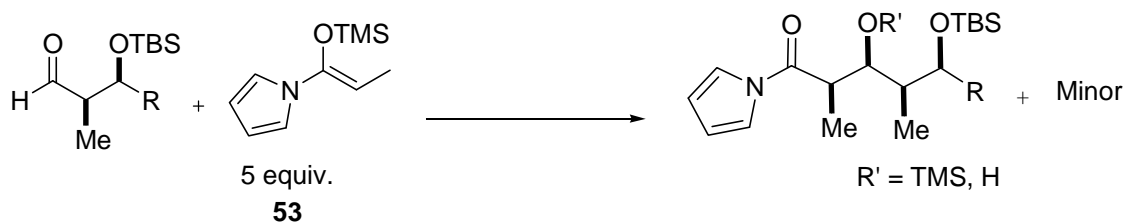
Figure 9. X-ray crystal structure of **78**.

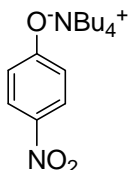
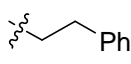
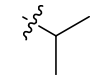
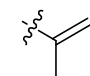
Generated with ORTEP 3 v2 and visualized with POV-Ray® software.

Different aldehydes were screened to determine the scope of this reaction (Table 7). Entry 1 and entry 3 demonstrated excellent diastereoselectivities and yields. Compared to the Lewis acid-mediated Mukaiyama aldol reaction (Table 7), overall selectivity was improved from moderate to excellent. The most important aldehyde **73**, which was used in total synthesis of

erythronolide B in our group, demonstrated excellent selectivity (94:6). The absolute stereochemistry of aldol product **83** also was confirmed by an X-ray crystal structure of the deprotected form of **84** (Figure 10).

Table 7. Comparison of Lewis base-catalyzed Mukaiyama aldol reaction and Lewis acid-mediated Mukaiyama aldol reaction for all-*syn* bispropionate synthesis



entry	aldehyde	Lewis Base: 		Lewis acid (BF ₃ ·Et ₂ O)	
		yield,	major:minor	yield,	major:minor
1	R =  Ph	96%	98:2	66%	5:1
	63		64	65	
2	R = 	62%	90:10	34%	1:1
	72		78	74	
3	R = 	90%	94:6	N/A	3:1
	73		83	76	

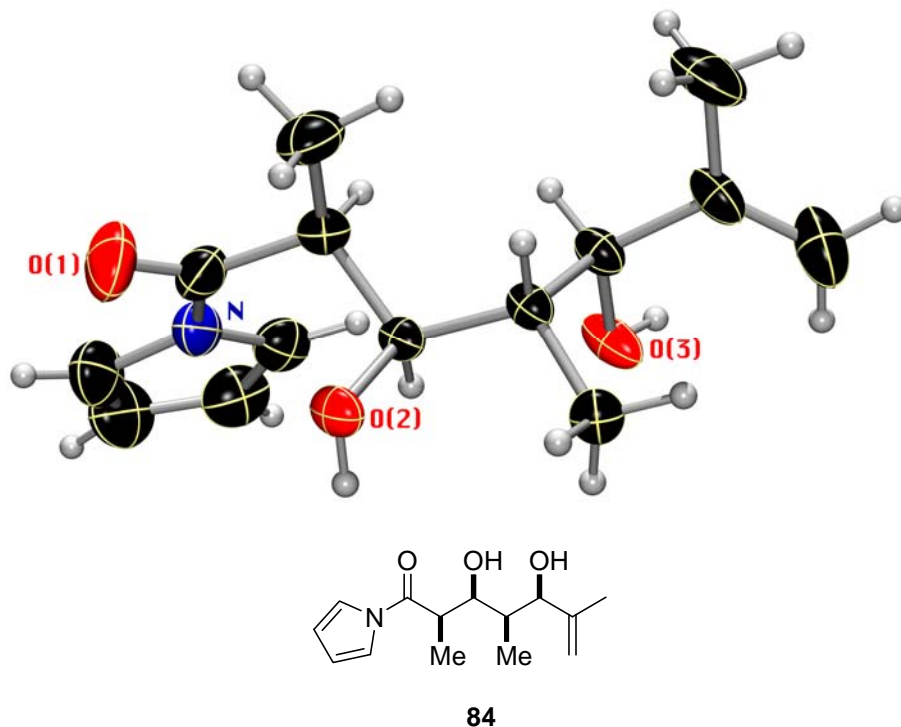


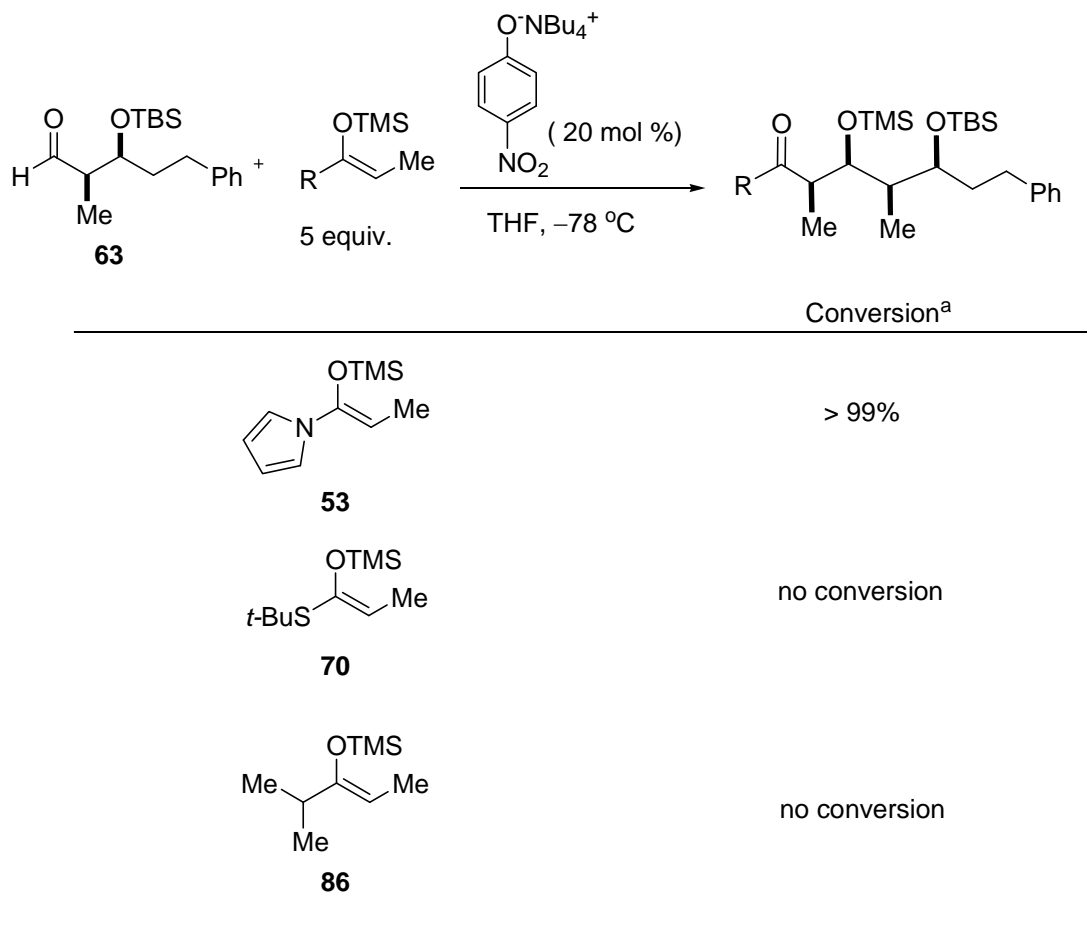
Figure 10. X-ray crystal structure of **84**

Generated with ORTEP 3 v2 and visualized with POV-Ray® software.

Since tetrabutylammonium phenoxide worked well in THF, lithium phenoxide was re-examined in the same solvent. It turned out that the reaction just stalled when the catalyst was switched from tetrabutylammonium phenoxide to lithium phenoxide. It appears that the counter ion had a significant impact on the reactivity of the Lewis base in THF.

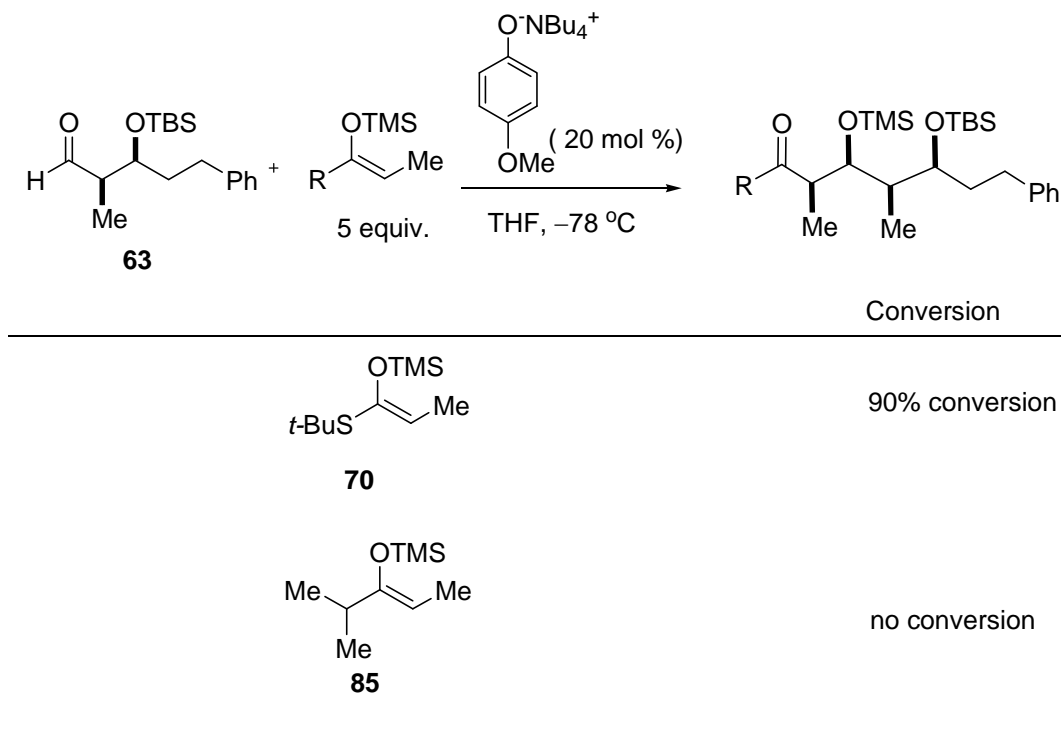
Different enol silanes were explored under the optimized condition (Table 8). At $-78\text{ }^{\circ}\text{C}$, tetrabutylammonium phenoxide was added to the solution of enol silane and aldehyde in THF. In Table 8, *p*-nitro phenoxides could only catalyze the reaction involving electron rich enol silane **53**. Enol silanes **70** and **86** had no conversion with this base catalyst in THF.

Table 8. Comparison of enol silanes for electronic properties



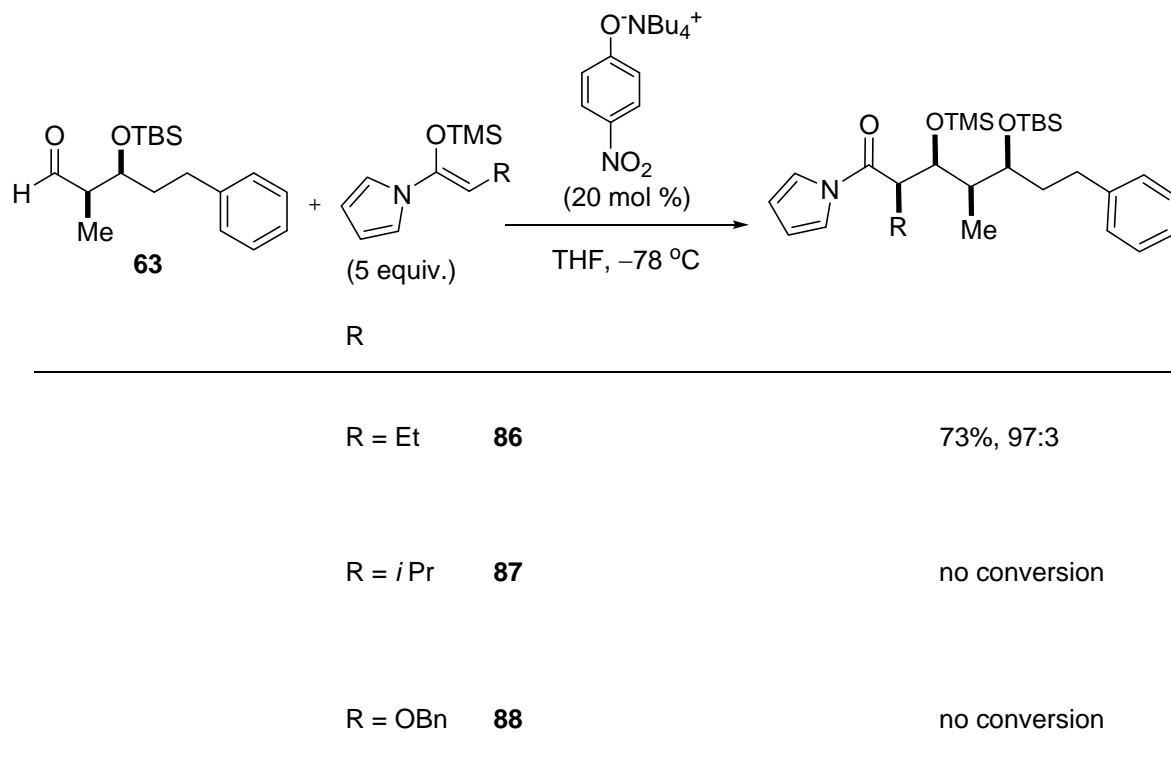
^a Monitored by GC-FID.

Next, in the presence of a stronger Lewis base, tetrabutylammonium *p*-methoxyphenoxide, the reaction of aldehyde **63** with enol silane **70** or **86** was repeated. The electron rich enol silane **70** reacted smoothly in 90% conversion, whereas ketone derived enol silane **86** gave no conversion. These results indicated that the reactivity of Lewis base-catalyzed Mukaiyama aldol relied on the electronic properties of the enol silane along with the electronic properties of Lewis base catalyst.

Table 9. Enol silane comparisons

Enol silane **86** has shown similar reactivity with aldehyde **63** and demonstrated high diastereoselectivity. But enol silane **87** didn't react with aldehyde **63** under the standard set of conditions. The steric bulk of the isopropyl group should be considered as the reason for its lack of reactivity. Enol silane **88** has also shown no reaction with aldehyde **63**. The non-reactivity of **88** probably resulted from low electron density on the enol moiety due to the α -effect.³⁵ The starting material did not decompose during this reaction. This behavior was different from our previous results in DMF. In DMF, aldehyde **63** was consumed completely if the reaction worked or not.

Table 10. Scope of enol silanes.



1.3 CONCLUSION

Thus far, a new methodology to synthesize all-*syn* bispropionate units has been developed in good yield and with excellent selectivity. In this endeavor, the catalysts, solvents and temperatures have been optimized to ultimately provide the best overall catalytic system. Through changing several couterions of the Lewis base catalyst, we discovered that tetrabutylammonium phenoxide dramatically improved the selectivity of these reactions. Through changing different substitutions on the aryl component of catalyst, the very mild Lewis

base catalyst tetrabutylammonium *p*-nitro phenoxide reduced the chance of deprotonation of the aldehyde. Next, several solvents were screened. THF was used to further temperature screen, since other solvents have high melting points. Gratifyingly, lower temperatures improved the selectivity to 90:10. We also applied this condition to other aldehydes and achieved similar yields and selectivity. The absolute stereochemistry of each bispropionate product was confirmed by X-ray crystallographic analysis. Furthermore, the target building block of erythronolide B has been synthesized by this method.

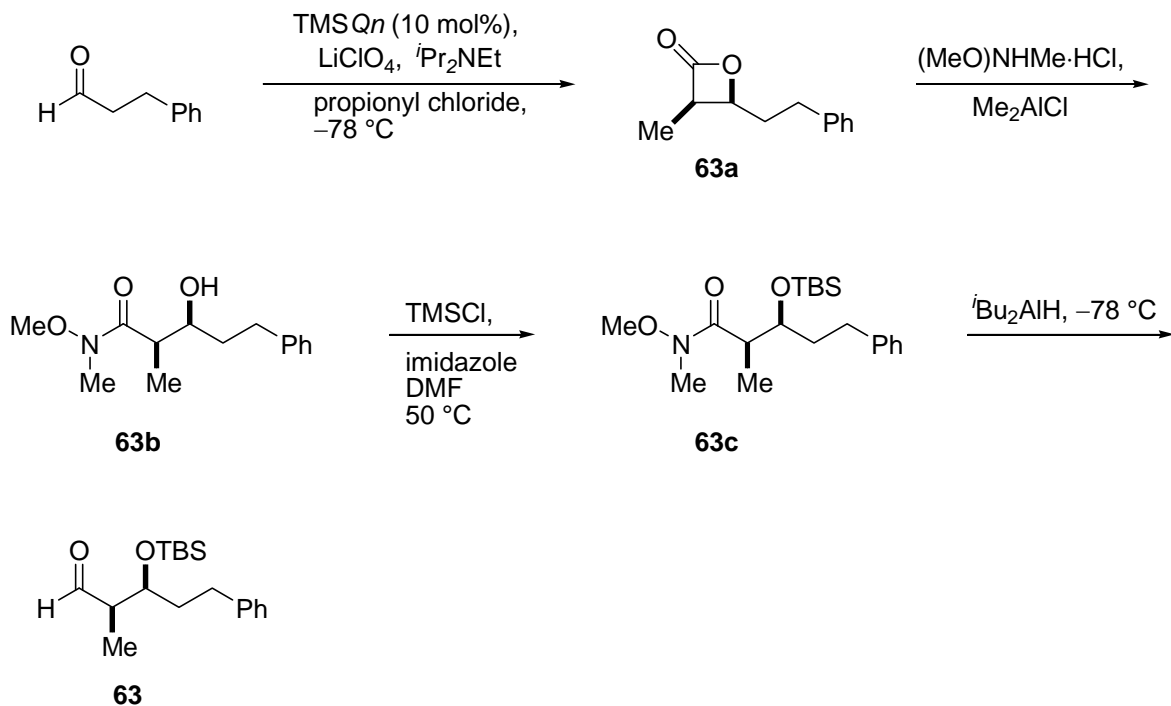
Compared to the known synthetic methods used to generate all-*syn* bispropionate units, ours is both catalytic and diastereoselective. In addition to a catalyst screen, we also investigated the reactivity of different enosilanes. Amide derived enol silane **53** demonstrated better reactivity compared to other enol silanes. Furthermore, the stronger Lewis base showed better reactivity to catalyze this reaction with unreactive enol silanes. Steric bulkiness of the enol silane also had dramatic effect on the reactivity. Lithium phenoxide ultimately catalyzed reaction to give an anti-Felkin product in good yield and selectivity. This indicated that this reaction might also provide us with a new route to construct *anti, anti, syn*-bispropionate units. A boat transition state was proposed to explain this product. Unfortunately, this reaction only gave good selectivity for two substrates. In summary, we have developed the only known way to generate all-*syn* bispropionate aldol products which is both catalytic and diastereoselective.

1.4 EXPERIMENTALS

General Information: Optical rotations were measured on a Perkin-Elmer 241 digital polarimeter with a sodium lamp at ambient temperature and are reported as follows: $[\alpha]_{\lambda}$ (c g/100mL). Infrared spectra were recorded on a Nicolet Avatar 360 FT-IR spectrometer. NMR spectra were recorded on a Bruker Avance-300 (^1H : 300 MHz; ^{13}C : 75 MHz) spectrometer with chemical shifts reported relative to residual CHCl_3 (7.26 ppm) for ^1H and CDCl_3 (77.0 ppm) for ^{13}C NMR spectra. Unless otherwise stated, all reactions were carried out in flame-dried glassware under a nitrogen atmosphere using standard inert atmosphere techniques for the manipulation of solvents and reagents. Analytical gas-liquid chromatography (GLC) was performed on a Varian 3900 gas chromatography equipped with a flame ionization detector and split mode capillary injection system using a ChiralDEX™ G-TA column (20 m x 0.25 mm) (Advanced Separation Technologies Inc.). Helium was used as the carrier gas at the indicated pressures. Mass spectra were obtained on a VG-7070 or Fisons Autospec high resolution magnetic sector mass spectrometer.

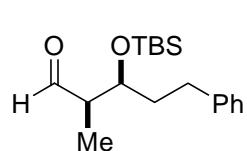
Unless otherwise stated, all reactions were carried out in dry glassware under a nitrogen atmosphere using standard inert atmosphere techniques for the manipulation of solvents and reagents. Anhydrous solvents (CH_2Cl_2 , THF, DMF, diethyl ether, pentane and toluene) were obtained by passage through successive alumina and Q5 reactant-packed columns on a solvent purification system. *N,N*-Diisopropylethylamine and triethylamine were distilled under nitrogen from CaH_2 . All the commercial chemicals are purchased from Aldrich Chemical Co. Flash chromatography was performed on EM silica gel 60 (230-240 mesh) unless noted otherwise.³⁶ If

the reaction was worked up with aqueous extraction, dr (diastereomer ratio) was determined from crude NMR or GLC. Enol silanes **53**, **86**, **87**,³⁷ **88**,³⁸ and **70**³⁹ were prepared according to the known procedures. Mass spectra were obtained on a VG-7070 or Fisons Autospec high resolution magnetic sector mass spectrometer.



(*2R,3S*)-3-Hydroxy-*N*-methoxy-*N*,2-dimethyl-5-phenylpentanamide (**63b**):⁴⁰ TMSQn (0.8 g, 2 mmol) and LiClO₄ (1.06 g, 10 mmol) were dissolved in 20 mL diethyl ether and 40 mL CH₂Cl₂ at room temperature and then cooled to -78 °C. To the above cooled mixture was added *N, N*-diisopropylethylamine (8.8 mL, 5 mmol), followed by hydrocinnamaldehyde (2.64 mL, 20 mmol). A solution of propionyl chloride (3.6 mL, 40 mmol) in 10 mL CH₂Cl₂ was then added over 2 h by syringe pump. After being stirred overnight, the reaction was quenched at the reaction temperature by

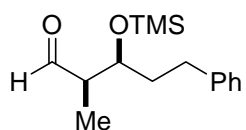
adding 100 mL Et₂O and filtered through a silica gel column and concentrated. The resulting crude product (2.96 g) was used without further purification. To a solution of Weinreb's salt (3.04 g, 31.2 mmol) in 80 mL CH₂Cl₂ at 0 °C, Me₂AlCl (32 mL, 1.0 M in hexane, 32 mmol) was added dropwise and then warmed to ambient temperature. After being stirred for 2 hours, a solution of crude lactone **90** (2.96 g, 15.6 mmol) in 40 mL CH₂Cl₂ was added -25 °C. The resulting mixture was stirred 2h, then quenched with aqueous Rochelle's solution and the biphasic mixture was stirred vigorously for an hour. Then the organic layer was separated and the aqueous layer was extracted with ether. The organic extracts were combined, dried (Na₂SO₄) and concentrated. The crude oil was then purified with flash column with 30% ethyl acetate in hexanes, affording 3.77 g (75% over 2 steps) of the title compound as a white solid. ¹H NMR (300 MHz, CDCl₃) δ 7.31-7.18 (m, 5H), 3.92-3.89 (br, 1H), 3.66 (s, 3H), 3.18 (s, 3H), 2.92-2.83 (m, 2H), 2.72-2.62 (m, 1H), 1.98-1.85 (m, 1H), 1.69-1.62 (m, 1H), 1.09 (d, J = 7.0 Hz, 3H), 0.89 (m, 9H), 0.09 (s, 3H), 0.04 (s, 3H);



(2R,3S)-3-(tert-Butyldimethylsilyloxy)-2-methyl-5-phenylpentanal (63):

To a solution of **91** (1.00 g, 3.98 mmol) in 40 mL of DMF at ambient temperature was added imidazole (0.80 g, 11.7 mmol) followed by TBSCl (1.20 g, 7.96 mmol). The reaction mixture was stirred overnight then was quenched by adding 100 mL saturated aqueous NH₄Cl solution. The mixture was extracted by ether (3 x 100 mL). The organic extracts were washed by brine, dried and concentrated. The crude product mixture was further condensed under high vacuum. The crude product was used without further purification. To a solution of crude product **92** (1.33 g, 3.64 mmol) in 30 mL of THF at -78 °C was slowly added DIBAL (4.0 mL, 1.0 M in hexanes, 4.0 mmol). The reaction mixture was

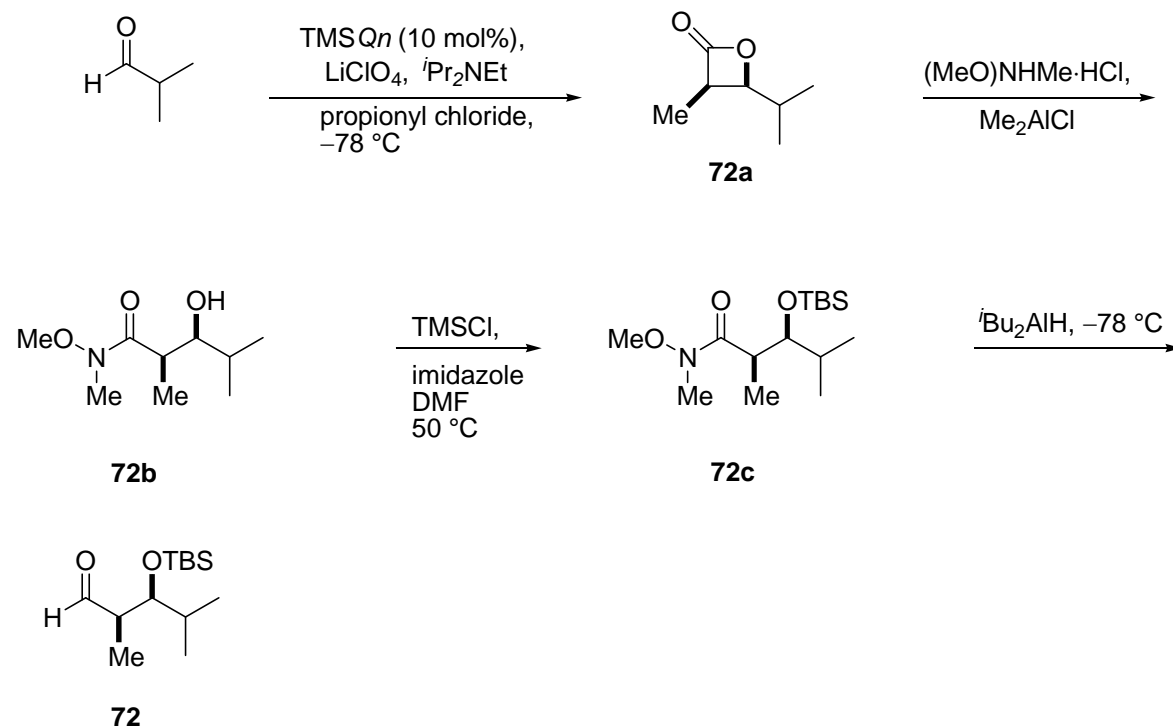
stirred for 3 h then was quenched by adding 50 mL aqueous Rochelle's solution. The mixture was extracted by Et₂O (3 x 50 mL). The organic extracts were combined and washed with Rochelle solution, brine and dried and concentrated. The crude product mixture was purified by flash chromatography (10% ethyl acetate in hexane) gave 826 mg (67% over 2 steps) of the title compound as a colorless oil. IR (thin film): 2953, 2857, 1726, 1254, 1034 cm⁻¹; [α]_D -26.8 (*c* 1.24, CHCl₃); ¹H NMR (300 MHz, CDCl₃) δ 9.78 (d, *J* = 9.0 Hz, 1H), 7.32-7.16 (m, 5H), 4.15 (td, *J* = 3.8, 6.4 Hz, 1H), 2.70-2.65 (m, 1H), 2.63-2.45 (m, 2H), 1.94-1.70 (m, 2H), 1.09 (d, *J* = 7.0 Hz, 3H), 0.89 (m, 9H), 0.09 (s, 3H), 0.04 (s, 3H); ¹³C NMR (75 MHz, CDCl₃) δ 205.07, 141.60, 128.48, 128.22, 125.99, 71.80, 51.27, 36.41, 32.15, 25.77, 18.03, 7.89, -4.23, -4.57; HRMS (*EI*) *m/z* calcd for (M-CH₃)⁺ C₁₇H₂₇O₂Si: 291.1780; found: 291.1778.



(2*R*,3*S*)-3-(*tert*-Trimethylsilyloxy)-2-methyl-5-phenylpentanal (67)⁴¹: To

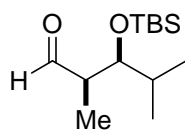
a solution of **91** (125 mg, 0.5 mmol) in 5 mL of DMF at ambient temperature was added imidazole (67 g, 1.0 mmol) followed by TMSCl (108 mg, 1.0 mmol). The reaction mixture was stirred at 50 °C overnight then was quenched by adding 15 mL saturated aqueous NH₄Cl solution. The mixture was extracted by ether (3 x 50 mL). The organic extracts were washed by brine, dried and concentrated. The crude product mixture was further condensed under high vacuum. The crude product was used without further purification. To a solution of crude product **92** in 10 mL of THF at -78 °C was slowly added DIBAL (0.60 mL, 1.0 M in hexanes, 0.6 mmol). The reaction mixture was stirred for 3 h then was quenched by adding 15 mL aqueous Rochelle's solution. The mixture was extracted by Et₂O (3 x 50 mL). The organic extracts were combined and washed with Rochelle solution, brine and dried and concentrated. The crude product mixture was purified by flash chromatography (10%

ethyl acetate in hexane) gave 105 mg (79% over 2 steps) of the title compound as a colorless oil. $^1\text{H NMR}$ (300 MHz, CDCl_3) δ 9.78 (d, $J = 0.9$ Hz, 1H), 7.34-7.19 (m, 5H), 4.16 (dt, $J = 3.9, 2.4$ Hz, 1H), 2.80-2.67 (m, 1H), 2.60-2.49 (m, 2H), 1.87-1.80 (m, 2H), 1.11 (d, $J = 7.2$ Hz, 3H), 0.15 (s, 9H);



(2*R*,3*S*)-3-(*tert*-Butyldimethylsilyloxy)-*N*-methoxy-*N*,2,4-trimethylpentanamide (72b): TMSQn (400 mg, 1 mmol) and LiClO_4 (2.1 g, 20 mmol) were dissolved in 10 mL diethyl ether and 20 mL CH_2Cl_2 at room temperature and then cooled to -78 °C. To the above cooled mixture was added *N*, *N*-diisopropylethylamine (4.4 mL, 2.5 mmol), followed by isobutyraldehyde (720 mg, 10 mmol). A solution of propionyl chloride (1.8 mL, 20 mmol) in 5 mL CH_2Cl_2 was then added over 2 h by

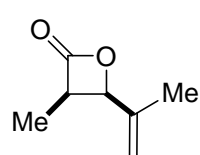
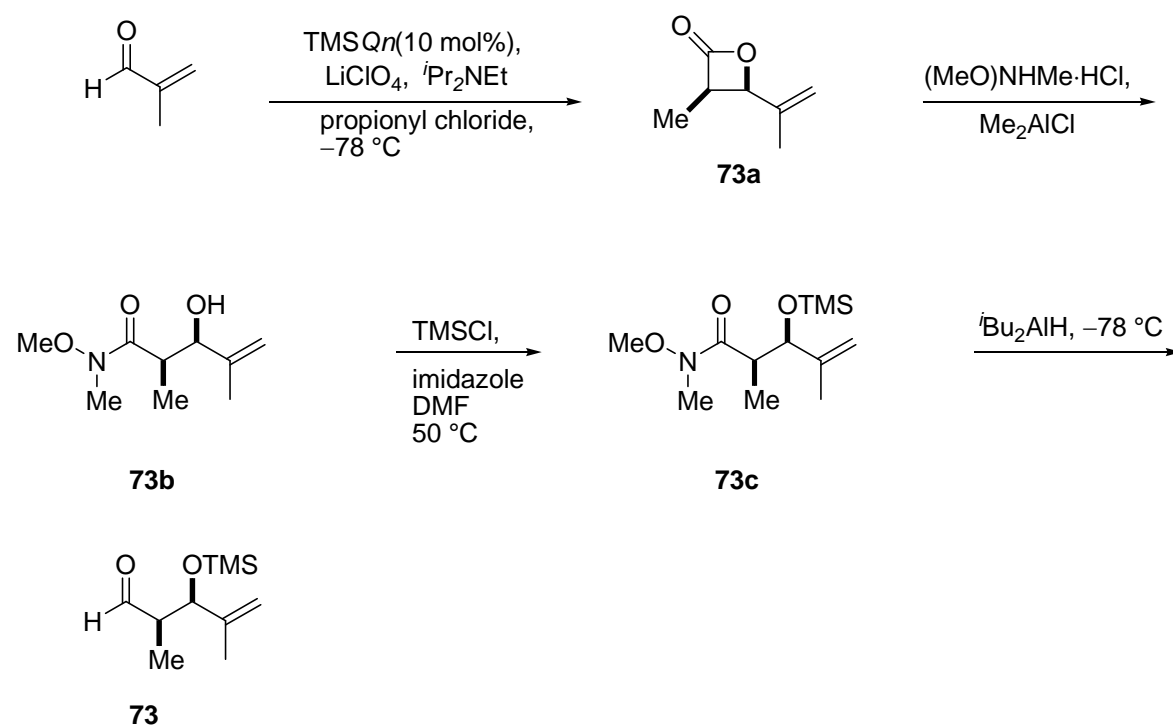
syringe pump. After being stirred overnight, the reaction was quenched at the reaction temperature by adding 50 mL Et₂O and filtered through a silica gel column and concentrated. The resulting crude product was used without further purification. To a solution of Weinreb's salt (1.36 g, 14.0 mmol) in 30 mL CH₂Cl₂ at 0 °C, Me₂AlCl (14.0 mL, 1.0 M in hexane, 14.0 mmol) was added dropwise and then warmed to ambient temperature. After being stirred for 2 h, a solution of crude lactone **93** (0.90 g, 7.1 mmol) in 60 mL CH₂Cl₂ was added at -30 °C. The resulting mixture was stirred for 2 h, then quenched with aqueous Rochelle solution and the biphasic mixture was filtered through celite. Then the organic layer was separated and the aqueous layer was extracted with ether. The organic extracts were combined, dried (Na₂SO₄) and concentrated. The crude product (1.35 g) was used without purification. The crude product **94** was then dissolved in 50 ml DMF at ambient temperature. Imidazole (1.43 g, 21 mmol) was added followed by TBSCl (3.15 g, 21 mmol). The reaction mixture was stirred for overnight then was quenched by adding 50 mL H₂O. The mixture was extracted with ether (5 x 50 mL). The organic extracts were washed with brine and dried over MgSO₄ and concentrated. The crude product mixture was purified by flash chromatography (5-20% ethyl acetate in hexane) gave 1.93 g (63% over 3 steps) of the title compound as a colorless oil.



(2R,3S)-3-(tert-Butyldimethylsilyloxy)-2,4-dimethylpentanal (72): To a

solution of **95** (1.9 g, 6.3 mmol) in 15 mL of THF at -78 °C was slowly added DIBAL (8.1 mL, 1.0 M in hexanes, 8.1 mmol). The reaction mixture was stirred for 2 h then was quenched by adding 50 mL aqueous Rochelle's solution. The mixture was extracted by Et₂O (3 x 50 mL). The organic extracts were combined and washed with Rochelle's solution, brine, dried and concentrated. The crude product mixture was purified by flash chromatography (2-5% ethyl

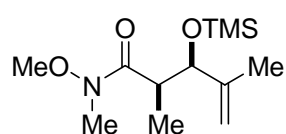
acetate in hexane) gave 1.2 g (79%) of the title compound as a colorless oil. IR (thin film): 2958, 2858, 1727, 1471, 1254, 1054 cm^{-1} ; $[\alpha]_{\text{D}} +55$ (c 0.82, CHCl_3); ^1H NMR (500 MHz, CDCl_3) δ 9.79 (s, 1H), 3.91 (dd, $J = 5, 3.5$ Hz, 1H), 2.52-2.50 (, 1H), 1.83-1.80 (m, 1H), 1.10 (d, $J = 7.0$ Hz, 3 H), 0.94 (d, $J = 8.0$ Hz, 3H), 0.92-0.89 (m, 12H), 0.08 (s, 3H), 0.02 (s, 3H); ^{13}C NMR (75 MHz, CDCl_3) δ 205.5, 76.4, 50.6, 32.2, 19.6, 18.3, 8.6, -4.0 , -4.2 ; HRMS (*EI*) m/z calcd for $[\text{M}]^+$ $\text{C}_{13}\text{H}_{28}\text{O}_2\text{Si}$: 244.1858; found:244.1855.



(3R,4R)-3-Methyl-4-(prop-1-en-2-yl)oxetan-2-one (73a)⁴²: TMSQn (1.20 g, 3.00 mmol) and LiClO_4 (6.36 g, 30.0 mmol) were dissolved in 30 mL diethyl ether and 60 mL CH_2Cl_2 at room temperature and then cooled to -78 $^\circ\text{C}$. To

the above cooled mixture was added *N,N*-diisopropylethylamine (13.2 mL, 7.50 mmol), followed

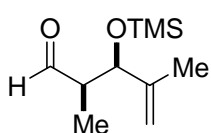
by methacrolein (2.1 g, 30 mmol). A solution of propionyl chloride (5.55 mg, 60 mmol) in 15 mL CH₂Cl₂ was then added over 3 h by syringe pump. After being stirred overnight, the reaction was quenched at the reaction temperature by adding 100 mL Et₂O and filtered through a silica gel column and concentrated. The resulting crude product was purified by flash chromatography (5% ethyl acetate in pentane) giving 1.91 g (51% yield with a tiny amount of ethyl acetate) of the title compound as a colorless volatile liquid. ¹H NMR (300 MHz, CDCl₃): δ 1.24 (d, J=7.5 Hz, 3H), 1.74 (s, 3H), 3.86 (pentet, J= 6.6 Hz, 1H), 4.92 (d, J=6.6 Hz, 1H), 5.16 (br s, 1H), 5.18 (br s, 1H);



(2*R*,3*R*)-*N*-Methoxy-*N*,2,4-trimethyl-3-(trimethylsilyloxy)pent-4-enamide (73b)⁴²: To a solution of Weinreb's salt (1.95 g, 20 mmol) in

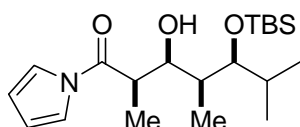
40 mL CH₂Cl₂ at 0 °C, Me₂AlCl (20 mL, 1.0 M in hexane, 20 mmol) was added dropwise and then warmed to ambient temperature. After being stirred for 2 h, a solution of lactone **96** (1.26 g, 10 mmol) in 20 mL CH₂Cl₂ was added at -30 °C. The resulting mixture was stirred for 2 h, then quenched with aqueous Rochelle solution and the biphasic mixture was filtered through celite. Then the organic layer was separated and the aqueous layer was extracted with ether. The organic extracts were combined, dried (Na₂SO₄) and concentrated. The crude product (1.35 g) was used without purification. To a solution of crude product **97** (600 mg, 3.20 mmol) in 20 mL CH₂Cl₂ at room temperature, 2,6-lutidine (0.560 mL, 3.85 mmol) was added. The reaction mixture was then cooled to -78 °C and TMSOTf (0.7 mL, 4.81 mmol) was added dropwise. The reaction was then warmed up to room temperature and stirred for 2 h. The reaction was quenched with 50 mL saturated aq. NaHCO₃ and extracted with CH₂Cl₂ (2 × 30 mL). All the organic extracts were then washed with brine, dried and concentrated. The crude oil was purified with

flash column (30% ethyl acetate in hexanes) giving 771 mg (90 % yield over 3 steps) of the title compound as a colorless oil. ¹H NMR (300 MHz, CDCl₃): δ 4.88 (s, 1H), 4.78 (s, 1H), 4.24 (d, J=8.7 Hz, 1H), 3.63 (s, 3H), 3.13 (s, 4H), 1.71 (s, 3H), 1.18 (d, J = 6.6 Hz, 3H), 0.08 (s, 9H).



(2R,3R)-2,4-Dimethyl-3-(trimethylsilyloxy)pent-4-enal (73)⁴²: To a

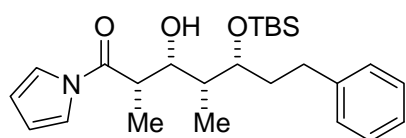
solution of Weinreb amide **61** (0.72 g, 2.78 mmol) in 30 mL THF at -78 °C, *t*Bu₂AlH (3.6 mL, 1.0 M in hexane, 3.6 mmol) was added dropwise. After being stirred for 3 h, the reaction was quenched with aqueous Rochelle salt solution at -78 °C and extracted with Et₂O. The organic extracts were combined and washed with brine, dried and concentrated. The crude oil was purified with flash column (10% ethyl acetate in hexanes), affording 484 mg (88% yield) of the title compound as a colorless oil. ¹H NMR (300 MHz, CDCl₃): δ 0.09 (s, 9H), 1.04 (d, J=6.9 Hz, 3H), 1.70 (s, 3H), 2.45-2.54 (m, 1H), 4.42 (d, J= 5.1 Hz, 1H), 4.92 (s, 1H), 4.98 (s, 1H), 9.67 (d, J= 1.8 Hz, 1H).



(2R,3S,4S,5S)-5-(*tert*-Butyldimethylsilyloxy)-3-hydroxy-2,4,6-

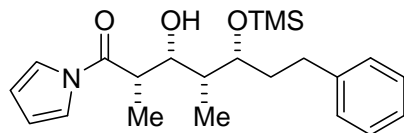
trimethyl-1-(1H-pyrrol-1-yl)heptan-1-one (74): To a solution of aldehyde **72** (36 mg, 0.13 mmol) and enol silane **53** (24 mg, 0.13 mmol) in 2 mL of CH₂Cl₂ was added BF₃·OEt₂ (0.015 mL, 0.16 mmol) at -78 °C. The reaction was then stirred for 1 h at -78 °C, the reaction was quenched with aqueous sat. NaHCO₃ (5 mL) and extracted with ether (3 x 20 mL). The combined organic extracts were washed with brine, dried (Na₂SO₄) and concentrated. The crude product mixture was purified by column chromatography (10% ethyl acetate in hexane) to give 20 mg (43%) of title compound as colorless oil and 20 mg. IR (thin film): 3517, 2957, 2857, 1710, 1468, 1251, 1047 cm⁻¹; [α]_D -4.3 (c 0.35, CHCl₃); ¹H NMR (300

MHz, CDCl₃) δ 7.34 (s, 2H), 6.34 (t, J = 2.4 Hz, 2H), 4.03 (ddd, J = 8.7, 4.2, 2.7 Hz, 1H), 3.59 (dd, J = 5.4, 2.1 Hz, 1H), 3.30 (pentet, J = 6.9 Hz, 1H), 2.83 (d, J = 2.7 Hz, 1H), 1.93-1.77 (m, 2H), 1.39 (d, J = 6.9 Hz, 3 H), 0.94 (d, J = 6.9 Hz, 3H), 0.92-0.90 (m, 12H), 0.88 (d, J = 2.7 Hz, 3H), 0.10 (s, 3H), 0.08 (s, 3H); ¹³C NMR (125 MHz, CDCl₃) δ 174.2, 119.0, 113.6, 80.4, 75.3, 41.5, 37.6, 32.7, 26.1, 19.0, 18.9, 18.4, 14.3, 9.2, -3.5, -4.1; HRMS (ESI) *m/z* calcd for [M+Na]⁺ C₂₀H₃₇NO₃NaSi: 390.2440; found: 390.2411



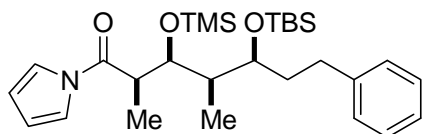
(2*R*,3*S*,4*S*,5*S*)-5-(*tert*-Butyldimethylsilyloxy)-3-hydroxy-4-dimethyl-7-phenyl-1-(1*H*-pyrrol-1-yl)heptan-1-one(65): To a

solution of aldehyde **63** (77 mg, 0.25 mmol) and enol silane **53** (48 mg, 0.25 mmol) in 2 mL of CH₂Cl₂, was added BF₃·OEt₂ (35 mg, 0.31 mmol) at -78 °C. The reaction was then stirred for 1 h at -78 °C. The reaction was quenched with aqueous sat. NaHCO₃ 5 mL and extracted with ether (3 x 20 mL). The combined organic extracts were dried (Na₂SO₄) and concentrated. The crude product mixture was purified by column chromatography (10% ethyl acetate in hexane) to give 76 mg (71%) of title compound as colorless oil. [α]_D +23 (*c* 0.21, CHCl₃); IR (thin film): 3524, 2953, 2857, 1710, 1467, 1251, 1072 cm⁻¹; ¹H NMR (300 MHz, CDCl₃) δ 7.35-7.12 (m, 7H), 6.36 (t, J = 2.4 Hz, 2H), 4.07 (ddd, J = 7.5, 3.3, 1.5 Hz, 1H), 3.89-3.87 (ddd, J = 8.4, 5.1, 2.7 Hz, 1H), 3.36-3.30 (pentet, J = 1.5 Hz, 1H), 3.28 (d, J = 1.5 Hz, 1H), 2.50 (t, J = 7.5 Hz, 2H), 1.86-1.78 (m, 3H), 1.40 (d, J = 6.9 Hz, 3 H), 0.90 (s, 9H), 0.09 (s, 3H), 0.08 (s, 3H); ¹³C NMR (150 MHz, CDCl₃) δ 174.0, 141.5, 128.4, 128.2, 126.0, 119.0, 113.5, 76.8, 75.5, 41.7, 37.5, 36.0, 31.9, 25.8, 18.0, 14.7, 7.0, -3.8, -4.5; HRMS (ESI) *m/z* calcd for [M+Na]⁺ C₂₅H₃₉NO₃SiNa: 452.2597; found:452.2566.



(2R,3S,4S,5S)-3-hydroxy-2,4-dimethyl-7-phenyl-1-(1H-pyrrol-1-yl)-5-(trimethylsilyloxy)heptan-1-one (68): To a solution of aldehyde **67** (66 mg, 0.25 mmol) and enol silane **53**

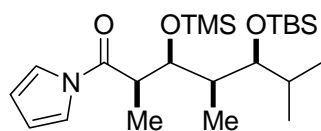
(49 mg, 0.25 mmol) in 2 mL CH₂Cl₂, was added BF₃·OEt₂ (35 mg, 0.313 mmol) at -78 °C. The reaction was then stirred for 1 hour at -78 °C. The reaction was quenched with aqueous saturated NaHCO₃ 5 mL and extracted with ether (3 x 100 mL). The organic layer was washed by brine and dried over Na₂SO₄ and concentrated. The crude product was purified with column chromatography (10% ethyl acetate in hexane) to give 64 mg (66%) of title compound as a white solid. mp 69-70 °C; IR (thin film): 3509, 2954, 1710, 1467, 1250 cm⁻¹; [α]_D +27 (c 0.43, CHCl₃); ¹H NMR (300 MHz, CDCl₃) δ 7.37-7.14 (m, 2H), 6.36 (t, J = 2.4 Hz, 2H), 4.09 (ddd, J = 8.7, 3.0, 1.5 Hz, 1H), 3.91 (ddd, J = 7.8, 5.7, 2.7 Hz, 1H), 3.38 (pentet, J = 7.2 Hz, 1H), 3.33 (d, J = 1.5 Hz, 1H), 2.56-2.50 (m, 2H), 1.89-1.77 (m, 3H), 1.42 (d, J = 6.9 Hz, 3 H), 0.94 (d, J = 7.2 Hz, 3H), 0.17 (s, 9H); ¹³C NMR (125 MHz, CDCl₃) δ 173.9, 141.5, 128.4, 128.2, 126.0, 119.1, 113.5, 77.1, 75.6, 41.9, 37.8, 35.9, 32.1, 14.8, 7.1, 0.6; HRMS (ESI) *m/z* calcd for [M+Na]⁺ C₂₂H₃₃NO₃NaSi: 410.2127; found:410.2123.



(2R,3S,4R,5S)-5-(*t*-Butyldimethylsilyloxy)-2,4-dimethyl-7-phenyl-1-(1H-pyrrol-1-yl)-3-(trimethylsilyloxy) heptan-1-one (64): To a solution of aldehyde **63** (30 mg, 0.1 mmol)

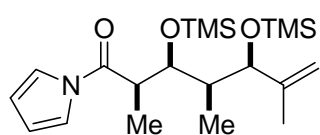
and enol silane **53** (58mg, 0.3 mmol) in 1 mL of THF, was added 0.01 mL tetrabutylammonium *p*-nitrophenoxide (2 M in THF) at -78 °C. The reaction was then stirred for overnight at -78 °C. The reaction was quenched with ether 5 mL and filtered through a plug of silica gel. The crude

product was purified by column chromatography (3% ethyl acetate in hexane) to give 40 mg (80%) of title compound as colorless oil. $[\alpha]_D +12$ (c 0.85, CHCl_3); IR (thin film): 2954, 2857, 1711, 1466, 1250, 1072 cm^{-1} ; ^1H NMR (300 MHz, CDCl_3) δ 7.37-7.21 (m, 7H), 6.32 (t, $J = 2.4$ Hz, 2H), 4.21 (dd, $J = 5.1, 3.6$ Hz, 1H), 3.71 (dt, $J = 7.5, 5.2$ Hz, 1H), 3.40 (pentet, $J = 6.9$ Hz, 1H), 2.64 (t, $J = 8.7$ Hz, 2H), 1.83-1.78 (m, 3H), 1.32 (d, $J = 6.9$ Hz, 3 H), 0.99- 0.89 (m, 12H), 0.13 (s, 9H), 0.11 (s, 3H), 0.08 (s, 3H); ^{13}C NMR (125 MHz, CDCl_3) δ 173.2, 142.9, 128.5, 128.5 125.7, 119.1, 113.3, 74.2, 73.3, 42.9, 40.9, 36.2, 26.0, 18.2, 14.8, 11.2, 0.8, $-4.0, -4.3$; HRMS (ESI) m/z calcd for $[\text{M}+\text{Na}]^+ \text{C}_{28}\text{H}_{47}\text{NO}_3\text{Na}$: 524.2992; found:524.3037.



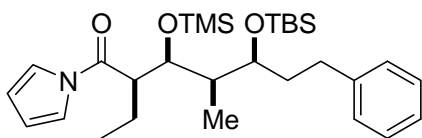
(2R,3S,4R,5S)-5-(tert-Butyldimethylsilyloxy)-2,4,6-trimethyl-1-(1H-pyrrol-1-yl)-3-(trimethylsilyloxy)heptan-1-one (78): To a solution of aldehyde **72** (24 mg, 0.1 mmol) and enol silane **53** (96 mg, 0.5 mmol) in 1 mL THF, was added 0.01 mL tetrabutylammonium *p*-nitrophenoxide (2 M in THF) at -88 °C. The reaction was then stirred for 6 h at -88 °C. The reaction was quenched with ether 5 mL and filtered through a plug of silica gel. The crude product was purified by column chromatography (3% ethyl acetate in hexane) to give 27 mg (61%) of title compound as colorless oil. IR (thin film): 2957, 2928, 1714, 1466, 1251, 1052 cm^{-1} ; $[\alpha]_D -20.9$ (c 1.04, CHCl_3); ^1H NMR (300 MHz, CDCl_3) δ 7.36-7.35 (m, 2H), 6.33 (t, $J = 2.4$ Hz, 2H), 4.11 (dd, $J = 7.8, 2.7$ Hz, 1H), 3.40 (dd, $J = 8.1, 2.1$ Hz, 1H), 3.35-3.30 (pentet, $J = 7.5$ Hz, 1H), 1.97-1.91 (m, 1H), 1.67-1.60 (m, 1H), 1.32 (d, $J = 6.9$ Hz, 3 H), 0.97 (d, $J = 6.9$ Hz, 3H), 0.91-0.88 (m, 12H), 0.81 (d, $J = 6.9$ Hz, 3H), 0.18 (s, 9H), 0.09 (s, 3H), 0.06 (s, 3H); ^{13}C NMR (125 MHz, CDCl_3) δ

173.3, 119.0, 113.4, 77.5, 74.9, 43.0, 40.8, 30.7, 26.3, 21.2, 18.6, 15.7, 15.1, 11.5, 0.9, -3.1, -3.4;
HRMS (EI) m/z calcd for ($M^+ - CH_3$) $C_{22}H_{42}NO_3Si_2$: 424.2703; found: 424.2700.



(2R,3S,4S,5R)-2,4,6-trimethyl-1-(1H-pyrrol-1-yl)-3,5-

bis(trimethylsilyloxy)hept-6-en-1-one (83): To a solution of aldehyde **73** (26 mg, 0.11 mmol) and enol silane **53** (96 mg, 0.50 mmol) in 1 mL THF, was added 0.01 mL tetrabutylammonium *p*-nitrophenoxide (2 M in THF) at -70 °C. The reaction was then stirred for 6 h at -70 °C. The reaction was quenched with ether 5 mL and filtered through a plug of silica gel. The crude product was purified by column chromatography (3% ethyl acetate in hexane) to give 38 mg (79%) of title compound as colorless oil. IR (thin film): 2959, 1713, 1466, 1250, 1071 cm^{-1} ; $[\alpha]_D -19$ (c 0.25, $CHCl_3$); 1H NMR (300 MHz, $CDCl_3$) δ 7.32 (s, 2H), 6.31 (t, $J = 2.4$ Hz, 2H), 4.98 (t, $J = 1.8$ Hz, 1H), 4.94 (s, 1H), 3.99 (dd, $J = 8.7, 1.5$ Hz, 1H), 3.93 (d, $J = 9$ Hz, 1H), 3.30 (dq, $J = 8.7, 6.9$ Hz, 1H), 1.64 (s, 3H), 1.29 (d, $J = 6.9$ Hz, 3H), 0.90 (d, $J = 6.6$ Hz, 3 H), 0.17 (s, 9H), 0.08 (s, 9H); ^{13}C NMR (125 MHz, $CDCl_3$) δ 173.2, 146.6, 119.0, 114.3, 113.4, 79.0, 74.1, 43.2, 40.6, 16.4, 16.0, 9.9, 1.1, 0.2; HRMS (ESI) m/z calcd for $[M+Na]^+$ $C_{20}H_{37}NO_3Si_2Na$: 418.2210; found: 418.2190.



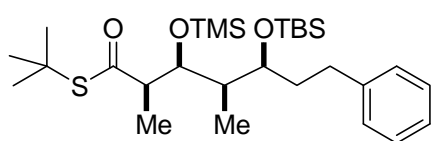
(2R,3S,4R,5S)-5-(*t*-Butyldimethylsilyloxy)-2-ethyl-4- methyl-

7-phenyl-1-(1H-pyrrol-1-yl)-3-(trimethylsilyloxy) heptan-1-

one (86) : To a solution of aldehyde **63** (30 mg, 0.10 mmol)

and enol silane **86** (96 mg, 0.5 mmol) in 1 mL of THF, was added 0.01 mL tetrabutylammonium *p*-nitrophenoxide (2 M in THF) at -78 °C. The reaction was then stirred for 6 h at -78 °C. The reaction was quenched with ether 5 mL and filtered through a plug of silica gel. The crude

product was purified by column chromatography (3% ethyl acetate in hexane) to give 38 mg (74%) of title compound as colorless oil. $[\alpha]_D +21.2$ (c 1.02, CHCl_3); IR (thin film): 2955, 2829, 1708, 1465, 1252, 838 cm^{-1} ; ^1H NMR (300 MHz, CDCl_3) δ 7.40-7.20 (m, 7H), 6.33 (t, J = 2.4 Hz, 2H), 4.17 (dd, J = 8.1, 2.4 Hz, 1H), 3.66 (m, 1H), 3.24 (m, 1H), 2.64 (qd, J = 11.4, 5.7 Hz, 2H), 1.93-1.80 (m, 4H), 1.70-1.65 (m, 1 H), 0.93- 0.89 (m, 15H), 0.14 (s, 9H), 0.09 (s, 3H), 0.04 (s, 3H); ^{13}C NMR (75 MHz, CDCl_3) δ 172.9, 143.0, 128.5, 128.4, 125.6, 119.1, 113.4, 74.2, 73.0, 50.6, 41.0, 36.5, 29.3, 26.0, 23.6, 18.2, 11.8, 10.9, 0.9, -4.1, -4.4; HRMS (ESI) m/z calcd for $[\text{M}+\text{Na}]^+ \text{C}_{28}\text{H}_{47}\text{NO}_3\text{Na}$: 538.3149; found:538.3198.

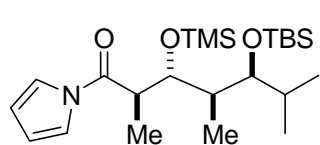


**(2R,3S,4R,5S)-S-*t*-Butyl 5-(*tert*-Butyldimethylsilyloxy) -
2,4-dimethyl-7-phenyl-3-(trimethylsilyloxy)**

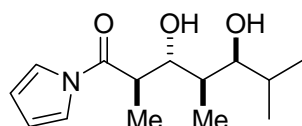
heptanethioate (89) : To a solution of aldehyde **63** (61 mg,

0.2 mmol) and enol silane **70** (132 mg, 0.6 mmol) in 2 mL of THF, was added 0.02 mL of tetrabutylammonium *p*-methoxyphenoxide solution (2 M in THF) at -70 °C. The reaction was then stirred for 5 h at -70 °C. The reaction was quenched with ether (5 mL) and filtered through a plug of silica gel. The crude product was purified by column chromatography (3% ethyl acetate in hexane) to give 47 mg (45%) of title compound as colorless oil. IR (thin film): 2956, 2857, 1675, 1455, 1252, 1033 cm^{-1} ; $[\alpha]_D -6.2$ (c 0.39, CHCl_3); ^1H NMR (300 MHz, CDCl_3) δ 7.33-7.19 (m, 5H), 4.02 (dd, J = 6.6, 2.1 Hz, 1H), 3.66 -3.63 (dt, J = 2.4, 2.1 Hz, 1H), 2.84-2.79 (pentet, J = 6.9 Hz, 1H) 2.64 -2.56 (m, 1H), 1.88-1.74 (m, 3H), 1.46 (s, 9H), 1.16 (d, J = 6.9 Hz, 3 H), 0.96- 0.94 (m, 12H), 0.10 (s, 9H), 0.08 (s, 3H), 0.05 (s, 3H); ^{13}C NMR (75 MHz, CDCl_3) δ 203.1, 142.9, 128.4, 128.4, 125.6, 74.2, 72.9, 52.7, 47.8, 40.8, 36.6, 29.8, 26.0, 18.2, 14.1, 10.8,

0.88, -4.0, -4.3; HRMS (ESI) m/z calcd for $[M+Na]^+$ $C_{28}H_{52}O_3NaSi_2S$: 547.3073; found:547.3068.

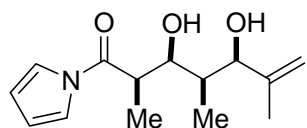


(2R,3R,4R,5S)-5-(*t*-Butyldimethylsilyloxy)-2,4,6-trimethyl-1-(1H-pyrrol-1-yl)-3-(trimethylsilyloxy)heptan-1-one (79): To a solution of aldehyde **72** (24 mg, 0.10 mmol) and enol silane **53** (98 mg, 0.50 mmol) in 1 mL of DMF, was added 0.01 mL lithium phenoxide (2 M in THF) at $-45\text{ }^\circ\text{C}$. The reaction was then stirred for 5 h at $-70\text{ }^\circ\text{C}$. The reaction was quenched with ether (5 mL) and filtered through a plug of silica gel. The crude product was purified with column chromatography (3% ethyl acetate in hexane) to give 34 mg (78%) of title compound as colorless oil. IR (thin film): 2957, 1716, 1467, 1252, 1071 cm^{-1} ; $[\alpha]_D -26.3$ (c 1.41, CHCl_3); ^1H NMR (300 MHz, CDCl_3) δ 7.35 (s, 2H), 6.29 (t, $J = 2.4$ Hz, 2H), 3.94 (dd, $J = 9.0, 3.0$ Hz, 1H), 3.64 (dd, $J = 6.3, 2.1$ Hz, 1H), 3.47-3.37 (dq, $J = 8.7, 6.9$ Hz, 1H), 1.98-1.87 (m, 2H), 1.22 (d, $J = 6.9$ Hz, 3 H), 1.02 (d, $J = 6.9$ Hz, 3H), 0.96-0.89 (m, 15H), 0.09 (s, 3H), 0.07 (s, 3H), -0.07 (s, 9H); ^{13}C NMR (75 MHz, CDCl_3) δ 174.2, 119.5, 112.8, 78.4, 76.8, 43.1, 41.2, 32.7, 26.3, 20.1, 18.6, 16.2, 14.2, 13.9, 0.19, -3.3, -3.4; HRMS (ESI) m/z calcd for $[M+Na]^+$ $C_{23}H_{45}NO_3Si_2Na$: 462.2836; found:462.2800.



(2R,3R,4R,5S)-3,5-Dihydroxy-2,4,6-trimethyl-1-(1H-pyrrol-1-yl)heptan-1-one (81): To a solution of compound **79** (45 mg, 0.1 mmol) in 2 mL of THF, was added TFA (0.011 mL, 0.15 mmol dissolved in 0.5 mL H_2O) at $0\text{ }^\circ\text{C}$. The reaction was then stirred for overnight at $0\text{ }^\circ\text{C}$. The reaction was quenched with aqueous saturated NaHCO_3 1 mL and filtered through a plug of silica gel and concentrated and dissolved in 2 mL CH_3CN . To this solution was added 2 drops of 48% aqueous HF at $0\text{ }^\circ\text{C}$, the reaction

was stirred for 3 h at 0 °C. The reaction was quenched with aqueous saturated NaHCO₃ 0.5 mL and filtered through a plug of silica gel and concentrated. The crude product was purified with column chromatography (20% ethyl acetate in hexane) to give 22 mg (88%) of title compound as a white wax. IR (thin film): 3374, 2964, 2933, 1707, 1283, 1071 cm⁻¹; [α]_D -40 (c 0.73, CHCl₃); ¹H NMR (300 MHz, CDCl₃) δ 7.38 (t, J = 2.4 Hz, 2H), 6.35 (t, J = 2.4 Hz, 2H), 3.96 (td, J = 8.1, 4.2 Hz, 1H), 3.60 (dt, J = 9.6, 2.1 Hz, 1H), 3.49 (pentet, J = 7.2 Hz, 1H), 3.37 (d, J = 7.5 Hz, 1H), 2.78 (d, J = 3.0 Hz, 1H), 1.95 (qdd, J = 6.9, 4.5, 1.8 Hz, 1H), 1.75 (m, 1H), 1.33 (d, J = 8.4 Hz, 3H), 1.07 (d, J = 5.7 Hz, 3H), 1.05 (d, J = 6.3 Hz, 3H), 0.86 (d, J = 6.6 Hz, 3H); ¹³C NMR (75 MHz, CDCl₃) δ 174.4, 119.2, 113.6, 78.2, 76.8, 41.2, 35.1, 31.2, 19.8, 18.9, 15.5, 10.4; HRMS (ESI) *m/z* calcd for [M+Na]⁺ C₁₄H₂₃NO₃Na: 276.1576; found:276.1562.



(2R,3S,4S,5R)-3,5-Dihydroxy-2,4,6-trimethyl-1-(1H-pyrrol-1-yl)hept-6-en-1-one (84): To a solution of compound **83** (27 mg, 0.061

mmol) in 2 mL THF, was added 2 drops of TFA at 0 °C. The reaction was then stirred for 8 h at room temperature. The reaction was quenched with aqueous saturated NaHCO₃ 0.5 mL and filtered through a plug silica gel and concentrated. The crude product was then purified with column chromatography (30% ethyl acetate in hexane) to give 14 mg (91%) of title compound as a white solid. [α]_D -42 (c 0.63, CHCl₃); mp 101 °C ; IR (thin film): 3392, 2974, 1705, 1467, 1275 cm⁻¹; ¹H NMR (300 MHz, CDCl₃) δ 7.37 (s, 2H), 6.33 (t, J = 2.4 Hz, 2H), 5.00 (d, J = 0.3 Hz, 1H), 4.94 (s, 1H), 4.30 (br, 1H), 4.22 (dd, J = 2.7, 1.2 Hz, 1H), 3.39-3.29 (pentet, J = 7.5 Hz, 1H), 1.94-1.81 (m, 1H), 1.67 (s, 3H), 1.44 (d, J = 6.9 Hz, 3 H), 0.85 (d, J = 6.9 Hz, 3H); ¹³C NMR (75 MHz, CDCl₃) δ 173.5, 145.9, 119.1, 113.6, 110.3, 78.8, 76.3, 42.0, 36.7, 19.4, 15.0, 5.7; HRMS (ESI) *m/z* calcd for [M+Na]⁺ C₁₄H₂₁NO₃Na: 251.1521; found:251.1521.

2.0 EFFORTS TOWARDS THE TOTAL SYNTHESIS OF AMPHIDINOLIDE H

2.1 INTRODUCTION

2.1.1 The Amphidinolides

2.1.1.1 Isolation

Dinoflagellates *Amphidinium* sp., which are symbionts of Okinawan marine flatworms *Amphiscolops* sp, produce a series of macrolide natural products, called amphidinolides.⁴³⁻⁴⁶ Due to their unique structures and potent cytotoxicity, amphidinolides have been attractive targets for total synthesis.⁴⁷⁻⁶⁷ Amphidinolide H1 is one of the most structurally interesting and biologically significant molecules in this class of macrolides. Amphidinolide H1 was isolated from the Y-72 strain of cultured dinoflagellate *Amphidinium* sp by the Kobayashi group in 1991, as well as amphidinolide G1.⁴⁴ In 2002, the Kobayashi group continued to discover four derivatives (amphidinolides H2, H3, H4, H5, H6) of amphidinolide H and two derivatives (amphidinolides G2, G3) of amphidinolide G from the dinoflagellate *Amphidinium* sp. (Y-42 strain) was isolated from an acoel flatworm *Amphiscolops* sp (Figure 11).⁶⁸

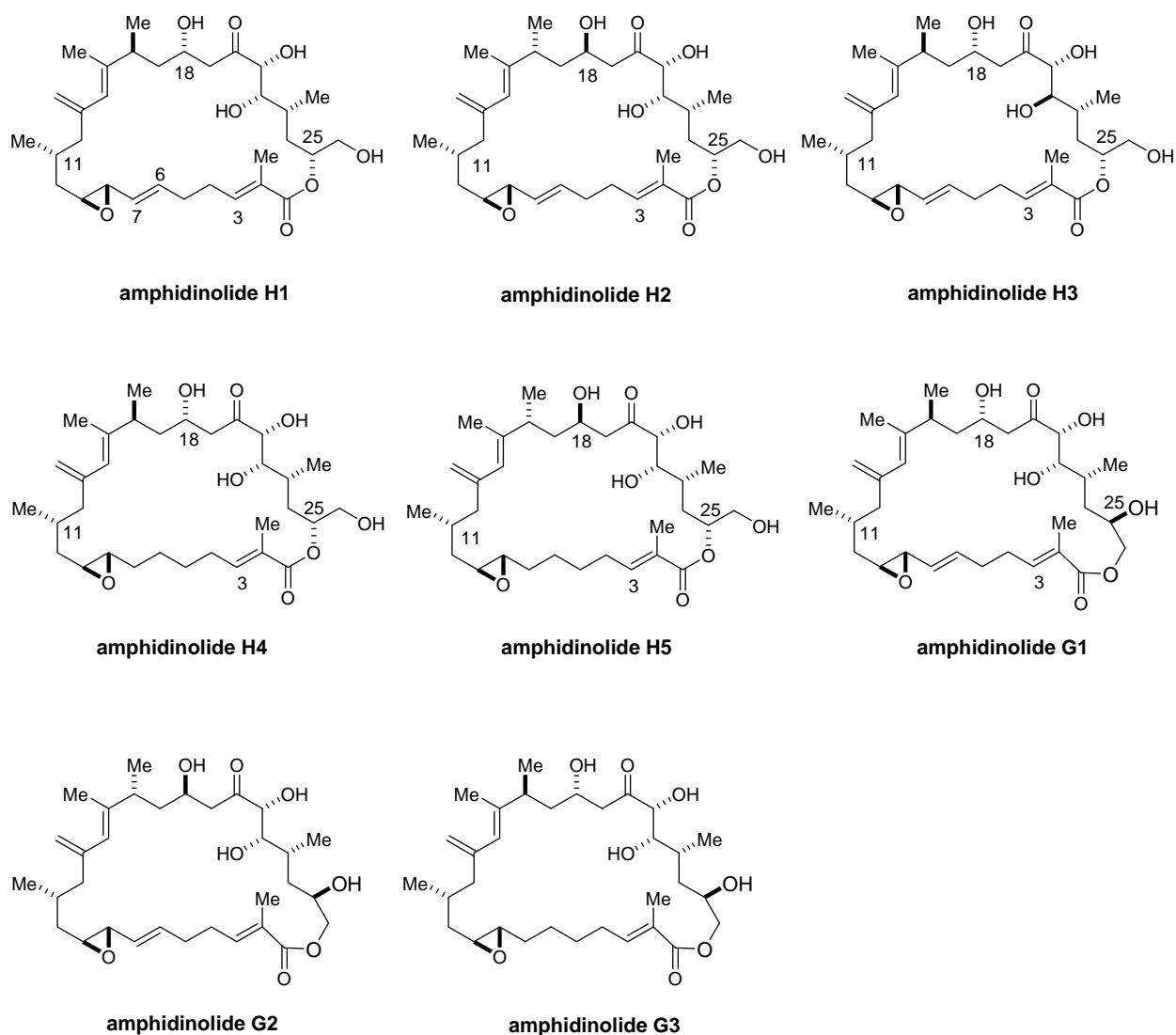


Figure 11. Amphidinolide H and G family

2.1.1.2 Structural Features and Biological Activity

The absolute stereochemistry of amphidinolides G and H was determined by a single-crystal X-ray diffraction analysis and interconversion between each other by the Kobayashi group in 2000 (Figure 12).⁴⁵ Amphidinolides G and H are 27- and 26-membered macrolides, respectively, with nine stereogenic centers and a unique allylic epoxide moiety. The final X-ray structure of amphidinolide H1 shows a rectangular shape that was bridged in across the

macrolactone by an intramolecular hydrogen bond between C₂₁-OH and the epoxide oxygen (O₃). The intramolecular hydrogen bond caused a significant distortion on the epoxide. Specifically the C₈-O bond (1.470 Å) is much longer than its C₉-O counterpart (1.448 Å). Through another intramolecular hydrogen bond between the C₂₂-OH and the oxygen atom at C₁₈, an envelope-boat-shaped eight-membered ring was constructed. In the X-ray structure the *S-cis* diene portion at C₁₅-C₁₄-C₁₃-C₂₉ was revealed to be twisted [torsion angle, $-35.6(5)^\circ$], resulted in the diene moiety non-conjugated in the natural product.⁴⁵

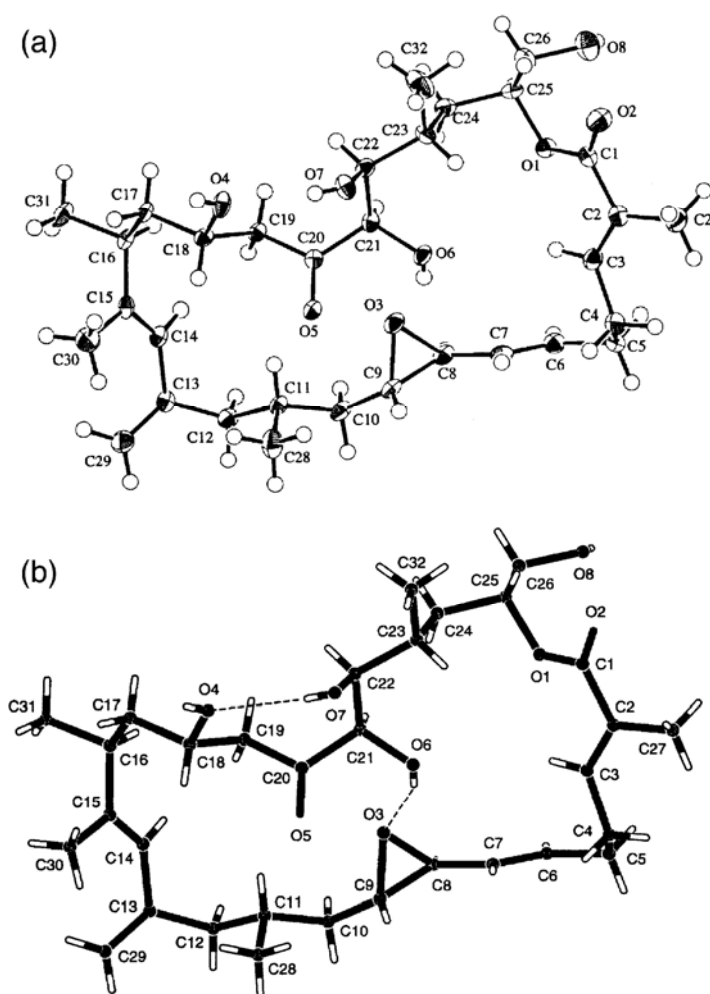


Figure 12. X-ray Crystal structure of amphidinolide H1

Amphidinolide H1 exhibited extremely strong cytotoxic activities against L1210 murine leukemia cells in vitro with an IC₅₀ value of 0.48 ng/mL and KB human epidermoid carcinoma cells in vitro with an IC₅₀ value of 0.52 ng/mL, respectively.^{43,44,46} Amphidinolide H1 was known to disrupt the actin organization in the cells, and the polymerization/depolymerization assay using purified actin indicated that amphidinolide H1 (8) stimulated actin polymerization and stabilized F-actin. The MALDI-TOF-MS analysis⁶⁹ and analysis with the halo assay using the yeast harboring site-directed mutagenized actin revealed that the covalent binding of amphidinolide H1 (8) to actin and the binding site was Tyr200 of actin subdomain 4. Impressive SAR studies performed with the naturally occurring amphidinolide derivatives, amphidinolide B1, B2, B3, B4, B5, B6, B7, D, H1, H2, H3, H4, H5, G1, G2, and G3 demonstrated that the sensitive *S-cis*-diene, the ketone at C₂₀, as well as the allylic epoxide are mandatory structural elements for high biological activity.^{70,71}

2.1.2 Previous Approaches to the Total Synthesis of Amphidinolide H1

In 1998, Chakraborty reported the first approach towards the total synthesis of amphidinolide H1 (Figure 13).⁷² The left fragment **92** was constructed by coupling the *E*- α,β -unsaturated aldehyde **96** and the functionalized sulfone unit **97**. The lower fragment, triphenylphosphine salt **93**, then underwent a Wittig reaction to give a mixture of olefins (*trans:cis* = 55:45) which was separated by preparative TLC to furnish the desired C₁-C₁₈ fragment **90**. Methyl ketone **91** was formed from aldehyde **95** by application of Evans' aldol reaction and the C₁₆- tertiary alcohol center was set by Seebach alkylation methodology.

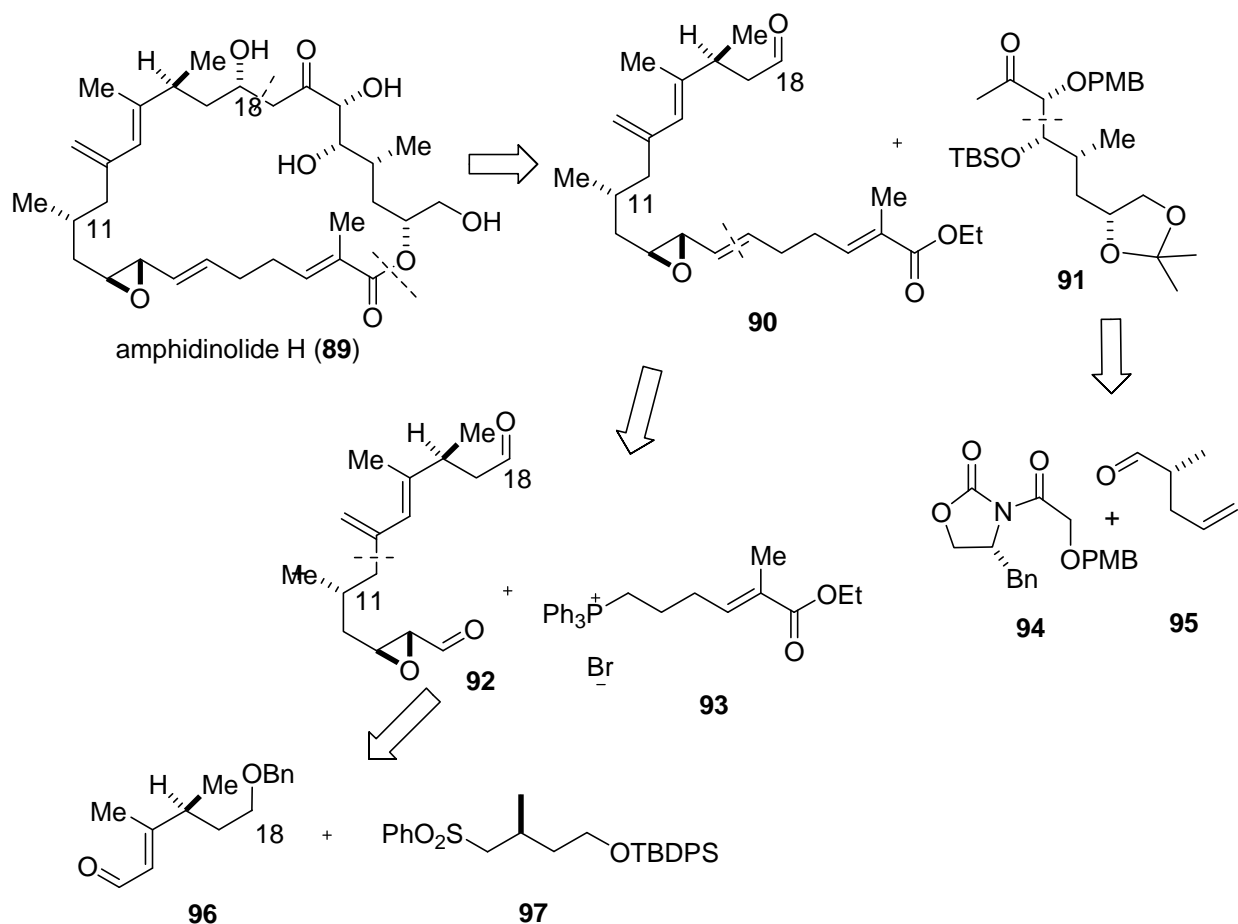


Figure 13. Chakraborty's approach to the synthesis of fragments of amphidinolide H1

In 2002, amphidinolide H2 was isolated by the Kobayashi group. As an amphidinolide H type macrolide, amphidinolide H2 has been assigned as a C₁₆- and C₁₈- epimer of amphidinolide H1 (Figure 14).⁶⁸ In 2005 and 2006, Kalesse proposed a retrosynthesis of amphidinolide H2 and synthesized fragments **99** and **100** (Figure 14).^{73,74} Kalesse proposed an aldol coupling between methyl ketone **100** and aldehyde **99**. It was further planned to construct the *S-cis*-diene moiety through an alkene–alkyne metathesis, followed by a macrolactonization, which should establish the carbon skeleton of amphidinolide H2. A vinylogous Mukaiyama aldol reaction was used to construct the C₂₃-C₂₄ bond using enolsilane **103** to add to 2,3-*O*-isopropylidene-*L*-

glyceraldehyde **104** with a substoichiometric amount of the sterically hindered Lewis acid tris(pentafluorophenyl)borane to afford fragment **102** in good yield and diastereoselectivity. However, the aldol coupling between methyl ketone **100** and aldehyde **99** turned out to be problematic. Only poor stereoselectivities were observed under a variety of conditions.

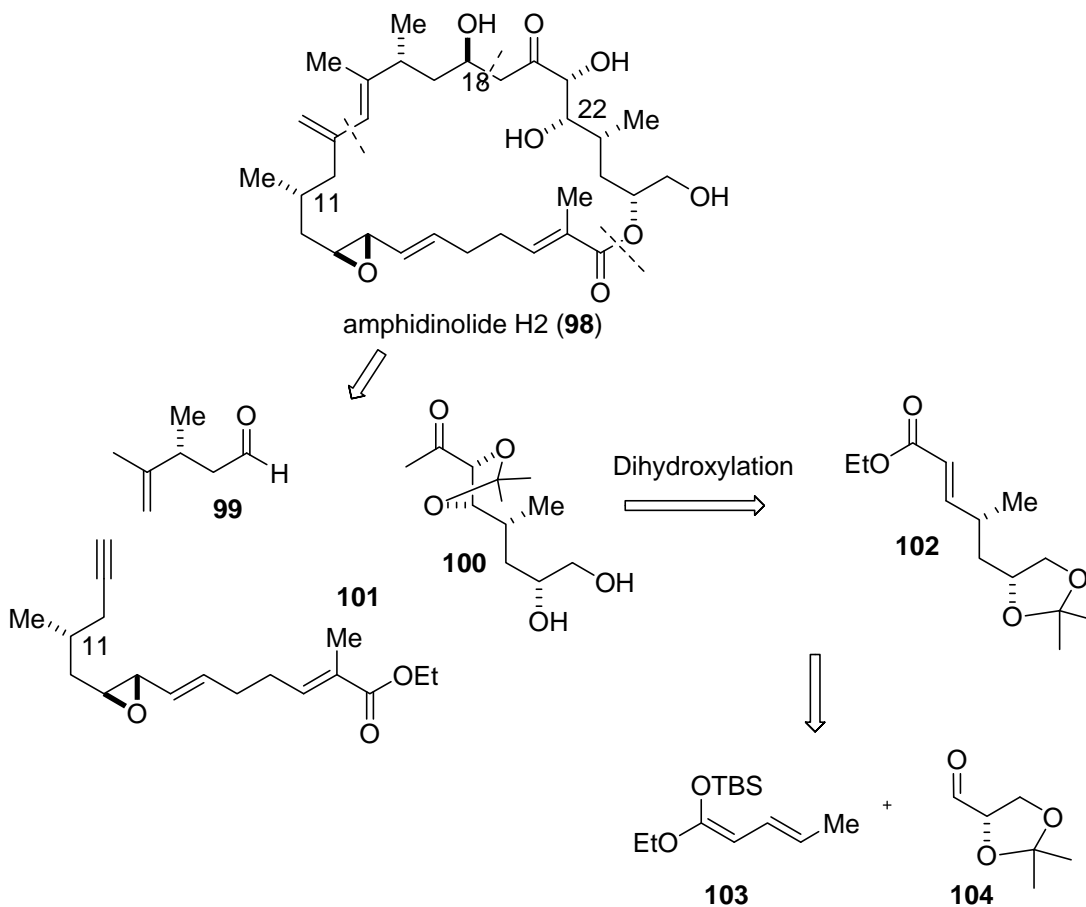


Figure 14. Kalesse's approach to the synthesis of fragments of amphidinolide H2

Murga's approach proceeded from the right fragment **105** that was prepared from lactone **109**. Enolation of **109** followed by methylation afforded **108** in 80% yield and 92:8 dr (Figure 15).⁷⁵ Reduction of **108** with DIBAL gave an aldehyde, which was immediately subjected to Wittig olefination. The resulting ester **107** was then submitted to a Sharpless asymmetric

dihydroxylation to afford triol **106** as a single stereoisomer. Protecting vicinal diol as an acetonide, followed by silylation of the remaining free hydroxyl group, furnished **105**, with all the stereogenic centers already in place. After hydrolysis and Weinreb amide formation, the methyl ketone **105** was achieved by methyl Grignard addition.

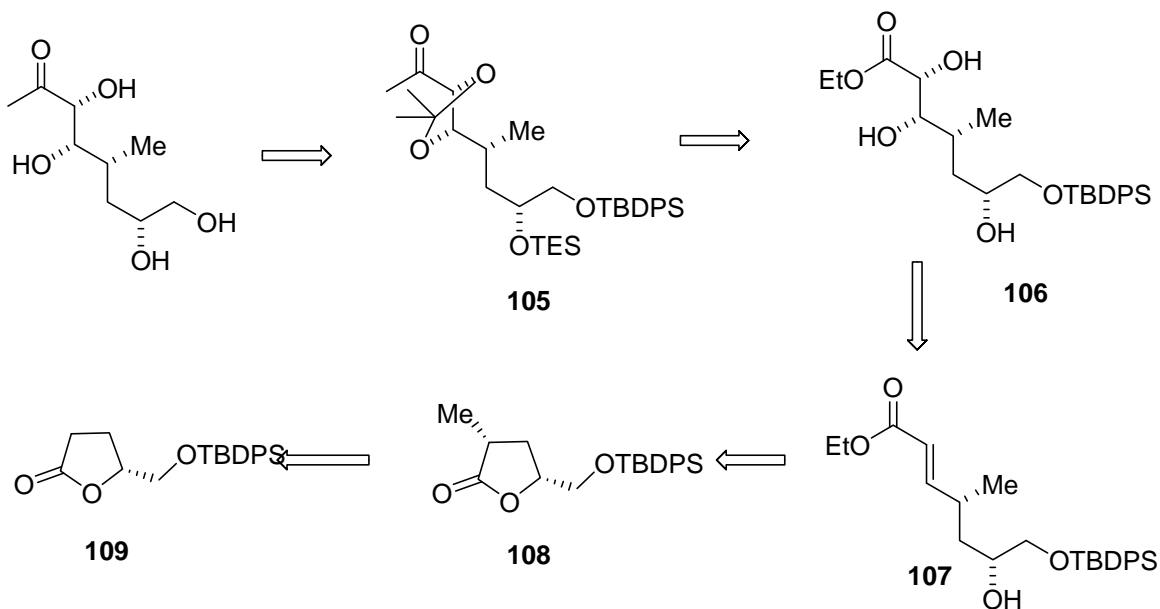


Figure 15. Murga's approach to amphidinolide H1 fragments

In Murga's publication in 2007, described an efficient synthetic route to the C₃-C₁₈ subunit **110** of amphidinolides G and H (Figure 16).⁷⁶ This paper demonstrated that the 1,3-diene moiety **116** can be assembled by an S_N2' reaction of an allenic acetate **117**. A Negishi-type cross-coupling between a vinyl iodide **116** and an alkylzinc species **115** was then used to assemble the left fragment **114**, which was combined with bottom fragment **113** by a lithiation/nucleophilic addition sequence to provide ketone **112**. Furthermore, they have shown that the allylic epoxide moiety of amphidinolides H was effectively synthesized from the protected *anti* mesylate **111**.

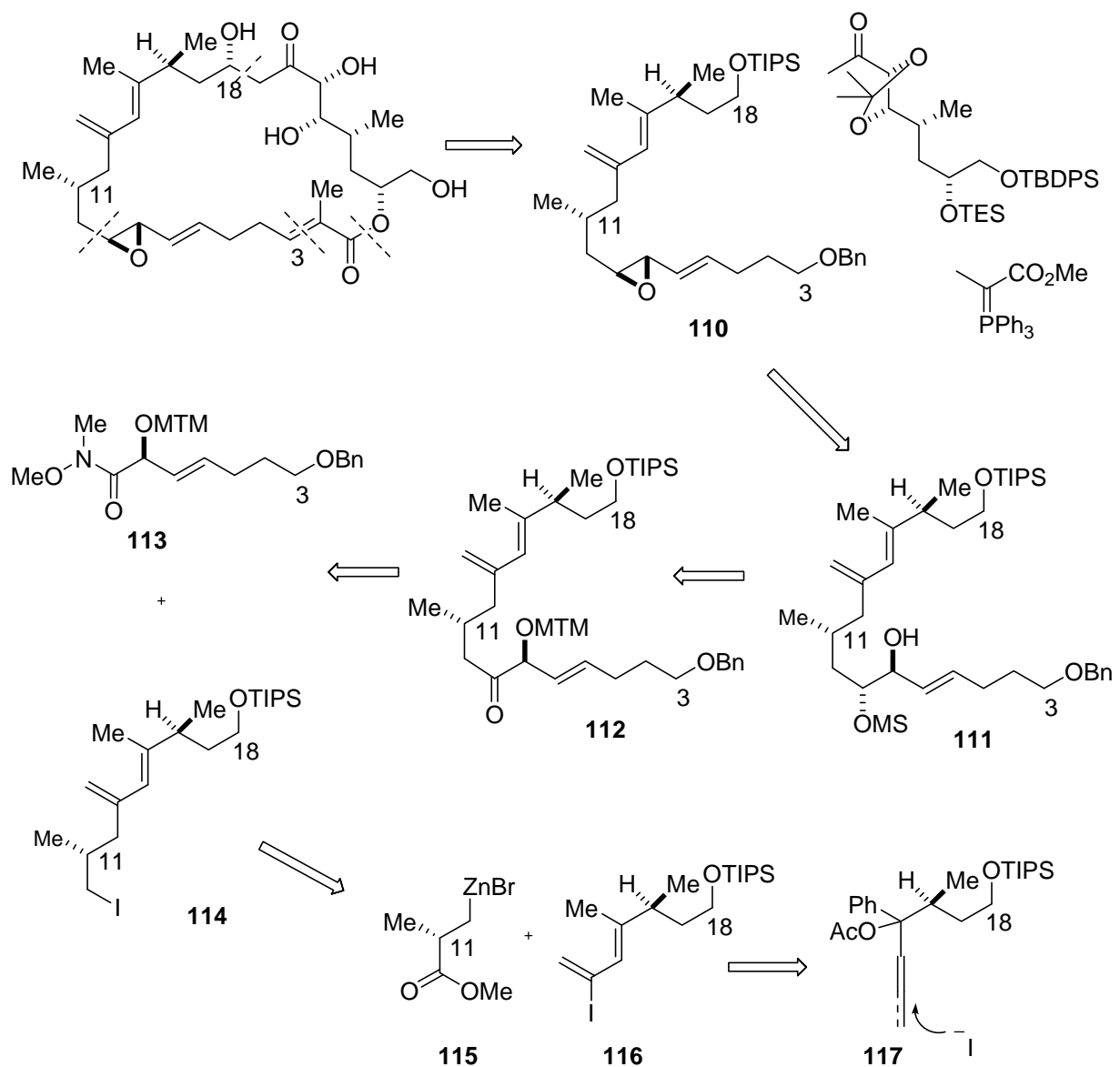


Figure 16. Crews's approach to amphidinolide H1 fragments

In the same year, the Zhao group has reported a nearly finished synthesis route of amphidinolide H1 (Figure 17).^{77,78} The core structure was completed by an intramolecular ring closing metathesis (RCM) reaction from alkene **118**, which was prepared by employing a highly diastereoselective aldol reaction between the aldehyde **119** and MOM protected methyl ketone **120**. The aldehyde **119** was assembled through a Stille coupling of fragments **121** and **122**. The

Methyl ketone **120** was achieved via Mitsunobu esterification from the bottom fragment **123** and the right fragment **124**. Murga's approach was employed to synthesize the right fragment **124** which was prepared from commercially available starting material **109** (Figure 15). However, the final deprotection of the MOM groups failed to achieve the completion of amphidinolide H1.

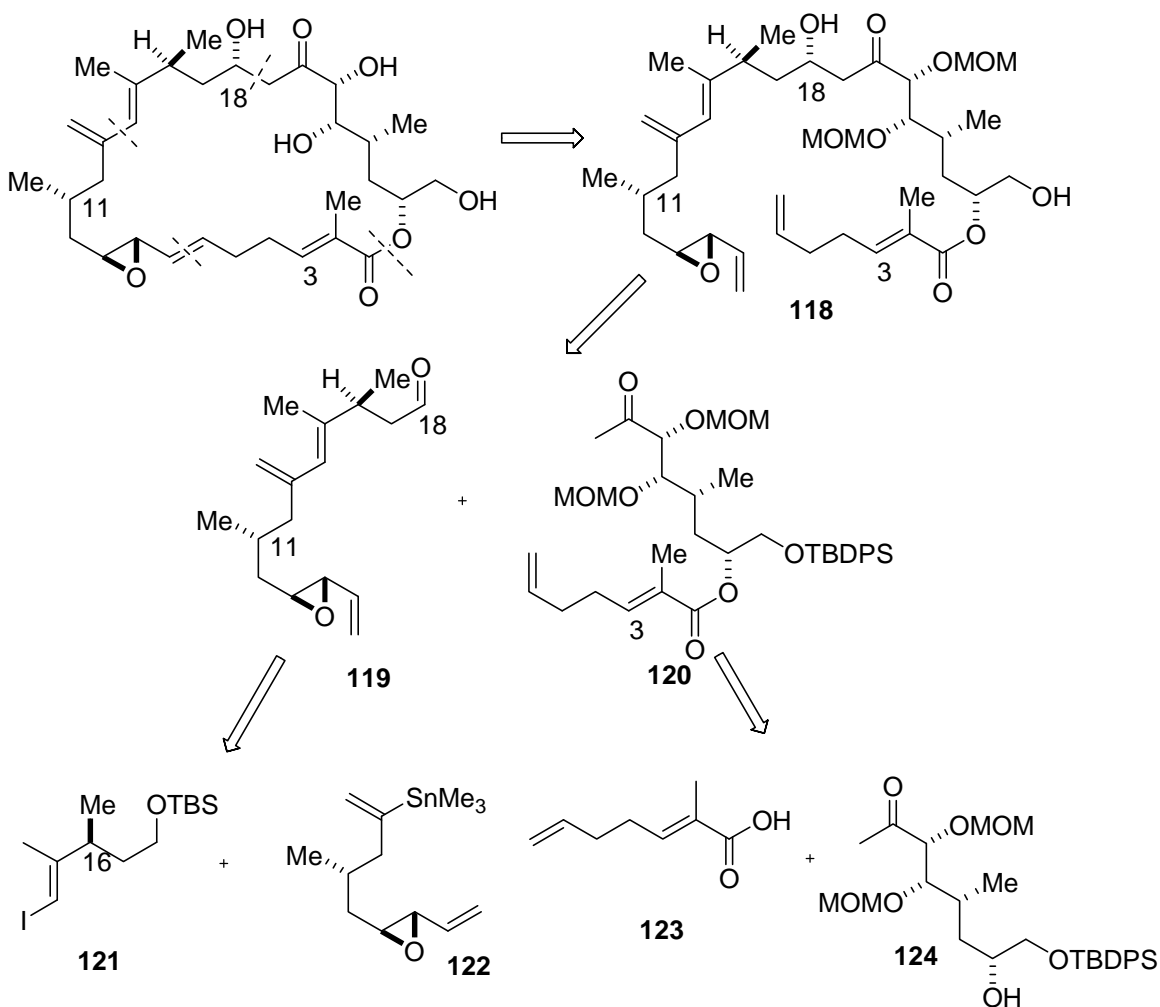


Figure 17. Zhao's approach to amphidinolide H1 fragments.

Finally, the first total synthesis of amphidinolide H1 was achieved in the Fürstner group in 2007 (Figure 18).^{49,79} The retrosynthesis was similar to the precedents of amphidinolid H: the

basic skeleton was assembled from four building blocks A – D by esterification, aldol reaction, Pd-catalyzed Stille coupling reaction, and olefin metathesis. The order of these crucial steps is the key to successfully accomplishing this complex molecule synthesis. The vinyl iodide fragment **126** was prepared through a multistep process from the itaconic acid monoester **130**, which delivered the C₁₆ methyl stereocenter through an asymmetric hydrogenation at C₁₆ alkene. The synthesis of C₇-C₁₃ fragment **128** commenced with chiral pool (*S*)-citronellal. Chakraborty's approach was then employed to deliver methyl ketone **127** by an Evans aldol reaction. The ultimate successful route relied on the early installation of the unsaturated ester, which was accomplished by esterification of alcohol **127** with acid **131** to give **129** as a fully functional surrogate of the 'south-eastern' part of amphidinolide H1. The fragments **126** and **129** were then coupled by an LDA-mediated aldol reaction to form an exclusive *R* C₁₈ hydroxyl functionality. Followed by a Stille-Migita coupling reaction with stannane **128** under the newly developed condition, the RCM precursor **125** was provided. The vinyl oxirane **125** proceeded a productive RCM reaction to form the required *E* isomer only, which eventually underwent a global deprotection to give the first total synthesis of amphidinolide H1.

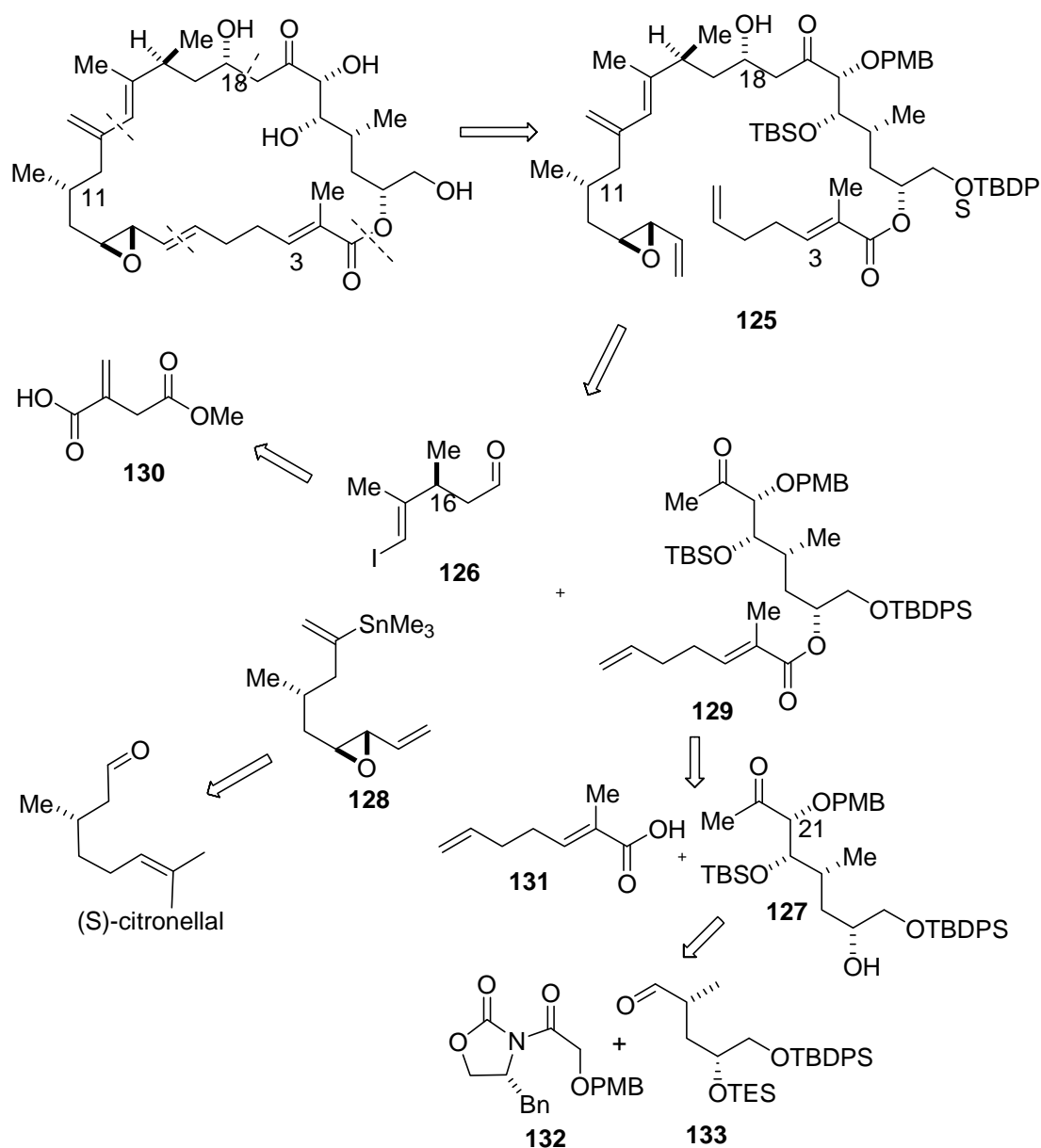


Figure 18. Fürstner's total synthesis of amphidinolide H1

In 2006, our group reported a catalytic asymmetric approach towards the total synthesis of amphidinolide B1 which has a very similar structure as amphidinolide H1 (Figure 19). The top fragment **137** and the left fragment **136** were coupled by an efficient Suzuki coupling to form sterically hindered diene and deliver C₇-C₂₀ subunit **135** in 80% yield. Catalytic asymmetric acyl

halidealdehyde cyclocondensation (AAC) methodology has been applied to efficiently generate the C₁₁- and the C₁₈- stereocenters in the requisite fragments **136** and **137** through β -lactones **138** and **139** respectively.

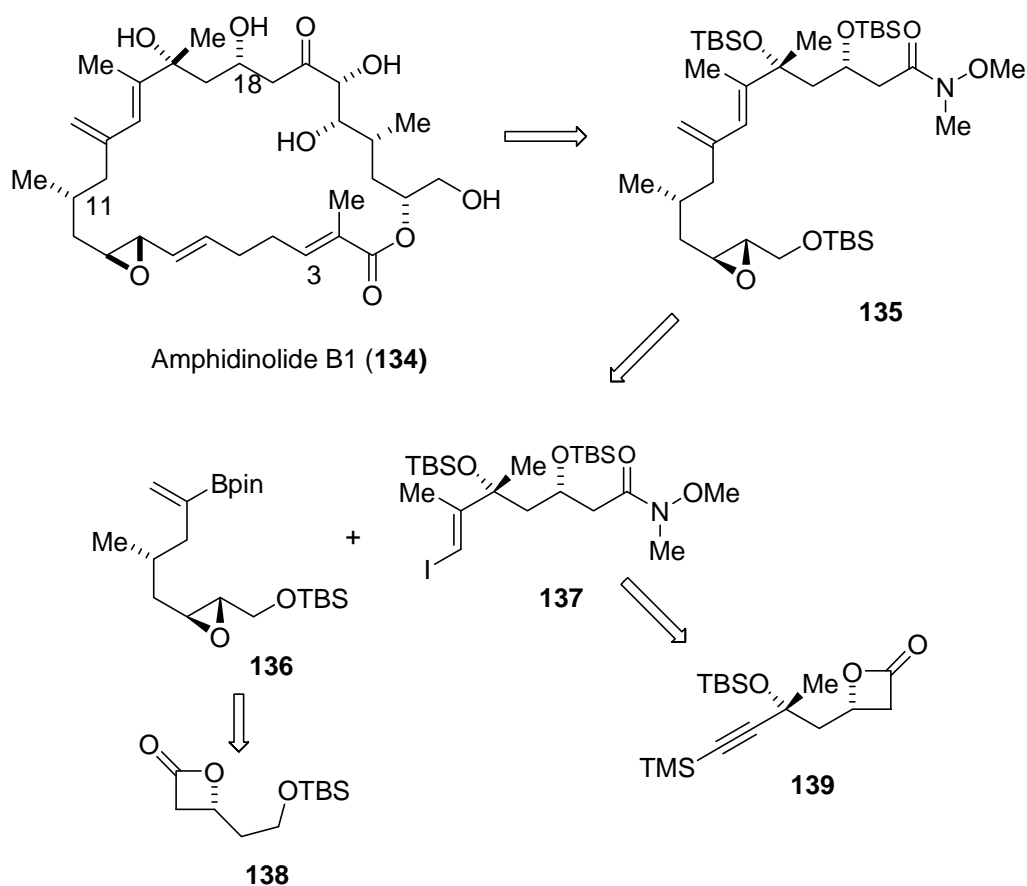


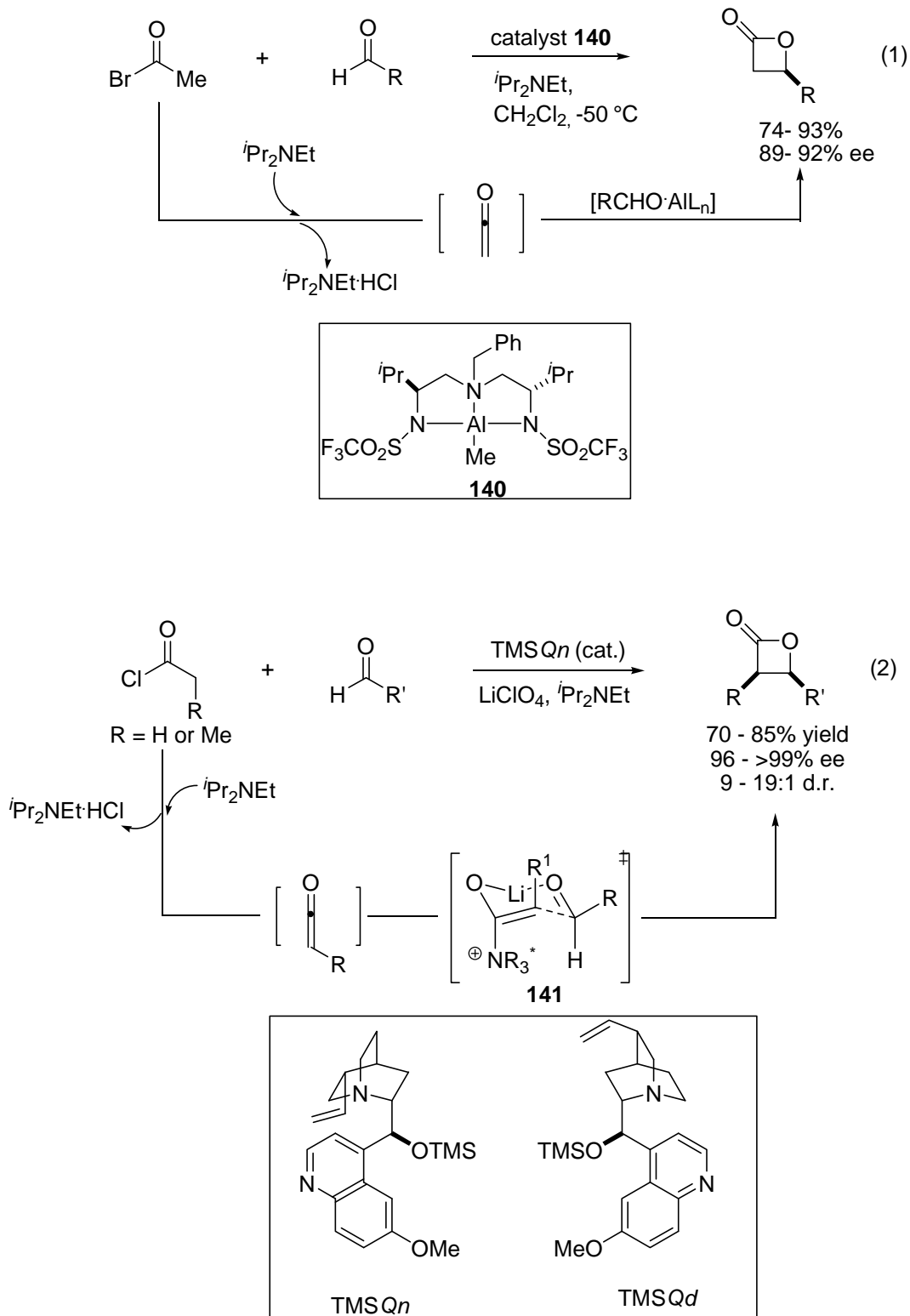
Figure 19. Our approach to the synthesis of amphidinolide B1

2.1.3 Application of AAC Reaction Technology in the Total Synthesis of Amphidinolide

H1

Methodology developed recently in our research group encouraged our pursuit of the total synthesis of amphidinolide H1.^{13,14,80,81} The catalytic, asymmetric acyl halide-aldehyde cyclocondensation (AAC) reactions gave us a powerful tool for efficiently preparing the highly enantioenriched β -lactones from a wide variety of aldehydes (Scheme 14, eq 1 and 2).^{13,14,80,81} As masked aldol products, β -lactones have proven useful in polypropionate and ployketide natural product total syntheses, (-)-pironetin,¹³ erythronolide B⁴² and apoptolidin C.⁸² Two versions of the AAC reactions have been developed in our group: 1) Lewis acid-catalyzed AAC reaction and 2) Lewis base-catalyzed AAC reaction. The Lewis acid-catalyzed AAC reaction employs substoichiometric amounts (10-15 mol %) of a chiral aluminum triamine catalyst **140** to promote an in situ generation between ketene and aldehyde to form a variety of enantiomerically enriched β -lactones.⁸⁰ Cinchona alkaloid Lewis bases *O*-trimethylsilylquinine (TMS*Qn*) or *O*-trimethylsilyl quinidine (TMS*Qd*) have also been used to catalyze AAC reaction from in situ generated ketene through an aldol process with a chair transition state **141**.¹⁴

Scheme 14. Two versions of β -lacton formation reactions



Enantioenriched β -lactones are useful building blocks in organic synthesis due to their unique electrophilicity (Figure 20). The addition of hard nucleophiles such as alkoxides, amine, and metal amide species into the carbonyl of the β -lactone could form β -hydroxyl carboxylic acids.⁸³ Soft nucleophiles such as dialkylcuprate reagents and azide could undergo nucleophilic attack in an S_N2 fashion at the C_4 position of the lactone to generate optically active β -disubstituted carboxylic acids.^{84,85} Use of the asymmetric AAC reaction in an iterative fashion leads to the formation of 1,3-stereochemical relationships, which is another important structural feature in our planned total synthesis. It was, therefore, speculated that the versatile reactivity demonstrated by enantiomerically enriched β -lactones would provide a novel and efficient approach to the total synthesis of amphidinolide H1.

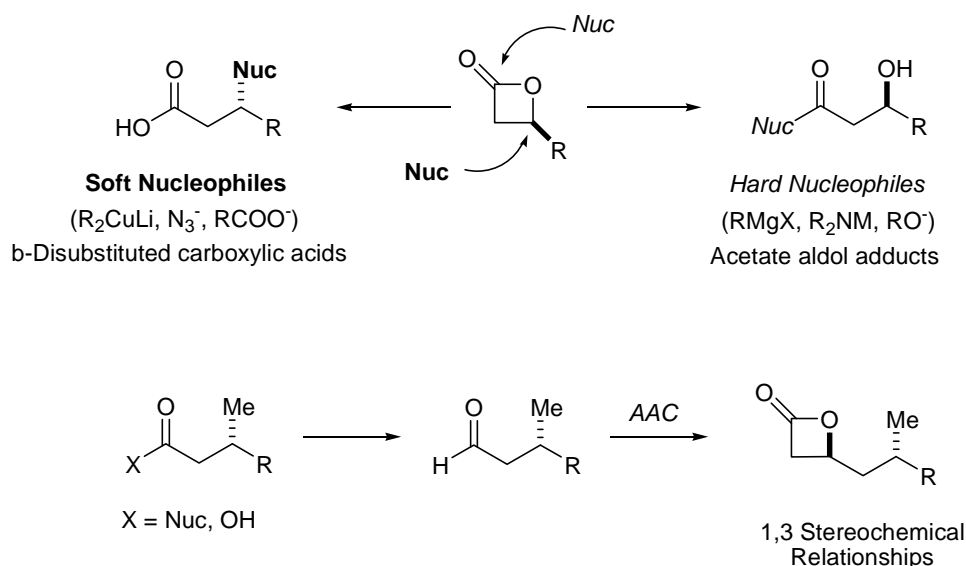


Figure 20. Accessible structural motifs from enantioenriched β -lactones

2.2 EFFORTS TOWARDS THE TOTAL SYNTHESIS OF AMPHIDINOLIDE H

2.2.1 The Retrosynthesis of Amphidinolide H1

Our retrosynthetic analysis of amphidinolide H1 is outlined in Figure 21. As in previous approaches, bond cleavages along the C₁-O macrolatone and C₆-C₇ of *E*-olefin divided the target molecule into two fragments, aldehyde **142** and the corresponding sulfone fragment **143**. Julia olefination was expected to unite the major fragments, to form the *E*-olefin moiety, and subsequent Yamaguchi macrolactonization would be employed to close the 26-membered ring. Palladium-mediated Suzuki coupling of the upper fragment vinyl iodide **144** and the pinacol boronate ester moiety **145** was expected to form the acid-sensitive diene moiety. Further disconnection at the C₂₁-C₂₂ bond in fragment **144** showed that aldol coupling between diazomethyl ketone **146** and enantioenriched **147** might selectively generate the C₂₂ hydroxyl group.

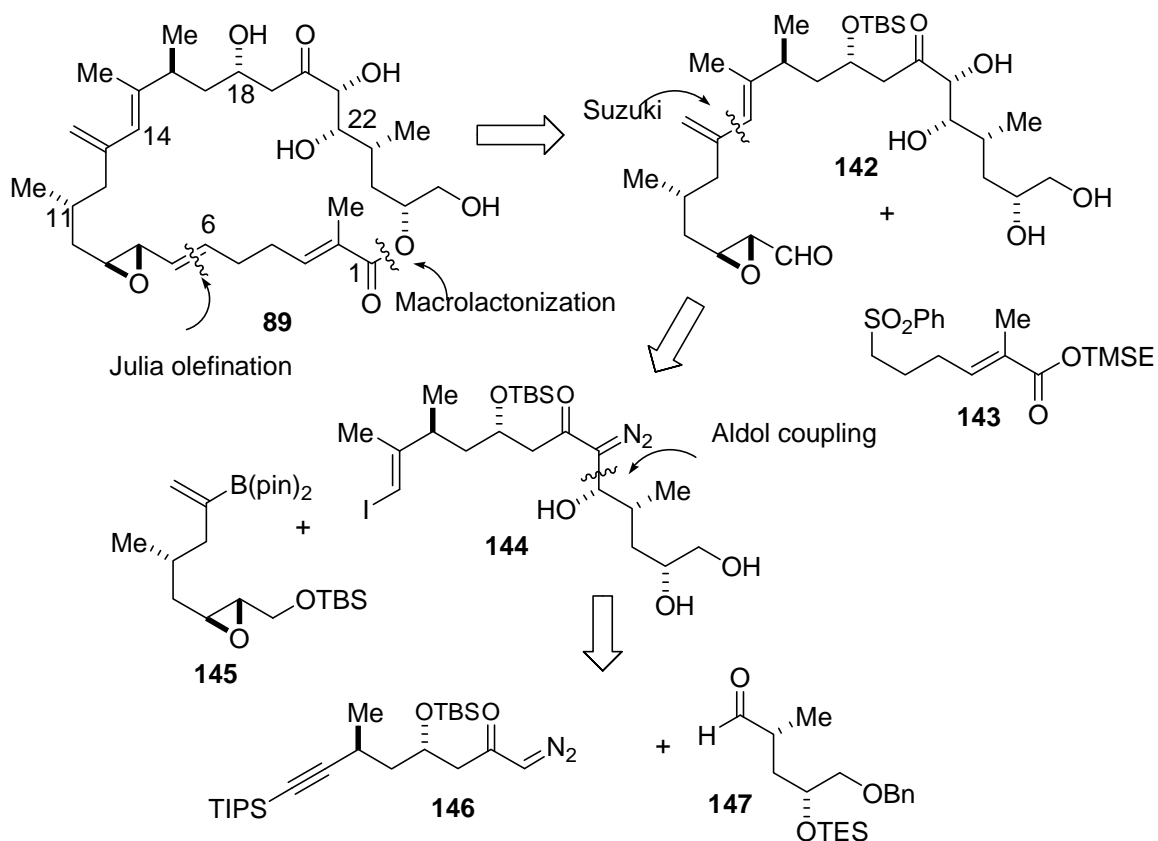


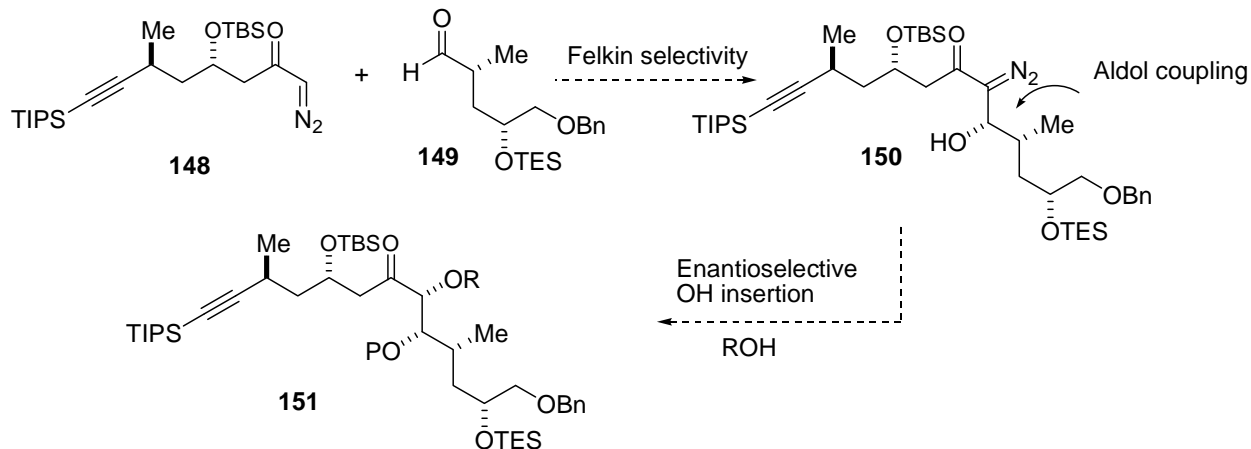
Figure 21. Retrosynthetic analysis of amphidinolide H1.

2.2.2 The First Generation of Synthesis of the C₁₄–C₂₆ Fragment

2.2.2.1 Model Study for preparing Fragment C₁₄–C₂₆

Three consecutive stereocenters from C₂₁ to C₂₃ posed a special challenge to set them up stereospecifically (Scheme 15). An aldol reaction was designed to couple fragments C₁₄–C₂₁ and C₂₂–C₂₆ in a Felkin fashion to construct the C₂₂ stereocenter directed by the preformed C₂₃ methyl stereocenter. Subsequently, a stereoselective O–H bond insertion to diazo ketone was proposed to form the C₂₁ stereocenter.

Scheme 15. Plan to set up upper fragment



It is well known that carboxylic esters can be formed by the reaction of carboxylic acids with diazomethane. Likewise, the α -diazoketone compounds also demonstrated the same reaction property to form the α -acetoxyketone with an acetic acid (Figure 22, eq 3).⁸⁶ Furthermore, the asymmetric O-H insertion reaction catalyzed by Rh(II) or Cu(I) showed potential to be an ideal synthetic strategy for preparing optically pure α -alkoxy, α -aryloxy, and α -hydroxy carboxylic acid derivatives, which are valuable building blocks for the construction of natural products and other biologically active molecules.⁸⁷⁻⁹² Through the use of copper catalysts carrying chiral ligands, the groups of Fu and Zhou have independently made remarkable advances in highly enantioselective insertions of α -diazocarbonyl compounds into the O-H bonds of alcohols,⁹³ phenols⁹⁴ and water⁹⁵ (Figure 22, eq 4). Through the O-H insertion reaction with a suitable ligand and protection group on the neighboring hydroxyl, α -diazocarbonyl compound **150** showed potential to be diastereoselectively converted into the upper fragment **151**.

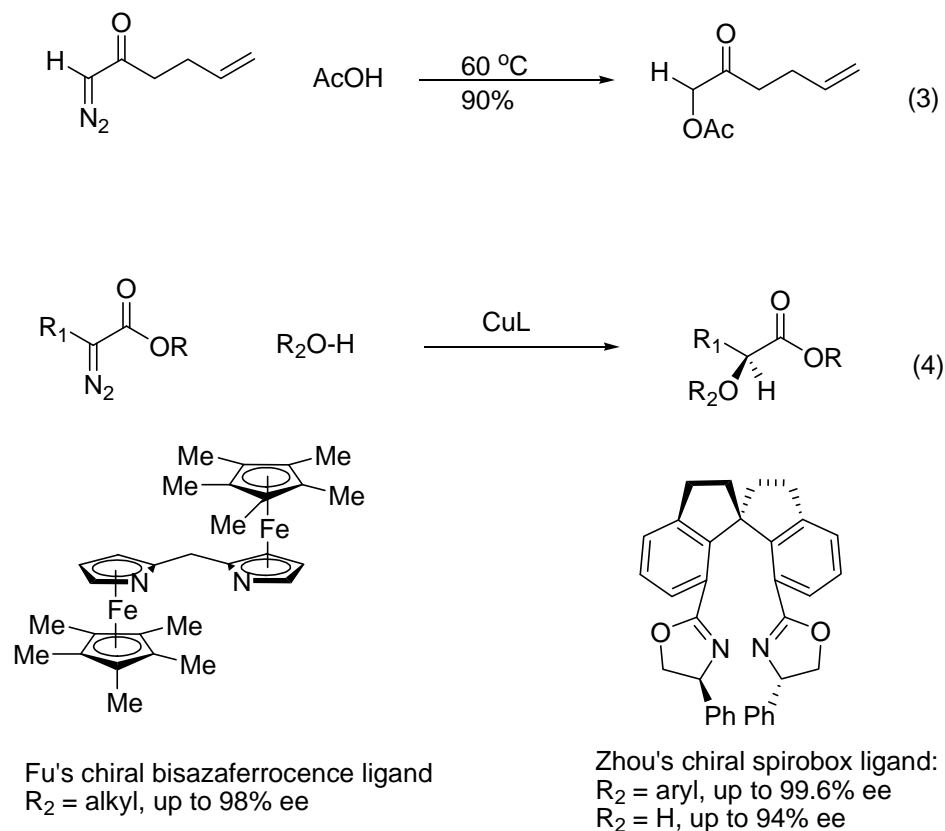


Figure 22. Copper-catalyzed asymmetric O-H bond insertion reaction

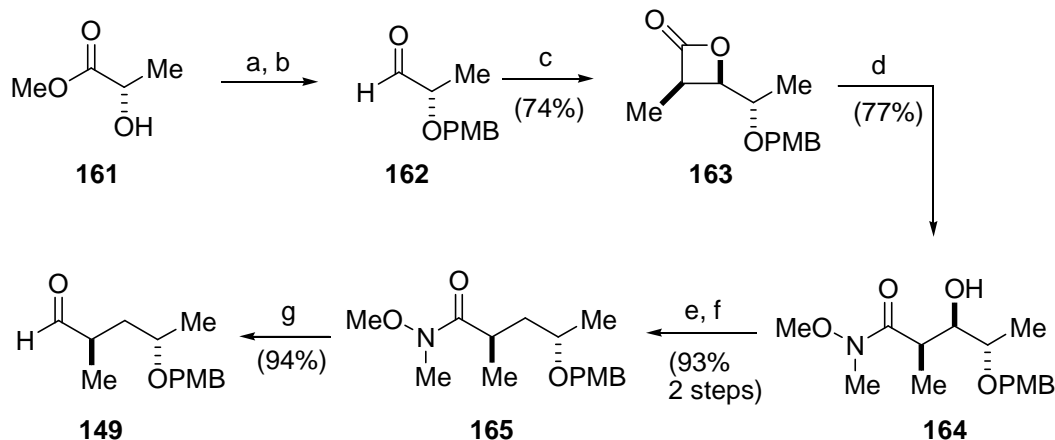
2.2.2.2 Synthesis of the C₁₄-C₂₁ Fragment 148

Synthesis of the C₁₄-C₂₁ synthon **148** commenced with the commercially available (triisopropylsilyl)acetylene (Scheme 16). Treating (triisopropylsilyl)acetylene with *n*-BuLi at –78 °C, followed by adding excess DMF, provided aldehyde **152** quantitatively.⁹⁶ The β-lactone **153** was prepared by an asymmetric AAC reaction with acetyl chloride and aldehyde **153**, catalyzed by 10 mol % TMS*Qn* in 78% yield. The copper-mediated S_N2 lactone ring opening reaction with methylmagnesium bromide established amphidinolide H1's C₁₆ methyl-bearing

stereocenter in delivering carboxylic acid **154** in 54% yield. It was essential that the bulky TIPS group was used to prevent conjugate addition at the alkyne position because TMS protected alkyne only gave the conjugated addition product **154a**. Even though several other Cu species, such as CuI, CuCN, Li₂CuCl₄, and (Ph₃P)₃CuI, were used to improve the selectivity, these catalysts just formed the allene **154a** as the major product. After esterification of **154** with trimethylsilyldiazomethane, followed by a DIBAL reduction of resulting methyl ester, aldehyde **157** was then formed in 94% over two steps and ready to undergo another round of AAC reaction. The AAC reaction was firstly carried under a Lewis base-catalyzed condition with 10 mol % TMSQ_n and 1 equiv. LiClO₄. However, a low yield (53%) was obtained due to the instability of the alkyne bearing aldehyde **157**. However, Lewis acid-catalyzed AAC reaction provided the solution for this problem. The aluminum catalyst **160** was used to improve the yield of the β-lactone formation reaction to 72%. Ring-opening of β-lactone **158** with KOH at 55 °C, protection of the resulting alcohol and carboxylic acid with a *tert*-butyldimethylsilyl group, followed by TFA deprotection of TBS ester gave carboxylic acid **159** in overall 90% yield for 3 steps. Finally, carboxylic acid **159** was then converted into an acid chloride with oxalyl chloride and then coupled with diazomethane to afford diazoketone in 78% yield over two steps.

diazoketone **148** and aldehyde **149**. A rapid synthesis of **149** was explored by employing AAC chemistry (Scheme 17). Commercially available (*S*)-methyl lactate reacted with 4-methoxybenzyl 2,2,2-trichloro-acetimidate catalyzed by substoichiometric amount of CSA at ambient temperature to yield the PMB protected ester in 74% yield, which was then reduced by 1.5 equiv. DIBAL to afford AAC precursor aldehyde **162** in 94% yield. Subsequently, the cyclocondensation of propionyl chloride with aldehyde **162** catalyzed by 10 mol % TMS*Qn* provided *syn* β -lactone **163** in 74% yield. It is worthwhile to point out that 2 equiv. of LiI are necessary to guarantee a good yield (74%) and diastereoselectivity (*syn:anti* = 13:1). The conversion of β -lactone **163** into amide **164** was carried out by employing *N,O*-dimethylhydroxylamine that mediated the β -lactone ring opening, and the subsequent Barton-McCombie deoxygenation reaction⁹⁷ afforded α -methyl amide **165** in 93% yield over 2 steps. Finally, synthesis of the aldehyde fragment **149** was accomplished by DIBAL reduction in 94% yield.

Scheme 17. Synthesis of the C₂₂-C₂₆ model fragment^a

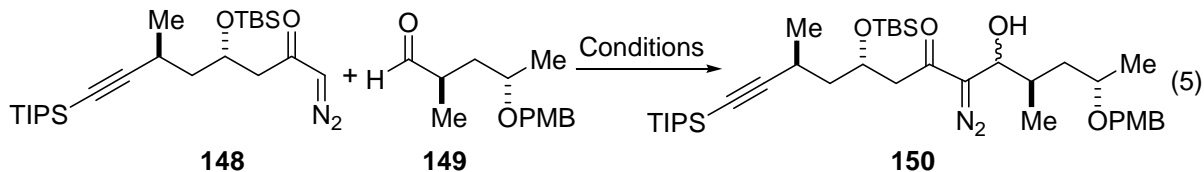


^aConditions: (a) 4-Methoxybenzyl-2,2,2-trichloroacetimidate, 10 mol % CSA, CH₂Cl₂, 74%; (b) DIBAL, CH₂Cl₂, -78 °C, 94%; (c) 10 mol % TMSQn, 2 eq. Lil, propionyl chloride, ⁱPr₂NEt, -78 °C; (d) MeO(Me)NH₂Cl, Me₂AlCl, 0 °C; (e) NaH, CS₂, MeI, THF, 0 °C to rt; (f) AIBN, ⁿBu₃SnH, toluene, reflux; (g) DIBAL-H, -78 °C;

2.2.2.4 Model Study of Aldol Coupling of C₁₄-C₂₁ Fragment With C₂₂-C₂₆

With diazoketone **148** and aldehyde **149** prepared, we metallated diazoketone **148** and subsequently added to aldehyde **149** under various conditions (Scheme 18, eq 5). Diazoketone **148** and aldehyde **149** had to be premixed in THF at -78 °C and then were treated with LDA to afford alcohol **150** in 79% yield. However, no diastereoselectivity was observed. We attempted to metallate diazoketone **148** through a transmetalation process from Li enolate to Zn and Mg enolate by using ZnCl₂ and MgBr₂. Unfortunately, it turned out that they were detrimental to the reaction efficiency. Since the diastereoselectivity was not improved, we decided to change the synthetic route.

Scheme 18. Aldol coupling for making C₁₄-C₂₆ fragment



Entry	Conditions	Yield	dr
a	LDA, THF, -78 °C;	79%	1:1
b	MgBr ₂ , THF, LDA, -78 °C	8%	
c	ZnCl ₂ , THF, LDA, -78 °C	10%	

2.2.3 The Second Generation of Synthesis of the C₁₄-C₂₆ Fragment

2.2.3.1 The Retrosynthesis of the C₁₄-C₂₆ Fragment

As shown in Figure 23, the second generation synthesis of the fragment C₁₄-C₂₆ was explored, since the aldol coupling between diazoketone **148** and aldehyde **149** failed to achieve satisfactory diastereoselectivity. The C₁₄-C₂₆ fragment would be obtained from dithiane **167**. This analysis would allow the C₂₀-C₂₁ bond to be constructed by dithiane coupling between dithiane **168** and aldehyde **169**. The synthesis of dithiane **168** started from entioenriched β -lactone **170**.

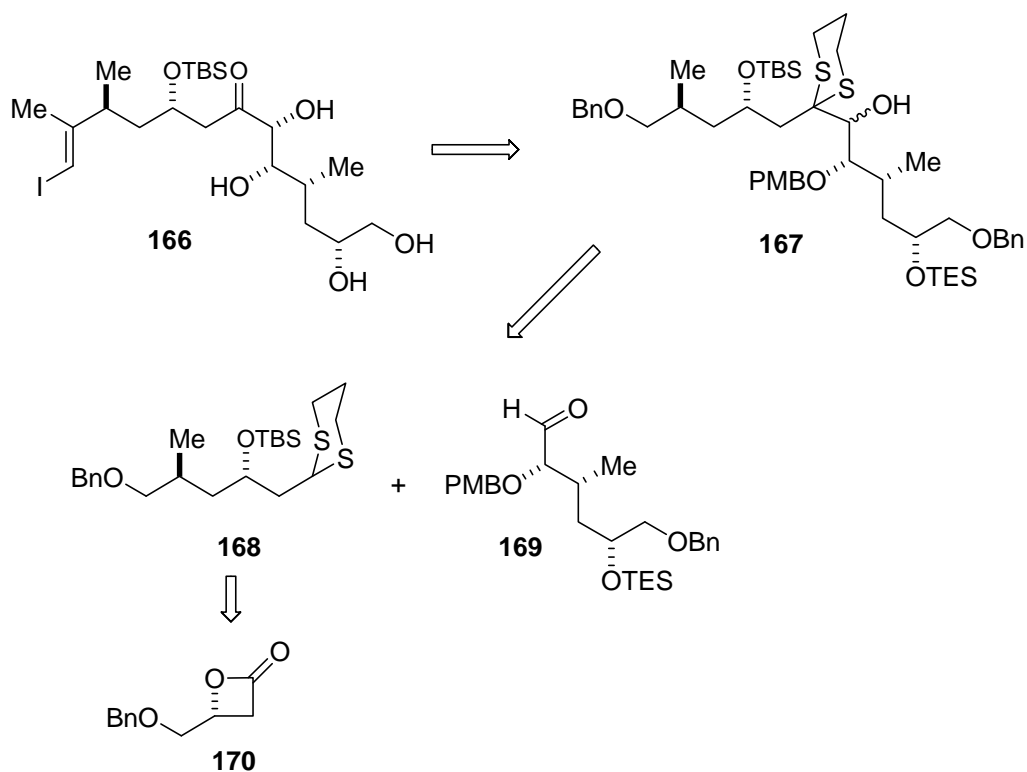


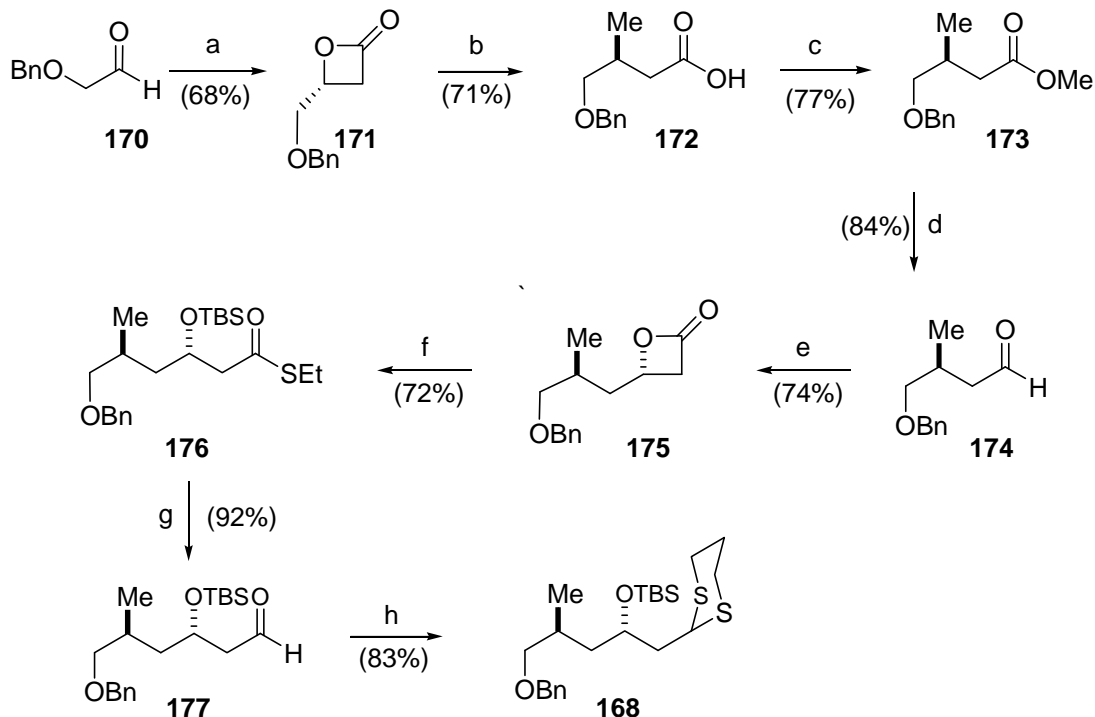
Figure 23. Retrosynthesis of top fragment **166**

2.2.3.2 The Synthesis of Fragment **168**

For the synthesis of C₁₅–C₂₀ dithiane subunit **168** (Scheme 19), we again sought the aid of the catalytic AAC reaction to prepare the enantioenriched β -lactone **171** in 68% yield and by employing 10 mol % of the TMSQ_n catalyst. It was also documented by our group that the aluminum catalyst would provide β -lactone **171** in higher yield and selectivity (91% yield, 92% ee). Cuprate-mediated S_N2 ring opening of lactone **171** afforded the corresponding carboxylic acid **172** in 71% yield and efficiently installed the C₁₆ methyl-bearing stereocenter. Anticipating the second AAC reaction to set up C₁₈ stereocenter, acid **172** was transformed into the corresponding aldehyde **174** by first treating **172** with excess trimethylsilyldiazomethane to provide the requisite methyl ester. Reduction of **173** with DIBAL at –78 °C formed the aldehyde

174 in 84% yield. Further homologation of **173** proceeded by *O*-trimethylsilylquinidine (TMS*Qn*)-catalyzed cyclocondensation with acetyl chloride to establish the C₁₆ stereocenter in providing β-lactone **175** in 74% yield. β-Lactone **175** was then elaborated to thioester **176** via a two-step sequence: 1) thiolate-mediated ring opening and in situ alkoxide silylation in 72% yield; 2) DIBAL-mediated thioester reduction in 92% yield. Aldehyde **177** was then converted to dithiane **168** by treatment with propane 1, 3-dithiol, MgBr₂ etherate in Et₂O in 83% yield.

Scheme 19. Synthesis of fragment **79**^a



^aConditions: (a) 10 mol % TMSQn, acetyl chloride, *i*-Pr₂NEt, -78 °C; (b) MeMgBr, CuBr, DMS, THF, TMSCl, -50 °C to -30 °C, then to rt; (c) trimethylsilyldiazomethane, methanol/toluene; (d) DIBAL, -78 °C; (e) 10 mol % TMSQn, acetyl chloride, *i*-Pr₂NEt, -78 °C; (f) EtSH, 20 mol %, KHMDS, THF, 0 °C; TBSOTf, 2,6-lutidine; (g) DIBAL, -78 °C; (h) MgBr₂·Et₂O, 1,3-propanedithiol, Et₂O.

2.2.3.3 The Synthesis of Fragment **169**

We aimed to prepare aldehyde **169** from alcohol **178** which possessed all desired stereocenters of fragment **169** (Figure 24). Alcohol **178** can be made from lactone **179** via a diastereoselective Davis' hydroxylation.⁹⁸ Lactone **179** would be the product of hydrogenation of α,β -unsaturated lactone **180** which in turn is produced from RCM reaction of diene **181**. The diene **181** was prepared from commercially available (*S*)-(-)-glycidol **182**.

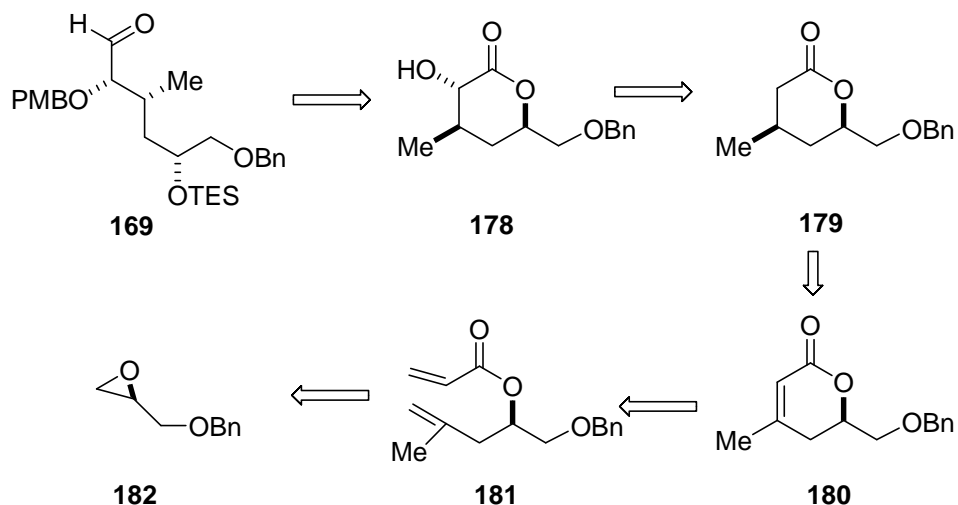
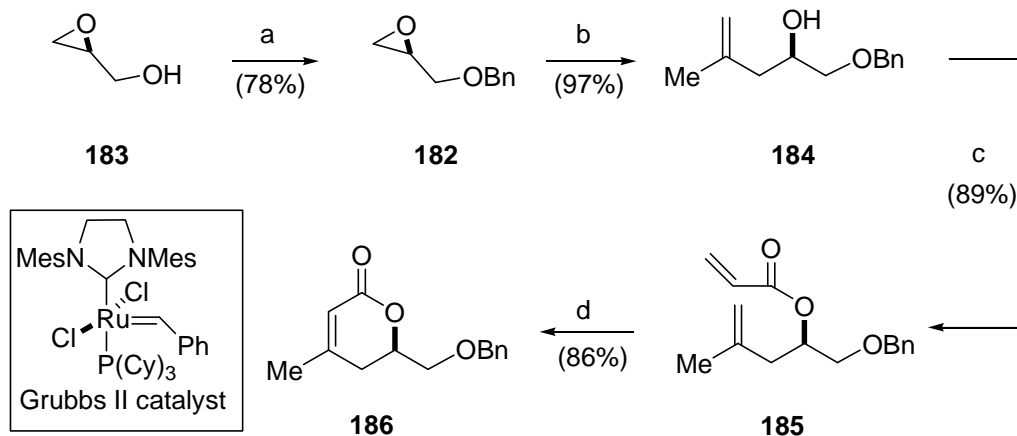


Figure 24. Retrosynthesis of right fragment **169**

As outlined in Scheme 20, the synthesis of the C₁₉–C₂₆ fragment **169** began with commercially available (*S*)-(-)-glycidol **183**, which was converted into **182** by benzyl protection of the free hydroxyl group in 78% yield. A CuI-catalyzed isoprenyl Grignard displacement followed by an esterification reaction with acryloyl chloride afforded ring closure metathesis precursor **185** in 89% yield. Exposure of **185** to substoichiometric amounts of the second generation Grubbs catalyst provided lactone **186** in 86% yield.

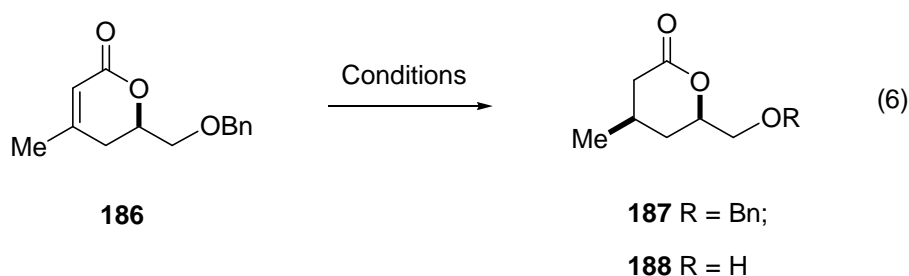
Scheme 20. Synthesis of **186**^a



^aConditions: (a) BnBr, NaH, DMF, 0 °C-rt; (b) Isopropenylmagnesium bromide, CuI, THF, -78 °C; (c) acryloyl chloride, DIPEA, DMAP, CH₂Cl₂; (d) Grubbs II, CH₂Cl₂, reflux;

Diastereoselective reduction of **186** to establish the β -methyl stereocenter in lactone **187** was carried under various conditions to achieve the best selectivity (Figure 25, eq 6). Treatment of lactone **186** with Stryker's reagent⁹⁹ in toluene led to a full conversion to the desired *syn* diastereomer of **187**. However, the product was contaminated with large amounts of triphenylphosphine impurities which could not be separated. Pd/C catalyzed hydrogenation conditions were then employed to diastereoselectively reduce the C=C double bond. These studies demonstrated that solvents played an important role in improving the diastereoselectivity. Two different solvents gave two completely different results: in methanol, the reduction underwent a complete non-selective process (dr = 1:1) and the benzyl group was cleaved simultaneously to form **188** in quantitative yield; benzene as a solvent slowed down the reaction rate and provided *syn* **187** in a 83% yield and excellent diastereoselectivity (dr = 95:5). The reduction reaction of **186** in methanol proceeded much faster than the reaction in benzene and

led to benzyl deprotected product **188**. However, the hydrogenation reaction of **186** in benzene proceeded in a much slower fashion and the benzyl group wasn't deprotected (an elongated reaction time would cause a slow deprotection of benzyl group). Therefore, the mild hydrogenation of **186** in benzene could not add hydrogens to the sterically hindered *si* face of alkene and only add hydrogens to *re* face to yield *syn* **188**. After deprotection of the benzyl group of *syn* **187**, the X-ray crystal structure of alcohol *syn* **188** was obtained, verifying the stereochemistry of *syn* **187**.



entry	Conditions:	yield	<i>syn</i> : <i>anti</i>
a	(((PPh ₃)CuH) ₆ , benzene	N/A (187)	only <i>syn</i> 187
b	10% Pd/C, H ₂ , methanol	quantitative yield (188)	1:1
c	10% Pd/C, H ₂ , benzene.	83% (187)	95:5

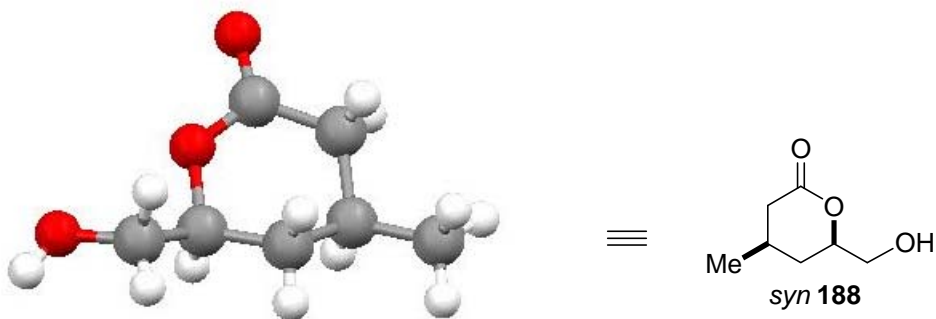
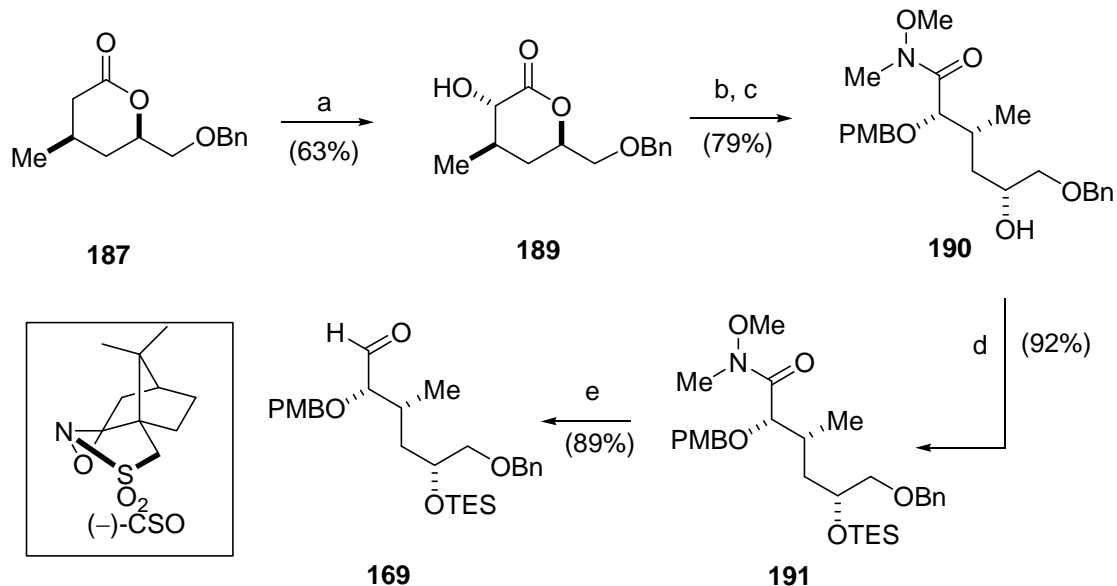


Figure 25. Synthesis of **187** and structure verification

After generating lactone **187** with the correct absolute stereochemistry, we could then further elaborate this intermediate to the C₂₁-C₂₆ subunit of amphidinolide (Scheme 21). In

attempt to establish the α -hydroxyl group of **189** with the desired diastereoselectivity, lactone **187** was enolized with LDA with the assistance of TMEDA and then oxidized with Davis' reagent ([(-)-(10-camphorsulfonyl)oxaziridine] or (-)-CSO)⁹⁸ at $-45\text{ }^{\circ}\text{C}$ to afford α -hydroxyl bearing lactone **189** in 63% yield as a single diastereomer. Completion of the right fragment required only a few routine synthetic manipulations (Scheme 21). After ring opening with *N,O*-dimethylhydroxylamine, silylation of the newly formed C₂₅ hydroxyl group with TESCl and imidazole furnished the fully protected upper synthon **191** in 92% yield. However, treating Weinreb's amide **191** with excess DIBAL provided only partial conversion to aldehyde fragment **169**. After the temperature was elevated to room temperature, DIBAL could not transform all starting material to product **169**. Surprisingly, the much stronger reducing reagent LiAlH₄ was applied at $0\text{ }^{\circ}\text{C}$ to provide aldehyde **169** in 89% yield.

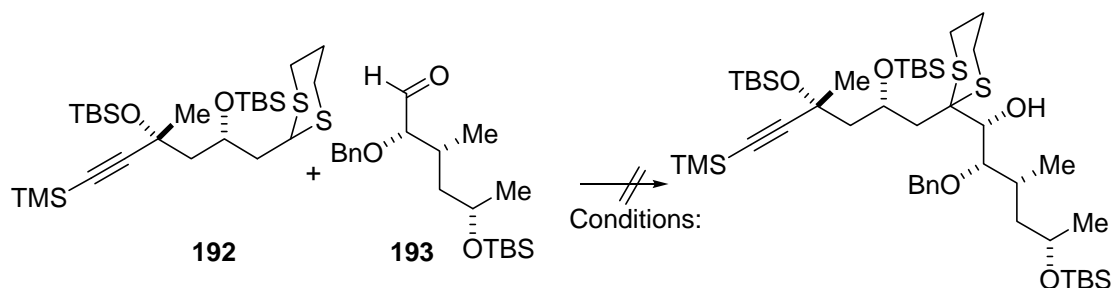
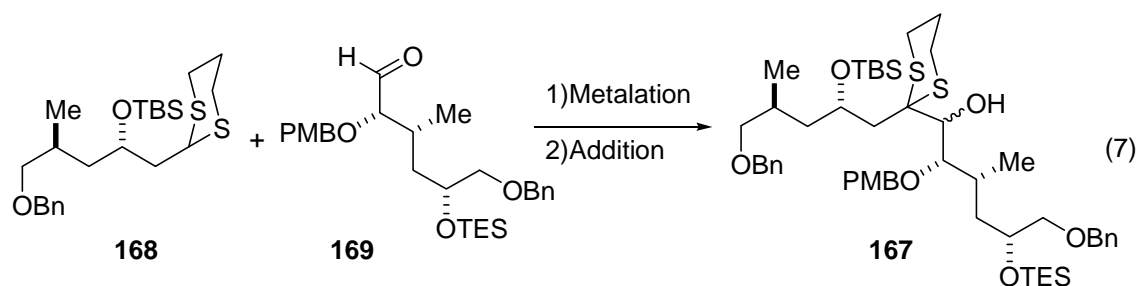
Scheme 21. Completion of fragment **169**^a



^aConditions: (a) (-)-CSO, LDA, TMEDA, -45 °C; (b) 4'-Methoxybenzyl-2,2,2-trichloroacetimidate, BF₃·EtO₂, CH₂Cl₂, -78 °C; (c) MeO(Me)NH₂Cl, Me₃Al, CH₂Cl₂, 0 °C; (d) TESCl, imidazole, DMF, 92%; (j) LiAlH₄, 0 °C;

2.2.3.4 Dithiane Addition Trials

With dithiane **168** and aldehyde **169** available, we attempted lithiation of the dithiane **168** and subsequent addition to aldehyde **169** (Figure 26, eq 7). The similar strategy has been explored in amphidinolide B synthesis.¹⁰⁰ Under a variety of conditions with bases such as *n*-BuLi, *t*-BuLi, and *n*-BuLi with HMPA, experiments to metalate dithiane **192** and add it to aldehyde **193** led to the complete recovery of dithiane **192**. Further controlled experiments with the same metalation conditions and trapping of the dithiane anion with TMSCl demonstrated the resistance of dithiane **192** toward metalation.



Conditions:

- (a) *n*-BuLi, THF, $-50\text{ }^{\circ}\text{C}$, then **193**
- (b) *t*-BuLi, THF, $-50\text{ }^{\circ}\text{C}$ – RT, then $-50\text{ }^{\circ}\text{C}$, **193**
- (c) *n*-BuLi, HMPA, $-50\text{ }^{\circ}\text{C}$, then **193**

Figure 26. Dithiane addition strategy in amphidinolide B synthesis

Based on these experiments, we attempted to evaluate the efficiency of the metalation with our dithiane subunit **192** (Figure 27). Treatment of dithiane **168** with *t*-BuLi and HMPA at $-78\text{ }^{\circ}\text{C}$ in THF and trapping of the dithiane anion with D_2O provided complete deuteration of dithiane **168**. Under the same condition, dithiane **194** also gave 25% deuterated product. Therefore, the metalated dithiane with *t*-BuLi and HMPA could generate dithiane anion which was then tested in the addition reaction to aldehyde **169** under a variety of conditions. Two equivalents of dithiane **194** were treated with *t*-BuLi and HMPA at $-78\text{ }^{\circ}\text{C}$ in THF and added to aldehyde **169** to form **195** in 38% yield and 1:1 dr. However, the addition of lithiated dithiane **168** to aldehyde **169** resulted in decomposition of the starting material aldehyde. Two additives, ZnCl_2 and CeCl_3 , were used to modify the reaction condition, but decomposition of the starting

fragment **199** and vinyl iodide **198**. Aldehyde **198** and methyl ketone **200** would be connected via a diastereoselective aldol reaction in delivering C₁₈ hydroxyl stereocenter.

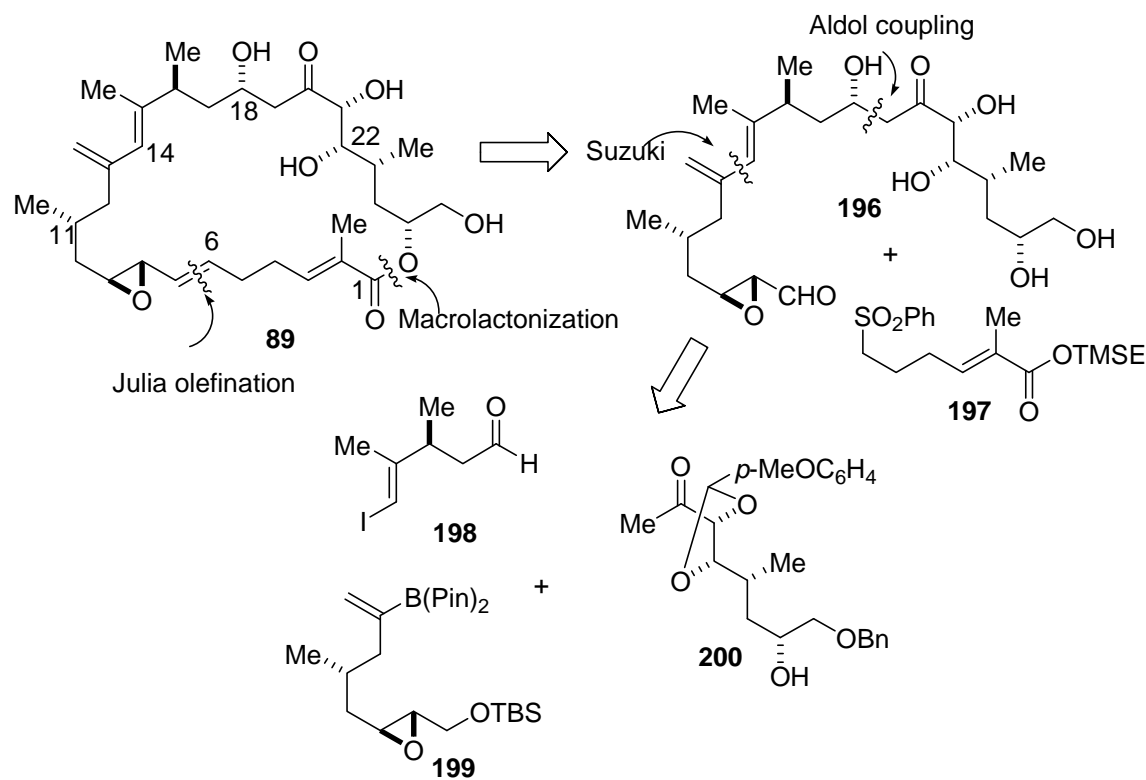


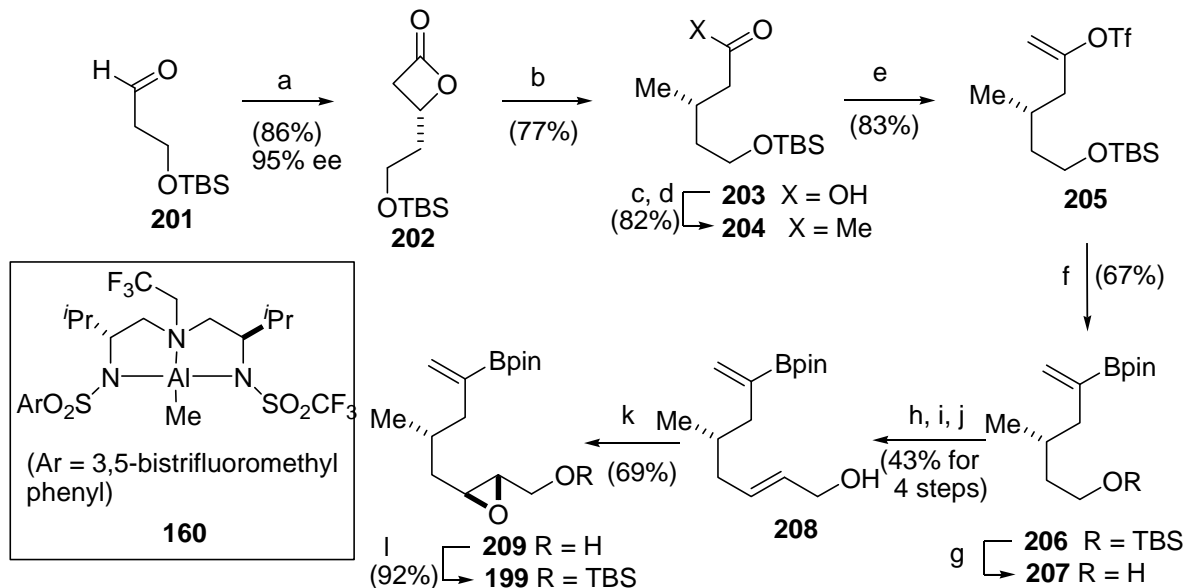
Figure 28. Revised retrosynthesis of amphidinolide H1

2.2.4.2 Synthesis of the C₇-C₁₃ Fragment **199**¹⁰⁰

Since the C₇-C₁₃ synthon **199** had a same structure as the left fragment of amphidinolide B which has been synthesized in our group before. The same route has been employed to complete the synthesis of fragment **199**, which began with a highly enantioselective AAC reaction of 2-*t*-butylsilyloxy propionaldehyde with acetyl bromide in the presence of Al(III) triamine catalyst **160**, delivering β-lactone **202** in 86% yield and 95% ee (Scheme 22). β-lactone **202** was subjected to a cuprate-mediated ring opening with methylmagnesiumbromide and CuBr to give carboxylic acid **203** in 77% yield. Coupling **203** with *N,O*-dimethylhydroxylamine and reacting

the resulting Weinreb amide with methyllithium provided methyl ketone **204** in 82% yield. Functionalizing **204** to serve as the requisite Suzuki cross-coupling partner proceeded by kinetic ketone enolization and enolate trapping with PhNTf₂ to provide vinyl triflate **205** in 83% yield. In anticipation of the planned fragment uniting the Suzuki reaction, vinyl triflate **205** was then converted into the corresponding pinacol boronate ester **206** through Pd(0)-catalyzed bis(pinacolato)diborane cross-coupling in 63% yield. The boronic ester functionality proved to be sufficiently robust that **207** could be further elaborated to the fully functionalized C₇-C₁₃ fragment. Thus, primary alcohol deprotection was followed by standard homologation to the allylic alcohol **208** by alcohol oxidation, Horner-Emmons-Wadsworth homologation, and enoate reduction. Subjecting allylic alcohol **208** to Sharpless epoxidation, therefore, afforded the epoxy alcohol **209** in 63% yield with subsequent protection of the primary alcohol affording the intact coupling partner **199** in 92% yield.

Scheme 22. Synthesis of the C₇-C₁₃ fragment **199**^a



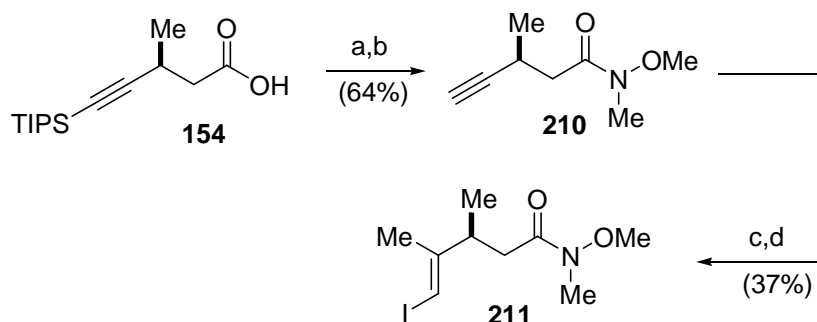
^aConditions: (a) 20 mol % catalyst **160**, *i*-Pr₂NEt, -78 °C. (b) MeMgBr, CuBr·DMS; (c) (OMe)MeNH₂Cl, EDCI, DMAP. (d) MeLi, THF; (e) KHMDS, PhNTf₂, -78 °C - 0 °C; (f) Bpin-Bpin, Pd(PPh₃)₂Cl₂, PPh₃, PhOK, DMF, 50 °C. (g) TBAF. (h) Dess-Martin/Py; (i) NaH, (O*i*Pr)₂P(O)CH₂CO₂Et. (j) DIBAL-H, CH₂Cl₂; (k) Ti(O*i*Pr)₄, (+)-DET, *t*BuOOH. (l) TBSCl, imidazole, DMF.

2.2.4.3 Synthesis of the C₁₄-C₁₈ Fragment **211**

Synthesis of the C₁₄-C₁₈ synthon **211** commenced with the known carboxylic acid **154** (Scheme 23).⁹⁶ Converting carboxylic acid **154** into alkyne **210** was carried out by coupling with *N,O*-dimethylhydroxylamine and the subsequent desilylation reaction with TBAF afforded alkyne **210** in 64% yield over two steps, thereby providing the conduit for stereoselective installation of the C₁₄-C₁₅ trisubstituted olefin. Thus, addition of Bu₃SnCu(Bu)(CN)Li₂¹⁰⁰ to **210** followed by the trapping of the intermediate alkenyl cuprate with MeI and stannane-iodine exchange provided vinyl iodide **211** in a low yield (37%). An alternative route was explored to

improve the yield.

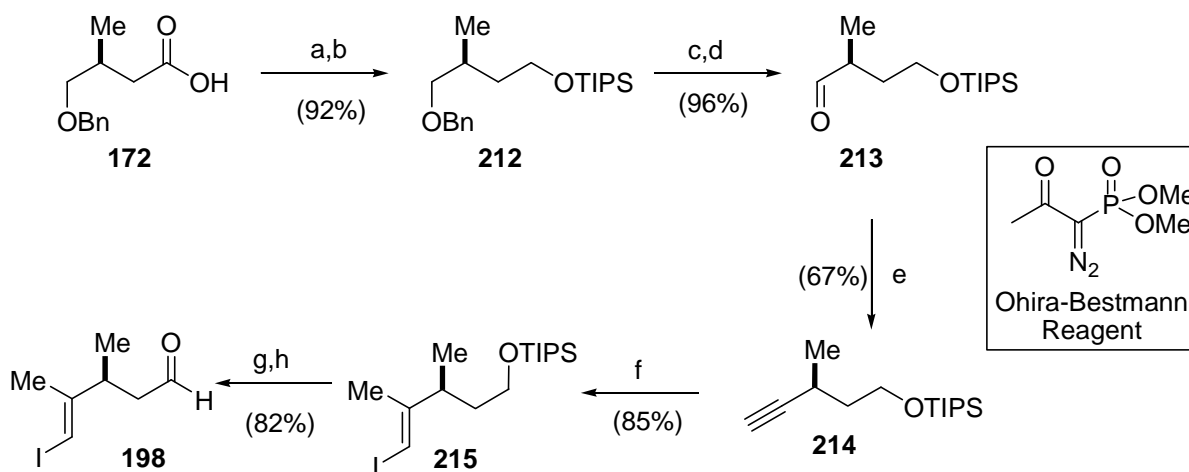
Scheme 23. Synthesis of the C₁₄-C₁₈ fragment **211**^a



^aConditions: (a) Me(MeO)NH₂Cl, DCC, DMAP. (b) TBAF, THF; (c) (Bu₃Sn)₂, CuCN, BuLi, MeI, -50 °C; (d) I₂, THF

The alternate route was commenced with carboxylic acid **172** (Scheme 24). Carboxylic acid **172** was converted into silyl ether **212** through a two-step sequence: reduction of carboxylic acid **172** with BH₃ followed by silyl deprotection with TBAF in 92% yield over two steps. The resulting silyl ether **212** was hydrogenated with 10% Pd/C and then oxidized by the Dess-Martin reagent¹⁰¹ to deliver aldehyde **213** in 96% yield over two steps. Subsequently, the carbozirconation reaction with the alkyne **214**, followed by I₂ quenching afforded vinyl iodide **215** in 85% yield. Finally, vinyl iodide **215** was desilylated with TBAF followed by the Dess-Martin oxidation¹⁰¹ to afford fragment **198** in 82% yield over two steps.

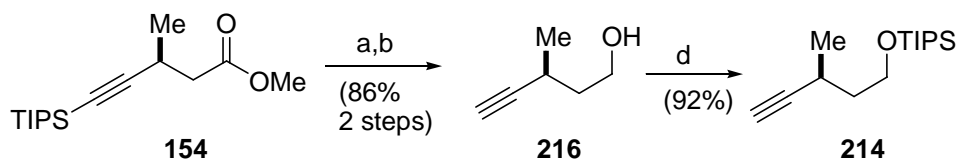
Scheme 24. Synthesis of the C₁₄-C₁₈ fragment **198**^a



^aConditions: (a) BH₃, THF, 0 °C- rt; (b) TIPSOTf, 0 °C; (c) 10% Pd/C, H₂, CH₃OH; (d) DMP, CH₂Cl₂; (e) Ohira-Bestmann reagent, NaOMe, MeOH. (f) AlMe₃, [ZrCp]₂Cl₂; I₂, CH₂Cl₂, -25 °C; (g) TBAF; (h) DMP, CH₂Cl₂.

The intermediate **214** was also synthesized from ester **154** (Scheme 25). DIBAL reduction of ester **154**, followed by desilylation with TBAF afforded the volatile alkyne **216** in 86% yield. Subsequently, exposure of **216** to TIPSOTf and 2,6-lutidine resulted in **214** in 92% yield.

Scheme 25. An alternative synthesis of intermediate **214**^a



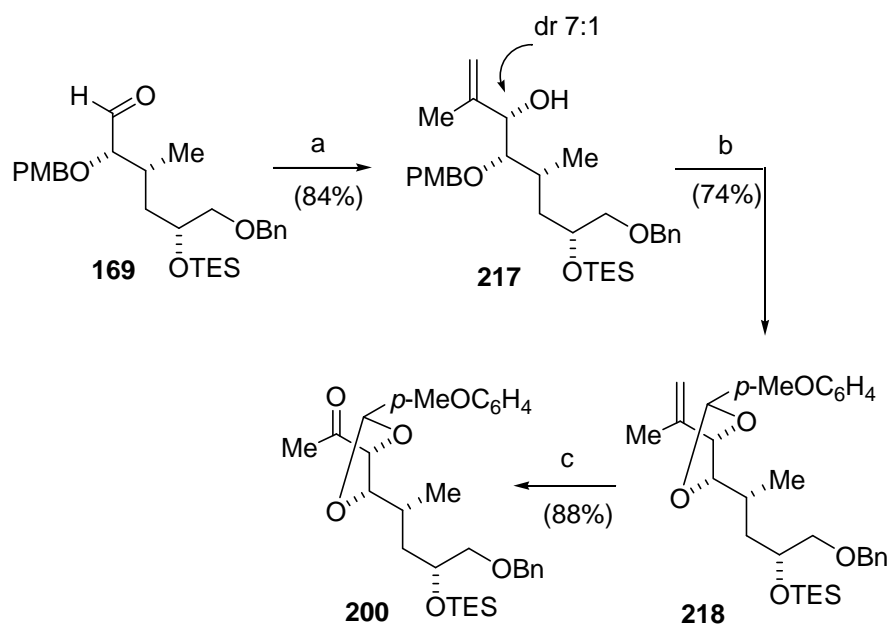
^aConditions: (a) DIBAL-H; (b) TBAF, THF; (c) TIPSOTf, 2,6-lutidine;

2.2.4.4 Synthesis of the C₁₉-C₂₆ Fragment 200

The right wing of amphidinolide, fragment **200**, was prepared from the previous

intermediate **200** (Scheme 26). A Cram-chelation¹⁰² type of isoprenyl Grignard addition to aldehyde **169** furnished **217** as the major isomer (dr 7:1). The newly formed hydroxyl group of **217** was then protected by *p*-anisyl acetal through anhydrous DDQ oxidation of PMB ether to provide **218**. Subsequently, ozonolysis of alkene of **218** successfully delivered the desired methyl ketone fragment **200** in 88% yield.

Scheme 26. Synthesis of the C₁₉-C₂₆ fragment **200**^a



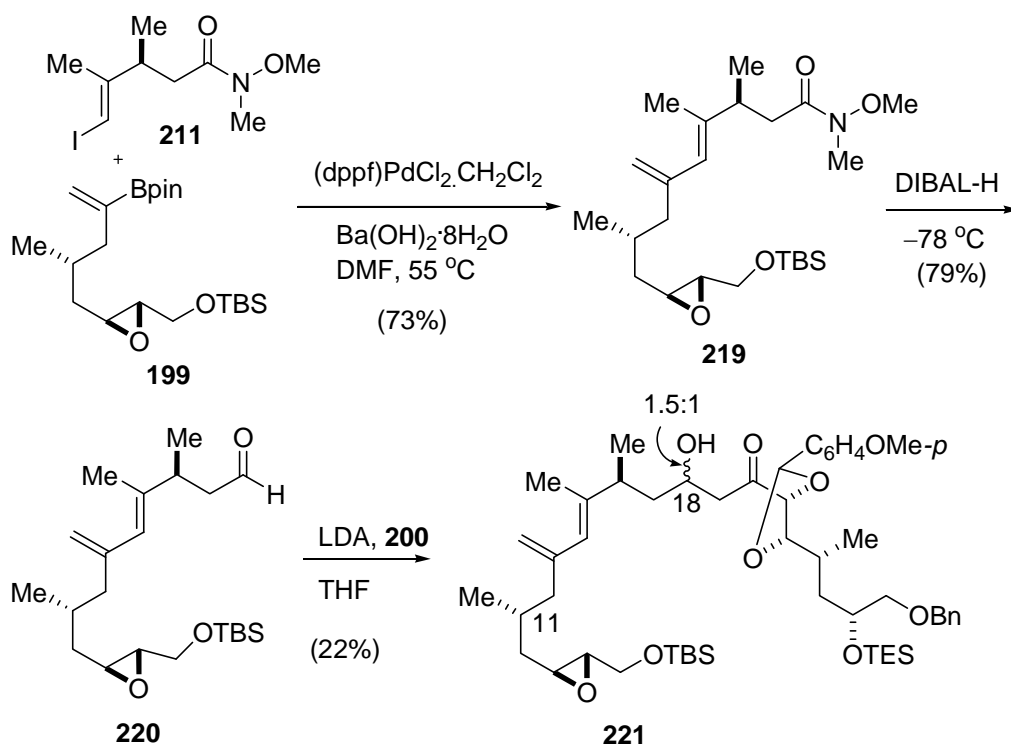
^aConditions: (a) Isopropenylmagnesium bromide, CH₂Cl₂, -78 °C; (b) DDQ, 0 °C, 74%; (c) O₃, Ph₃P, -78 °C.

2.2.4.5 Fragments Coupling

With three major fragments in hand, we are trying to develop a reliable assembly process. The potentially challenging Suzuki coupling of **199** and the sterically compromised iodide **198** was tested, which gave the desired diene **219** in 73% yield, provided that it was performed with a

combination of Pd(dppf)Cl₂·CH₂Cl₂, Ba(OH)₂·H₂O in DMF (Scheme 27).¹⁰⁰ Reduction of **219** with DIBAL afforded aldehyde **220**. Next, the LDA-mediated aldol reaction of methyl ketone **200** with aldehyde **220** proceeded with poor selectivity (dr 1.5:1). However, Kalesse has reported a low yield and poor selective aldol reaction when C₂₁ and C₂₂ diol was protected as the acetonide.⁷³ In future work, protecting group adjustment at the C₂₁ hydroxyl will be tested in order to get good selectivity in the aldol coupling reaction.

Scheme 27. Fragments coupling.



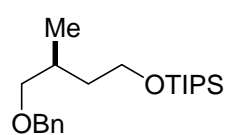
2.3 CONCLUSIONS

In efforts towards asymmetric synthesis of the cytotoxic macrolide amphidinolide H1, asymmetric AAC reactions have been used to set key stereochemical relationships in major fragments **211** and **199**. Iodide **211** was coupled with boronic ester **199** via an efficient Suzuki reaction to form a C₇-C₁₈ fragment **219**. Subsequent homologation was attempted by the aldol coupling between fragment **220** and **200**. However, the low yield and low selectivity was obtained and needs to be improved in the further study.

2.4 EXPERIMENTALS

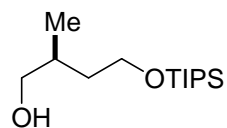
General Information: Optical rotations were measured on a Perkin-Elmer 241 digital polarimeter with a sodium lamp at ambient temperature and are reported as follows: $[\alpha]_{\lambda}$ (c g/100mL). Infrared spectra were recorded on a Nicolet Avatar 360 FT-IR spectrometer. NMR spectra were recorded on a Bruker Avance-300 (^1H : 300 MHz; ^{13}C : 75 MHz) spectrometer with chemical shifts reported relative to residual CHCl_3 (7.26 ppm) for ^1H and CDCl_3 (77.0 ppm) for ^{13}C NMR spectra. Unless otherwise stated, all reactions were carried out in flame-dry glassware under a nitrogen atmosphere using standard inert atmosphere techniques for the manipulation of solvents and reagents. Analytical gas-liquid chromatography (GLC) was performed on a Varian 3900 gas chromatography equipped with a flame ionization detector and split mode capillary injection system using a ChiralDEX™ G-TA column (20 m x 0.25 mm) (Advanced Separation Technologies Inc.). Helium was used as the carrier gas at the indicated pressures.

Unless otherwise stated, all reactions were carried out in dry glassware under a nitrogen atmosphere using standard inert atmosphere techniques for the manipulation of solvents and reagents. Anhydrous solvents (CH_2Cl_2 , THF, DMF, diethyl ether, pentane and toluene) were obtained by passage through successive alumina and Q5 reactant-packed columns on a solvent purification system. *N, N*-Diisopropylethylamine and triethylamine were distilled under nitrogen from CaH_2 . Anhydrous solvents Flash chromatography was performed on EM silica gel 60 (230-240 mesh) unless noted otherwise. If the reaction was worked up with aqueous extraction, dr (diastereomer ratio) was determined from crude NMR or GLC. Compound **198** was prepared according to the procedure.⁷²



(S)-4-(Benzyloxy)-3-methylbutoxy)triisopropylsilane (212): To a solution

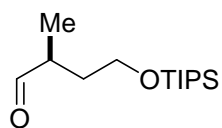
of 416 mg of carboxylic acid **172** (2.00 mmol) in 10 mL of THF was added 3 mL of a 1.0 M solution of $\text{BH}_3 \cdot \text{THF}$ (3.0 mmol) at 0 °C. The solution was then stirred at 0 °C for 3 h, warmed up to room temperature and the solvent evaporated *in vacuo* to afford 386 mg crude product and submit to next step without further purification. To a solution of 386 mg crude alcohol **212a** (2.00 mmol) in 10 mL of CH_2Cl_2 was added 0.347 mL of a 2,6-lutidine (321 mg, 3.0 mmol) at 0 °C, followed by adding 0.550 mL of TIPSOTf. The solution was then stirred at 0 °C for 3 h, warmed up to room temperature. The reaction was then quenched with aqueous saturated NaHCO_3 and extracted with ether (3 x 20 mL). The organic layer was dried over Na_2SO_4 and concentrated. The crude product was purified with column chromatography (5% ethyl acetate in hexane) to give 636 mg (92%, 2 steps) of title compound as colorless oil. $[\alpha]_D^{25} +4.5$ (*c* 2.9, CHCl_3); IR (thin film): 2942, 2865, 1461, 1099 cm^{-1} ; ^1H NMR (700 MHz, CDCl_3) δ 7.29-7.37 (m, 5H), 4.53 (s, 1H), 3.74-3.77 (m, 1H), 3.40 (dd, *J* = 8.8 Hz, 5.7 Hz, 1H), 3.29 (t, *J* = 7.0 Hz, 1H), 1.96-2.01 (m, 1H), 1.72 (dt, *J* = 13.3 Hz, 7.0 Hz, 1 H), 1.41 (dt, *J* = 14.0 Hz, 7.0 Hz, 1H), 1.07-1.16 (m, 21H), 1.00 (d, *J* = 7.0 Hz, 3H); ^{13}C NMR (150 MHz, CDCl_3) δ 138.9, 128.3, 127.5, 127.4, 76.0, 72.9, 61.6, 37.0, 30.4, 18.0, 17.4, 12.0.



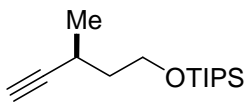
(S)-2-Methyl-4-(triisopropylsilyloxy)butan-1-ol (213a): To a solution of 84

mg of **212** (0.25 mmol) in 5 mL of MeOH under nitrogen atmosphere, 12 mg of Pd/C was added. After two vacuum/ H_2 cycles to replace nitrogen atmosphere with hydrogen, the reaction was stirred for over night under 1 atm pressure of hydrogen (balloon). The reaction mixture was then filter through a plug of celite, the filtrate was concentrated. The crude product

was submitted to the next step without further purification. $[\alpha]_D -9.2$ (c 0.80, CHCl_3); IR (thin film): 3348, 2942, 2866, 1462, 1099 cm^{-1} ; ^1H NMR (600 MHz, CDCl_3) 3.86 (dt, $J = 10.3$, 1H), 3.74-3.77 (m, 1H), 3.3 (pentet, $J = 6.9$ Hz, 1H), 2.83 (d, $J = 2.7$ Hz, 1H), 1.93-1.77 (m, 2H), 1.39 (d, $J = 6.9$ Hz, 3 H), 0.94 (d, $J = 6.9$ Hz, 3H), 0.92-0.90 (m, 12H), 0.88 (d, $J = 2.7$ Hz, 3H), 0.10 (s, 3H), 0.08 (s, 3H); ^{13}C NMR (150 MHz, CDCl_3) δ 174.2, 119.0, 113.6, 80.4, 75.3, 41.5, 37.6, 32.7, 26.1, 19.0, 18.9, 18.4, 14.3, 9.2, -3.5 , -4.1 ; HRMS (ESI) m/z calcd for $[\text{M}+\text{Na}]^+$ $\text{C}_{14}\text{H}_{32}\text{O}_2\text{NaSi}$: 283.2069; found: 283.2052

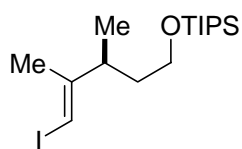


(S)-2-Methyl-4-(triisopropylsilyloxy)butanal (213): To a 0°C solution of the crude alcohol **213a** in 5 mL of CH_2Cl_2 was added 159 mg of Dess-Martin periodinane (0.375 mmol). The reaction mixture was allowed to warm to ambient temperature and stirred for 2 h. It was then direct loaded on the silica gel column and carefully eluted with 5% ethyl acetate in hexanes to afford 64 mg the title compound as colorless oil (96% 2 steps); $[\alpha]_D -12$ ($c = 12$, CHCl_3); IR (thin film): 2942, 2866, 1708, 1462, 1106 cm^{-1} ; ^1H NMR (700 MHz, CDCl_3) 9.68 (s, 1H), 3.82-3.77 (m, 1H), 3.79-3.74 (m, 1H), 2.57 (sextet, $J = 7.0$ Hz, 1H), 1.99 (td, $J = 7.0$, 14 Hz, 1H), 1.64 (td, $J = 7.0$, 14.0 Hz, 1H), 1.13 (d, $J = 7.0$ Hz, 3H), 1.10-1.05 (m, 21 H); ^{13}C NMR (175 MHz, CDCl_3) δ 205.0, 60.6, 43.5, 33.9, 18.0, 13.1, 11.9; HRMS (EI) m/z calcd for $[\text{M}-\text{C}_3\text{H}_7]^+$ $\text{C}_{11}\text{H}_{23}\text{O}_2\text{Si}$: 215.1467; found: 215.1435



(S)-Triisopropyl(3-methylpent-4-ynoxy)silane (214): To 2 mL of MeOH, Na metal (63 mg, 2.7 mmol) was added. The mixture was stirred for 30 min and cooled to -78°C . Dimethyl-1-diazo-2-oxopropylphosphonate (518 mg, 2.70 mmol) in 5 mL THF was added dropwise. The resulting mixture was stirred at this temperature

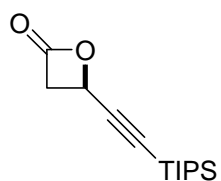
for 0.5 h. Aldehyde **213** (174 mg, 0.67 mmol) in 5 mL THF was slowly introduced. The mixture was stirred for 0.5 h at -78°C and then warmed up to ambient temperature. After stirred overnight at ambient temperature, 5 mL H_2O was added and extracted with CH_2Cl_2 (3x30 mL). The combined organic phases were dried over Na_2SO_4 and evaporated, and the residue was purified by flash chromatography (1% hexanes in ethyl acetate) to give alkyne **214** as a pale yellow oil (104 mg, 61%). $[\alpha]_{\text{D}} + 25$ (c 7.3, CHCl_3); IR (thin film): 2942, 2866, 1708, 1462, 1106 cm^{-1} ; ^1H NMR (600 MHz, CDCl_3) 3.84 (br, 2H), 3.70 (sextet, $J = 6.0$ Hz, 1H), 2.03 (s, 1H), 1.69 (dt, $J = 6.0, 12.0$ Hz, 2H), 1.24 (d, $J = 6.0$ Hz, 3H), 1.12-1.04 (m, 21 H); ^{13}C NMR (150 MHz, CDCl_3) δ 88.9, 68.2, 61.0, 39.8, 22.1, 20.9, 18.0, 12.0; HRMS (APCI) m/z calcd for $[\text{M}]^+$: $\text{C}_{15}\text{H}_{31}\text{OSi}$: 255.2144; found: 255.2165.



(S,E)-(5-Iodo-3,4-dimethylpent-4-enyloxy)triisopropylsilane (215): To a suspension of Cp_2ZrCl_2 (76 mg, 0.30 mmol) in CH_2Cl_2 (2 mL), was added 0.40 mL of AlMe_3 (2.0 M, 0.80 mmol) under N_2 atmosphere. After stirring

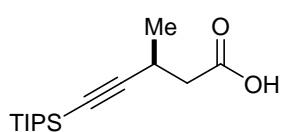
for 0.5 h, a solution of alkyne **214** (53 mg, 0.21 mmol) in CH_2Cl_2 (2 mL) was added dropwise. The resulting solution was stirred for 16 h at ambient temperature until all starting material was consumed as monitored by TLC. The mixture was cooled to -20°C and a solution of iodine (318 mg, 1.2 mmol) in THF (2 mL) was slowly introduced. After stirring for 30 min at -20°C , the reaction was warmed to 0°C . The reaction was then quenched with sat. aq. K_2CO_3 (1 mL) and extracted with ether (3 x 20 mL). The organic layer was washed with sat. aq. Na_2SO_3 solution, dried over Na_2SO_4 and concentrated. The residue was purified by flash chromatography (5% ethyl acetate in hexanes) to afford the title compound as a colorless oil (67 mg, 85%). $[\alpha]_{\text{D}} -2.9$ (c 1.1, CHCl_3); IR (thin film): 2939, 2865, 1458, 1105 cm^{-1} ; ^1H NMR

(300 MHz, CDCl₃) 5.97 (s, 1H), 3.67-3.54 (m, 2H), 2.03 (sextet, J = 6.9 Hz, 1H), 1.78 (s, 3H), 1.67 (dt, J = 5.7, 7.5 Hz, 1H), 1.56 (q, J = 6.9 Hz, 1H), 1.08-0.99 (m, 24H); ¹³C NMR (75 MHz, CDCl₃) δ 151.7, 61.1, 39.8, 37.9, 20.5, 19.4, 18.0, 12.0; HRMS (ESI) *m/z* calcd for (M⁺+H) C₁₆H₃₄OSi: 397.1424; found: 397.1438.



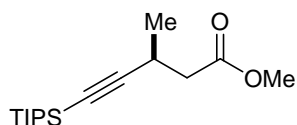
(S)-4-((Triisopropylsilyl)ethynyl)oxetan-2-one (153): TMS_{Qn} (2.0 g, 5.00 mmol) and MgCl₂ (4.75 g, 50.0 mmol) were dissolved in 50 mL diethyl ether

and 100 mL CH₂Cl₂ at room temperature and then cooled to -78 °C. To the above cooled mixture was added *N,N*-diisopropylethylamine (21.8 mL, 125 mmol), followed by aldehyde **152** (10.5 g, 50 mmol). A solution of acetyl chloride (7 mL, 100 mmol) in 50 mL CH₂Cl₂ was then added over 2 h by syringe pump. After being stirred overnight, the reaction was quenched at the reaction temperature by adding 200 mL Et₂O and filtered through a silica gel column and concentrated. The resulting crude product was purified by flash chromatography (10% ethyl acetate in hexanes) giving 9.88 g (78% yield) of the title compound as a colorless oil. [α]_D -0.76 (*c* 0.92, CHCl₃); IR (thin film): 2944, 2866, 1839, 1458, 1095 cm⁻¹; ¹H NMR (700 MHz, CDCl₃) 5.06 (dd, J = 4.2, 4.9 Hz, 1H), 3.81 (dd, J = 6.3, 16.1 Hz, 1H), 3.53 (dd, J = 4.9, 16.8 Hz, 1H), 1.11-1.06 (m, 21H); ¹³C NMR (150 MHz, CDCl₃) δ 167.0, 101.2, 92.9, 58.7, 46.6, 18.5, 11.0; HRMS (APCI) *m/z* calcd for [M]⁺ C₁₄H₂₄O₂Si: 252.1546; found: 252.1585.



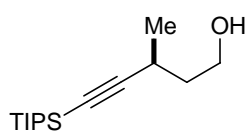
(S)-3-Methyl-5-(triisopropylsilyl)pent-4-ynoic acid (154): To a -50 °C solution of 1.28 g of CuBr (9.0 mmol) in 90 mL of THF and 3 mL of dimethylsulfide was added 6.0 mL of a 3 M ethereal solution of methylmagnesium bromide (18.0 mmol) slowly dropwise via syringe. The resulting heterogeneous mixture was stirred at -

50 °C for 30 min then warmed to –30 °C for 30 min. The reaction was then cooled to –50 °C and 1.50 g of lactone **153** (6.0 mmol) in 10 mL of THF was added via cannula. The resulting mixture was maintained at –50 °C for 45 min, then 1.1 mL of TMSCl (9.0 mmol) was added and the reaction was allowed to warm to ambient temperature overnight. Saturated aqueous NH₄Cl (300 mL) and 1 M HCl (100 mL) was added and the mixture was extracted with Et₂O (3 × 100 mL). The combined organics were washed with saturated aqueous NH₄Cl and brine (100 mL), dried over Na₂SO₄, filtered, and concentrated. The crude product was purified by MPLC three times (0-5% EtOAc/hexanes, then 30-100%, EtOAc/hexanes) to afford the title compound as a yellow oil (883 mg, 52% with about 5% of unisolatable impurity). [α]_D +9.8 (*c* 2.9, CHCl₃); IR (thin film): 2939, 2865, 2165, 1713, 1462 cm⁻¹; ¹H NMR (300 MHz, CDCl₃) 3.00 (sextet, *J* = 6.9 Hz, 1H), 2.62 (dd, *J* = 6.9, 16.0 Hz, 1H), 2.47 (dd, *J* = 8.4, 16.0 Hz, 1H), 1.27 (d, *J* = 6.9, 3H), 1.09-0.99 (m, 21H); ¹³C NMR (175 MHz, CDCl₃) δ 176.9, 111.1, 81.0, 41.5, 23.6, 20.8, 18.5, 11.1; HRMS (*ESI*) *m/z* calcd for (M–H)[–] C₁₅H₂₇O₂Si: 267.1780; found: 267.1792.

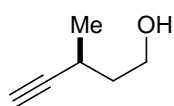


(S)-Methyl 3-methyl-5-(triisopropylsilyl)pent-4-ynoate (155): To a solution of 1.34 g of carboxylic acid **154** (5.0 mmol) in 21 mL of MeOH and 63 mL of toluene, was added 5.0 mL of a 2 M ethereal solution of trimethylsilyl diazomethane (10.0 mmol) slowly dropwise via syringe. The reaction was stirred for 2 h and concentrated. The residue was directly used to the next step with further purification. [α]_D +13 (*c* 0.6, CHCl₃); IR (thin film): 2943, 2865, 2165, 1744, 1462, 1168 cm⁻¹; ¹H NMR (700 MHz, CDCl₃) 3.80 (s, 3H), 3.01 (sextet, *J* = 9.0 Hz, 1H), 2.57 (dd, *J* = 7.8, 15.0 Hz, 1H), 2.44 (dd, *J* = 6.6, 15.6 Hz, 1H), 1.26 (d, *J* = 6.6 Hz, 3H), 1.09-1.00 (m, 21H); ¹³C NMR (150 MHz, CDCl₃) δ

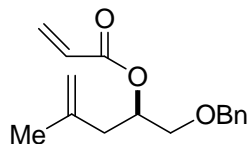
171.9, 111.5, 80.6, 51.6, 41.8, 23.9, 20.9, 18.6, 11.2; HRMS (APCI) m/z calcd for $[M+H]^+$ $C_{16}H_{31}O_2Si$:283.2093; found: 283.2065



(S)-3-Methyl-5-(triisopropylsilyl)pent-4-yn-1-ol (216a): To a 0 °C solution of 187 mg of ester **154** (0.66 mmol) in 10 mL of THF, was added 2.0 mL of a 1 M hexanes solution of DIBAL (2.0 mmol) dropwise via syringe. The reaction was stirred for 1 h at 0 °C and quenched with a saturated aqueous Rochelle's solution. The mixture was extracted by Et₂O. The organic extracts were combined and washed with Rochelle solution, brine and dried and concentrated. The residue was purified with MPLC (5%-20% ethyl acetate in hexanes) to afford the title compound as colorless oil (152 mg, 91%). $[\alpha]_D^{+21}$ (c 2.6, CHCl₃); IR (thin film): 3335, 2941, 2866, 2164, 1462, 1052 cm⁻¹; ¹H NMR (600 MHz, CDCl₃) 3.84 (m, 2H), 2.68 (sextet, J = 7.2 Hz, 1H), 1.83 (br, 1H), 1.79-1.74 (m, 1H), 1.72-1.66 (m, 1H), 1.25 (d, J = 7.2 Hz, 3H), 1.08-1.04 (m, 21H); ¹³C NMR (75 MHz, CDCl₃) δ 113.1, 81.0, 61.4, 39.5, 24.1, 21.5, 18.6, 11.2; HRMS (APCI) m/z calcd for $[M]^+$ $C_{15}H_{31}OSi$: 255.2144; found: 255.2178



(S)-3-Methylpent-4-yn-1-ol (216): To a solution of alcohol **216a** (152 mg, 0.60 mmol) in 2 mL of THF, was added 0.72 mL of a 1 M solution of TBAF (0.72 mmol) dropwise via syringe. The reaction was stirred for 3 h and quenched by adding 0.5 mL saturated aqueous NH₄Cl solution. The mixture was filtered through a plug of silica gel with ether/pentane (1:1) solution and concentrated carefully with rotavapor (low boil point) to afford 58 mg product with a trace amount of solvent (95%). ¹H NMR (300 MHz, CDCl₃) 3.84 (m, 2H), 2.68 (m, 1H), 2.09 (d, J = 2.4 Hz, 1H), 1.79-1.74 (m, 2H), 1.78-1.61 (m, 1H), 1.25 (d, J = 6.9 Hz, 3H); ¹³C NMR (125 MHz, CDCl₃) δ 88.4, 68.9, 61.0, 39.3, 22.6, 21.0, 15.3, 14.0;



(R)-1-(Benzyloxy)-4-methylpent-4-en-2-yl acrylate (185): To a 0 °C

solution of 2.06 g of alcohol **184** (10.0 mmol), 3.15 ml of diisopropylethylamine (2.34 g, 19 mmol) and 0.122 g of DMAP (1 mmol)

in 60 mL of CH₂Cl₂, was added 1.22 mL of acryloyl chloride (15 mmol) dropwise via syringe.

The reaction was stirred for 24 h and quenched with aq. sat. NaHCO₃ solution, extracted with ether, dried with Na₂SO₄ and concentrated. The residue was purified by flash chromatography

(10% ethyl acetate in hexane) to afford 2.32 g (89%) of the title compound as a colorless oil.

[α]_D +7.0 (c 3.4, CHCl₃); IR (thin film): 3073, 2862, 1723, 1453, 1405, 1269, 1193 cm⁻¹; ¹H

NMR (300 MHz, CDCl₃) 7.40-7.28 (m, 5H), 6.16 (dd, J = 17.4, 1.5 Hz, 1H), 6.44 (dd, J = 17.1,

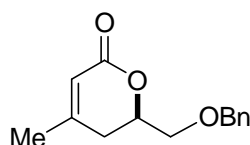
9.9 Hz, 1H), 5.84 (dd, J = 10.5, 1.5 Hz, 1H), 5.33 (tdd, J = 6.6, 4.9, 4.8 Hz, 1H), 4.79 (dd, J =

15.1, 1. Hz, 12H), 4.57 (q, J = 12.3 Hz, 1H), 3.60 (d, J = 4.8 Hz, 2H), 2.40 (d, J = 7.2 Hz, 2H),

1.79 (s, 3H); ¹³C NMR (75 MHz, CDCl₃) δ 165.8, 141.1, 138.1, 130.8, 128.6, 128.4, 127.7,

127.6, 113.6, 73.2, 71.0, 70.9, 39.3, 22.5; HRMS (APCI) *m/z* calcd for [M+H]⁺ C₁₆H₂₁O₃:

261.1491; found: 261.1481.



(R)-6-(Benzyloxymethyl)-4-methyl-5,6-dihydropyran-2-one (186): 1.78

g of ester **185** (6.8 mmol) was dissolved in 350 mL of degassed CH₂Cl₂

and heated to reflux. A solution of 462 mg of Grubbs II catalyst (0.54

mmol) in 5 ml of CH₂Cl₂ was added via cannula to the refluxed solution. The resulting mixture

was refluxed for overnight and condensed. The residue was purified with flash chromatography

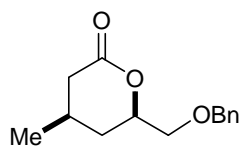
(20%, 50% ethyl acetate in hexanes) to yield 1.37 g of the title compound as a slightly red oil

(86%). [α]_D +117 (c 3.0, CHCl₃); IR (thin film): 2910, 2866, 1720, 1453, 1387, 1247, 1125 cm⁻¹;

¹H NMR (300 MHz, CDCl₃) 7.41-7.27 (m, 5H), 5.80 (s, 1H), 4.59 (s, 2H), 4.59-4.52 (m, 1H),

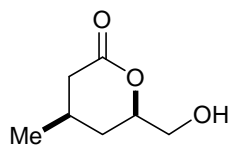
3.68 (d, J = 3 Hz, 2H), 2.55 (dd, J = 12.0, 18.0 Hz, 1H), 2.26 (dd, J = 3.0, 18.0 Hz, 1H), 1.98 (s,

3H); ^{13}C NMR (75 MHz, CDCl_3) δ 164.6, 157.3, 137.7, 128.5, 127.9, 127.8, 116.2, 76.0, 73.6, 70.8, 31.4, 23.1; HRMS (APCI) m/z calcd for $[\text{M}]^+$: $\text{C}_{14}\text{H}_{17}\text{O}_3$: 233.1178; found: 233.1198.



(4R,6R)-6-(Benzyloxymethyl)-4-methyl-tetrahydropyran-2-one (187):

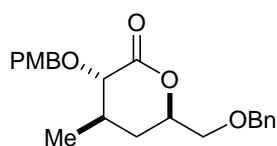
To a solution of 1.37 g of **186** (5.90 mmol) in 40 mL of benzene under nitrogen atmosphere, 611 mg of 10% Pd/C was added. After two vacuum/ H_2 cycles to replace nitrogen with hydrogen, the reaction was stirred for overnight under 1 atm pressure of hydrogen (balloon). The reaction mixture was then filtered through a plug of celite, the filtrate was concentrated. The crude product was purified with flash chromatography (30-50% ethyl acetate in hexanes) to afford 1.15 g of the title compound as colorless oil (83%). $[\alpha]_{\text{D}} +4.7$ (c 2.0, CHCl_3); IR (thin film): 2910, 2866, 1720, 1453, 1387, 1247, 1125 cm^{-1} ; ^1H NMR (600 MHz, CDCl_3) 7.38-7.28 (m, 5H), 5.80 (s, 1H), 4.59 (s, 2H), 4.47 (dddd, 12.1, 4.5, 4.5, 3.4 Hz, 1H), 3.65-3.60 (m, 2H), 2.69 (dd, $J = 9.6, 2.4$ Hz, 1H), 2.08-2.03 (m, 2H), 1.97 (d, $J = 13.2$ Hz, 1H), 1.43 (dd, $J = 12.0, 2.4$ Hz, 1H), 1.09 (d, $J = 6.4$ Hz, 3H); ^{13}C NMR (150 MHz, CDCl_3) δ 170.9, 137.7, 128.4, 127.7, 127.6, 79.2, 73.5, 71.9, 38.1, 33.4, 26.5, 21.5; HRMS (APCI) m/z calcd for $[\text{M}]^+$: $\text{C}_{14}\text{H}_{17}\text{O}_3$: 233.1334; found: 233.1365



(4R,6R)-6-(Hydroxymethyl)-4-methyl-tetrahydropyran-2-one (188):

To a solution of 240 mg of **187** (1.0 mmol) in 20 mL of methanol under nitrogen atmosphere, 52 mg of 10% Pd/C was added. After two vacuum/ H_2 cycles to replace nitrogen with hydrogen, the reaction was stirred for overnight under 1 atm pressure of hydrogen (balloon). The reaction mixture was then filter through a plug of celite, the filtrate was concentrated to afford 142 mg of the title compound as white solid (98%). $[\alpha]_{\text{D}} -11$

(*c* 1.7, CHCl₃); IR (thin film): 3432, 2961, 2930, 1708, 1457, 1376, 1265, 1064, 1091 cm⁻¹; ¹H NMR (700 MHz, CDCl₃) 4.43 (tdd, *J* = 11.9, 2.8, 2.8 Hz, 1H), 3.83 (d, *J* = 11.9 Hz, 1H), 3.67 (dd, *J* = 11.9, 4.2 Hz, 1H), 2.71 (dd, *J* = 16.8, 4.2 Hz, 1H), 2.38 (br, 1H), 2.15-2.06 (m, 1H), 2.10-2.05 (m, 1H), 1.88 (dd, *J* = 16.8, 5.6 Hz, 1H), 1.44 (q, *J* = 14.0 Hz, 1H), 1.08 (d, *J* = 6.3 Hz, 3H); ¹³C NMR (150 MHz, CDCl₃) δ 171.1, 81.1, 64.9, 38.0, 32.4, 26.4, 21.5; X-ray crystallography was used to verify the stereochemistry.

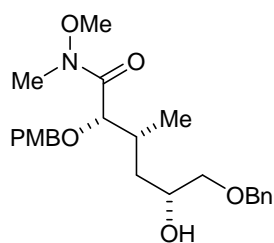


(3*S*,4*R*,6*R*)-6-(Benzyloxymethyl)-3-hydroxy-4-methyl-

tetrahydropyran-2-one (190a): To a 0 °C solution of diisopropylamine (101 mg, 1 mmol) in 3.4 mL THF, was added 0.63 mL BuLi (1.6 M in

hexanes, 1 mmol). After stirred at 0 °C for 10 min, 4 mL LDA (0.25 M) stock solution was made. A round bottom flask was charged with dry nitrogen and filled with 3.67 mL LDA (0.25 M, 0.91 mmol) and 0.3 mL of TMEDA (1.9 mmol) at -45 °C. To the resulting solution, was added a solution of 180 mg of lactone **187** in 1 mL of THF. Reaction was stirred at the same temperature for 30 min and then cooled to -78 °C. A solution of (1*R*)-(-)-(10-camphorsulfonyl)oxaziridine (351 mg, 1.53 mmol) in 5 mL of THF was cannulated to the reaction and stirred for 2 h. The reaction was quenched with aq. sat. NH₄Cl and extracted with ether (3 x 50 mL), dried with Na₂SO₄ and concentrated. The residue was purified with MPLC (20% to 50% ethyl acetate in hexanes) to afford title compound as colorless oil (125 mg, 63%, contains tiny amount of unisolatable impurities). To a -78 °C solution of alcohol **189** (680 mg, 2.72 mmol) and 4-methoxybenzyl-2,2,2-trichloroacetimidate (1.15 g, 4.08 mmol) in 10 mL CH₂Cl₂, was added a solution of BF₃ etherate (0.4 mL, 1 M in CH₂Cl₂, 0.4 mmol). After stirring for 4 h, the reaction was quenched by adding a saturated aqueous solution of NaHCO₃ and

extracted with CH₂Cl₂ (3×30 mL). The combined organic extracts were dried (Na₂SO₄), and concentrated to provide a yellow oil that was triturated with CH₂Cl₂ and hexanes and the resulting white solid was removed by filtration. The filtrate was concentrated and purified by flash chromatography (2.5-5% ethyl acetate in hexanes) to afford 887 mg (88%) of the title compound as a clear colorless oil. $[\alpha]_D -40$ (*c* 2.3, CHCl₃); IR (thin film): 2917, 2851, 1736, 1161, 1511, 1454, 1243, 1094, 1028 cm⁻¹; ¹H NMR (600 MHz, CDCl₃) 7.39-7.31 (m, 7H), 6.90 (d, *J* = 7.8 Hz, 2H), 5.00 (d, *J* = 11.4 Hz, 1H), 4.61 (d, *J* = 11.4 Hz, 1H), 4.59 (s, 2H), 4.68-4.55 (m, 1H), 3.82 (s, 3H), 3.61 (dd, *J* = 4.8, 11.4 Hz, 2H), 3.55 (d, *J* = 9.6 Hz, 1H), 2.20-2.13 (m, 1H), 1.99 (dt, *J* = 14.3, 3.8 Hz, 1H), 1.61 (dd, *J* = 12.6, 25.6 Hz, 1H), 1.06 (d, *J* = 6.4 Hz, 3H); ¹³C NMR (150 MHz, CDCl₃) δ 171.3, 159.5, 137.7, 130.2, 129.5, 128.5, 127.8, 127.7, 113.8, 79.4, 78.3, 73.6, 73.5, 71.7, 33.2, 32.9, 18.9; HRMS (*ESI*) *m/z* calcd for [M+Na]⁺ C₂₂H₂₆O₅Na: 393.1678; found: 393.1674.

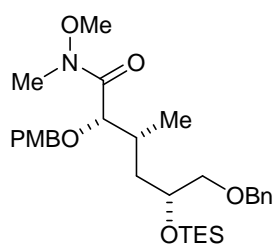


(2*S*,3*R*,5*R*)-6-(Benzyloxy)-5-hydroxy-*N*-methoxy-2-(4-

methoxybenzyloxy)-*N*,3-dimethylhexanamide (190): To a solution of Weinreb's salt (624 mg, 6.40 mmol) in 20 mL CH₂Cl₂ at 0 °C, Me₃Al (3.2 mL, 2.0 M in hexane, 6.40 mmol) was added dropwise and then

warmed to ambient temperature. After being stirred for 1 h, a solution of crude lactone **190a** (470 mg, 1.28 mmol) in 10 mL CH₂Cl₂ was added at 0 °C. The resulting mixture was stirred 1.5 h, then quenched with aqueous saturated Rochelle's solution and the biphasic mixture was stirred vigorously for 1 h. Then the organic layer was separated and the aqueous layer was extracted with ether. The organic extracts were combined, dried (Na₂SO₄) and concentrated. The residue was purified by flash chromatography (70% ethyl acetate in hexanes), affording 495 mg (90%)

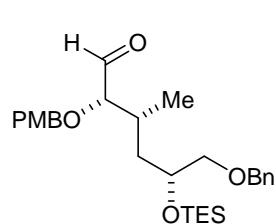
of the title compound as a colorless oil. $[\alpha]_D -16$ (c 1.0, CHCl_3); IR (thin film): 3445, 2931, 1734, 1698, 1651, 1512, 1456, 1247, 1097, 1031 cm^{-1} ; ^1H NMR (300 MHz, CDCl_3) 7.40-7.25 (m, 7H), 6.87 (d, $J = 8.4$ Hz, 2H), 4.67 (d, $J = 12.0$ Hz, 1H), 4.56 (s, 2H), 4.29 (d, $J = 12.0$ Hz, 1H), 4.21 (br, 1H), 3.89-3.84 (m, 1H), 3.81 (s, 3H), 3.57 (s, 3H), 3.48 (dd, $J = 9.0, 3.3$ Hz, 2H), 3.32 (dd, $J = 9.0, 7.2$ Hz, 2H), 3.23 (s, 3H), 2.24 (br, 2H), 1.54 (dddd, $J = 14.4, 9.3, 5.1$ Hz, 1H), 1.44-1.35 (m, 1H), 0.99 (d, $J = 7.2$ Hz, 3H); ^{13}C NMR (175 MHz, CDCl_3) δ 172.7, 159.3, 138.0, 130.2, 129.6, 128.5, 127.8, 127.8, 113.7, 78.3, 75.1, 73.4, 71.2, 68.5, 61.2, 55.3, 36.9, 33.2, 32.1, 14.2; HRMS (ESI) m/z calcd for $[\text{M}+\text{Na}]^+ \text{C}_{24}\text{H}_{33}\text{NO}_6\text{Na}$: 454.2206; found: 454.2186.



(2S,3R,5R)-6-(Benzyloxy)-N-methoxy-2-(4-methoxybenzyloxy)-N,3-dimethyl-5-(triethylsilyloxy)hexanamide (191): To a solution of alcohol **190** (43 mg, 0.01mmol) in 2 mL DMF was added imidazole (0.21 mg, 0.03 mmol). Triethylsilyl chloride (23 mg, 0.015 mmol) was added

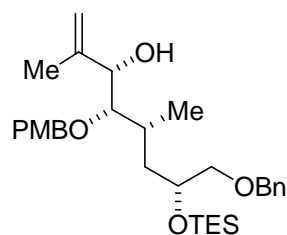
and the reaction was allowed to stir for overnight. The reaction was quenched by adding a saturated aqueous solution of NaHCO_3 and extracted with ether (3×10 mL). The combined organic extracts were dried (Na_2SO_4) and concentrated. The residue was purified by flash chromatography (30% ethyl acetate in hexanes), affording 50 mg (92%) of the title compound as a colorless oil. $[\alpha]_D -13.5$ (c 1.2, CHCl_3); IR (thin film): 2917, 2851, 1736, 1511, 1454, 1243, 1094, 1028 cm^{-1} ; ^1H NMR (600 MHz, CDCl_3) 7.38-7.28 (m, 7H), 6.87 (d, $J = 8.4$ Hz, 2H), 4.67 (d, $J = 12.0$ Hz, 1H), 4.53 (s, 2H), 4.29 (d, $J = 12$ Hz, 1H), 4.11 (br, 1H), 3.91-3.89 (m, 1H), 3.82 (s, 3H), 3.55 (s, 3H), 3.40-3.35 (m, 2H), 3.22 (s, 3H), 2.20 (br, 1H), 1.58-1.56 (m, 1H), 1.51-1.47 (m, 1H), 0.98 (d, $J = 6.6$ Hz, 3H), 0.94 (t, $J = 8.4$ Hz, 9H), 0.64-0.54 (m, 6H); ^{13}C NMR (150 MHz, CDCl_3) δ 172.8, 159.2, 138.4, 130.1, 129.6, 128.3, 127.6, 127.5, 113.7, 79.3, 75.4, 73.3,

71.2, 69.2, 61.1, 55.3, 39.0, 32.3, 31.3, 13.8, 6.9, 5.1; HRMS (*ESI*) m/z calcd for $[M+Na]^+$ $C_{30}H_{47}NO_6NaSi$: 568.3070; found: 568.3074.



(2*S*,3*R*,5*R*)-6-(Benzyloxy)-2-(4-methoxybenzyloxy)-3-methyl-5-(triethylsilyloxy)hexanal (169): To a solution of amide **191** in 20 mL

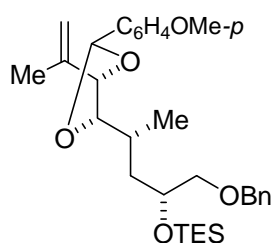
THF at 0 °C was added a solution of $LiAlH_4$ (0.46 mL, 1M in THF, 0.46 mmol). The reaction was allowed to stir for 15 min at 0 °C and quenched by adding a saturated aqueous solution of Rochelle salt and extracted with diethyl ether (3×30 mL). The combined organic extracts were dried (Na_2SO_4) and concentrated. The resulting crude oil was purified by flash chromatography (10-20% ethyl acetate in hexanes), affording 135 mg (89%) of the title compound as a colorless oil. $[\alpha]_D -2.3$ (c 1.1, $CHCl_3$); IR (thin film): 2954, 2875, 1731, 1612, 1513, 1456, 1248, 1110, 1033, 1010 cm^{-1} ; 1H NMR (300 MHz, $CDCl_3$) 9.63 (d, $J = 2.1$ Hz, 1H), 7.37-7.27 (m, 7H), 6.89 (d, $J = 6.6$ Hz, 2H), 4.63 (d, $J = 11.4$ Hz, 1H), 4.52 (s, 2H), 4.29 (d, $J = 11.4$ Hz, 1H), 3.93-3.91 (m, 1H), 3.82 (s, 3H), 3.62 (dd, $J = 4.5, 2.1$ Hz, 1H), 3.42-3.30 (m, 2H), 2.26 (br, 1H), 1.57-1.48 (m, 2H), 0.98-0.92 (m, 12H), 0.64-0.56 (m, 6H); ^{13}C NMR (75 MHz, $CDCl_3$) δ 204.4, 159.4, 138.3, 129.7, 129.6, 128.4, 127.7, 127.6, 113.8, 87.3, 75.3, 72.5, 69.0, 55.3, 38.0, 30.8, 14.2, 6.9, 5.1; HRMS (*ESI*) m/z calcd for $[M+Na]^+$ $C_{28}H_{42}O_5NaSi$: 509.2699; found: 509.2679.



(3*S*,4*S*,5*R*,7*R*)-8-(Benzyloxy)-4-(4-methoxybenzyloxy)-2,5-dimethyl-7-(triethylsilyloxy)oct-1-en-3-ol (217): A solution of isoprenyl

magnesium bromide (2.2 mL, 0.5 M in THF, 0.55 mmol) was evaporated to dried under vacuo at -78 °C. The residue was redissolved

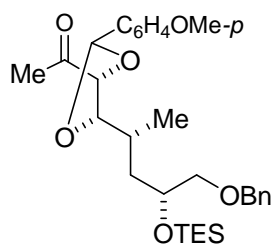
in 10 mL CH₂Cl₂ at -78 °C. To the resulting solution, a solution of aldehyde **169** (135 mg, 0.278 mol) in 5 mL CH₂Cl₂ was added dropwise at -78 °C. After stirred at the same temperature for 10 min, the reaction was quenched with a saturated aqueous solution of NH₄Cl and extracted with ether (3×30 mL). The combined organic extracts were dried and concentrated. The residue was purified by flash chromatography (10-20% ethyl acetate in hexanes), affording 124 mg (84%, d.r 7:1) of the title compound as a colorless oil. [α]_D +21 (*c* 1.1, CHCl₃); IR (thin film): 3500, 2952, 2876, 1612, 1513, 1456, 1248, 1080, 1035 cm⁻¹; ¹H NMR (700 MHz, CDCl₃) 7.36-7.29 (m, 7H), 6.89 (d, *J* = 8.4 Hz, 2H), 5.06 (s, 1H), 4.94 (s, 1H), 4.65 (d, *J* = 10.5 Hz, 1H), 4.55 (d, *J* = 10.5 Hz, 1H), 4.54 (s, 2H), 4.09 (t, *J* = 6.3 Hz, 1H), 3.92 (t, *J* = 6.3 Hz, 1H), 3.83 (s, 3H), 3.43-3.41 (m, 1H), 3.38-3.35 (m, 2H), 2.63 (d, *J* = 4.2 Hz, 1H), 2.01 (br, 1H), 1.77 (s, 3H), 1.60-1.58 (m, 2H), 0.97-0.94 (m, 12H), 0.64-0.58 (m, 6H); ¹³C NMR (75 MHz, CDCl₃) δ 159.3, 144.9, 138.3, 130.6, 129.5, 128.3, 127.7, 127.5, 113.8, 113.6, 84.9, 76.1, 75.5, 74.4, 73.3, 69.1, 55.3, 40.0, 30.7, 17.8, 13.4, 6.9, 5.1; HRMS (*ESI*) *m/z* calcd for [M+Na]⁺ C₃₁H₄₈O₅NaSi: 551.3169; found: 551.3150.



((2R,4R)-1-(Benzyloxy)-4-((4S,5S)-2-(4-methoxyphenyl)-5-(prop-1-en-2-yl)-1,3-dioxolan-4-yl)pentan-2-yloxy)triethylsilane (218): To a

mixture of azeotropically dried 113 (37 mg, 0.070 mmol) and 128 mg of activated powdered 4 Å molecular sieves in 1 mL of CH₂Cl₂ was added the azeotropically dried DDQ (19 mg, 0.084 mmol) at 0 °C by syringe. After stirring 2 h, the reaction was load on silica gel column and eluted with 5-10% EtOAc in hexanes to afford the title compound as colorless oil (29 mg, 74%). [α]_D +4.3 (*c* 0.53, CHCl₃); IR (thin film): 2953, 2876, 1615, 1517, 1457, 1249, 1080, 1033 cm⁻¹; ¹H NMR (300 MHz, CDCl₃) 7.45 (d, *J* = 6.6 Hz,

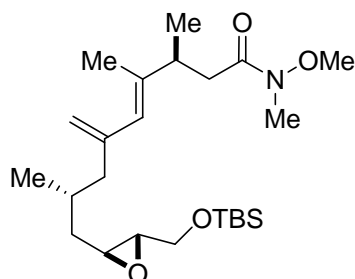
2H), 7.36-7.28 (m, 5H), 6.92 (d, $J = 6.6$ Hz, 2H), 5.91 (s, 1H), 5.08 (s, 1H), 4.95 (s, 1H), 4.53 (s, 2H), 4.39 (d, $J = 7.2$ Hz, 1H), 3.99-3.92 (m, 1H), 3.87 (dd, $J = 7.2, 4.2$ Hz, 1H), 3.83 (s, 3H), 3.42-3.36 (m, 2H), 2.06 (m, 1H), 1.67 (s, 3H), 1.63-1.54 (m, 2H), 1.09 (d, $J = 6.6$ Hz, 3H), 0.97 (t, $J = 8.1$ Hz, 12H), 0.67-0.58 (m, 6H); ^{13}C NMR (75 MHz, CDCl_3) δ 160.4, 143.4, 138.3, 130.3, 128.3, 128.2, 127.7, 127.6, 113.7, 113.2, 103.7, 84.9, 82.3, 75.5, 73.4, 69.1, 55.3, 39.5, 30.9, 18.0, 13.4, 6.9, 5.1; HRMS (ESI) m/z calcd for $[\text{M}+\text{Na}]^+$ $\text{C}_{31}\text{H}_{46}\text{O}_5\text{NaSi}$: 549.3012; found: 549.3027.



1-((4R,5S)-5-((2R,4R)-5-(Benzyloxy)-4-(triethylsilyloxy)pentan-2-yl)-2-(4-methoxyphenyl)-1,3-dioxolan-4-yl)ethanone (200): A gaseous stream of ozone in O_2 (generated using a standard ozonizer) was bubbled through a -78 °C solution of **218** (17 mg, 0.032 mmol) in 5 mL CH_2Cl_2

until the reaction mixture becomes blue. Triphenylphosphine (20 mg, 0.076 mmol) was added at -78 °C and the reaction was warmed to ambient temperature and stirred for 2 h. The reaction was then condensed under vacuuo. The residue was loaded on the a silica gel and firstly eluted with 5% ethyl acetate in hexanes to get rid of triphosphine then eluted with 20% ethyl acetate in hexanes to afford 15 mg of the tile compound as colorless oil (88%). $[\alpha]_{\text{D}} +14$ (c 1.4, CHCl_3); IR (thin film): 2954, 2876, 1718, 1615, 1517, 1456, 1250, 1088, 1033 cm^{-1} ; ^1H NMR (700 MHz, CDCl_3) 7.46 (d, $J = 8.4$ Hz, 2H), 7.37-7.29 (m, 5H), 6.94 (d, $J = 8.4$ Hz, 2H), 5.85 (s, 1H), 4.53 (s, 2H), 4.31 (d, $J = 6.3$ Hz, 1H), 4.05 (t, $J = 5.6$ Hz, 1H), 3.97-3.96 (m, 1H), 3.85 (s, 3H), 3.42 (dd, $J = 9.1, 5.6$ Hz, 1H), 3.37 (dd, $J = 9.1, 5.6$ Hz, 1H), 2.34 (s, 3H), 2.15-2.11 (m, 1H), 1.66 (m, 1H), 1.52 (ddd, $J = 13.8, 10.7, 2.9$ Hz, 1H), 1.09 (d, $J = 7.0$ Hz, 3H), 0.97 (t, $J = 7.7$ Hz, 9H), 0.66-0.60 (m, 6H); ^{13}C NMR (75 MHz, CDCl_3) δ 209.2, 160.7, 138.2, 128.7, 128.3, 127.7, 127.5,

113.8, 104.4, 83.4, 82.9, 75.3, 73.3, 69.0, 55.3, 38.7, 31.9, 26.8, 14.0, 6.9, 5.1; HRMS (ESI) m/z calcd for $[M+Na]^+$ $C_{30}H_{44}O_6NaSi$: 551.2805; found: 551.2773.



(3*S*,8*R*,*E*)-9-((2*S*,3*S*)-3-((*tert*-

Butyldimethylsilyloxy)methyl)oxiran-2-yl)-*N*-methoxy-*N*,3,4,8-

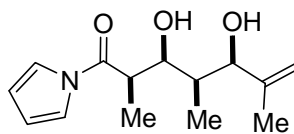
tetramethyl-6-methylenenon-4-enamide (130): A mixture of of

iodide **211** (6 mg, 0.02 mmol) boronic ester **199** (12 mg, 0.03

mmol) and palladium(dppf)dichloride (7 mg, 0.008 mmol) was evacuated and refilled under nitrogen twice. To this was added DMF 0.5 mL and $Ba(OH)_2 \cdot 8H_2O$ (19 mg, 0.06 mmol) followed by 2 rapid evacuation and N_2 refilling cycles. The resulting red solution was stirred at 45 °C for 20 min, during which time it developed a dark brown color. The reaction mixture was directly loaded on the silica gel column and eluted with (10% ethyl acetate in hexanes) to afford 6.6 mg of title compound as colorless oil (73%). 1H NMR (300 MHz, $CDCl_3$) 5.62 (s, 1H), 4.97 (s, 1H), 4.82 (s, 1H), 3.78 (dd, $J = 12.0, 6.3$, Hz, 1H), 3.75 (s, 3H), 3.76-3.70 (m, 1H), 3.18 (s, 3H), 2.84-2.76 (m, 3H), 2.58 (dd, $J = 14.7, 6.3$ Hz, 1H), 2.38 (dd, $J = 15.0, 8.4$, 1H), 2.12 (11.1, 4.2 Hz, 1H), 1.94 (dd, $J = 13.2, 7.8$ Hz, 1H), 1.59 (s, 3H), 1.29-1.19 (m, 3H), 1.09 (d, $J = 6.9$ Hz, 3H), 0.92 (dd, $J = 9.0$ Hz, 3H), 0.89 (s, 9H), 0.08 (s, 3H), 0.07 (s, 3H).

APPENDIX

X-RAY DATA



84

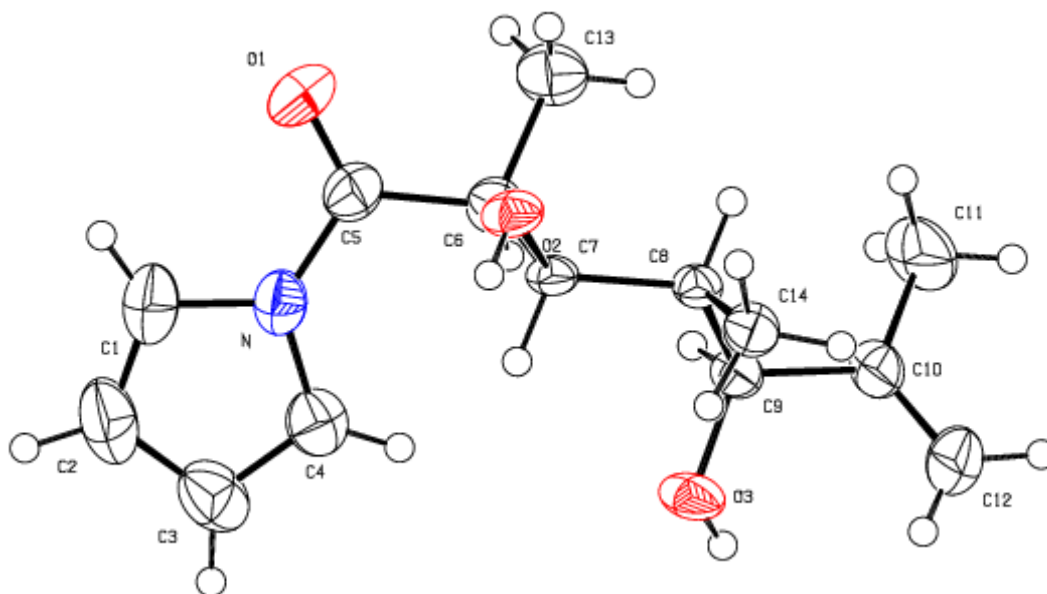


Table 11. Crystal data and structure refinement for **84**

Identification code	df82208s	
Empirical formula	C ₁₄ H ₂₁ N O ₃	
Formula weight	251.32	
Temperature	203(2) K	
Wavelength	0.71073 Å	
Crystal system	Monoclinic	
Space group	P 21	
Unit cell dimensions	a = 10.009(3) Å	α = 90°.
	b = 6.8235(18) Å	β = 105.554(5)°.
	c = 10.630(3) Å	γ = 90°.
Volume	699.4(3) Å ³	
Z	2	
Density (calculated)	1.193 Mg/m ³	
Absorption coefficient	0.083 mm ⁻¹	
F(000)	272	
Crystal size	0.32 x 0.18 x 0.02 mm ³	
Theta range for data collection	1.99 to 32.27°.	
Index ranges	-14 ≤ h ≤ 14, -10 ≤ k ≤ 9, -15 ≤ l ≤ 15	
Reflections collected	8690	
Independent reflections	2512 [R(int) = 0.0564]	
Completeness to theta = 30.00°	100.0 %	
Absorption correction	Semi-empirical from equivalents	
Max. and min. transmission	0.9983 and 0.9738	
Refinement method	Full-matrix least-squares on F ²	
Data / restraints / parameters	2512 / 1 / 174	
Goodness-of-fit on F ²	0.963	
Final R indices [I > 2σ(I)]	R1 = 0.0607, wR2 = 0.1267	
R indices (all data)	R1 = 0.1144, wR2 = 0.1524	
Largest diff. peak and hole	0.255 and -0.173 e.Å ⁻³	

Table 12. Atomic coordinates ($\times 10^4$) and equivalent isotropic displacement parameters ($\text{\AA}^2 \times 10^3$) for **81**

U(eq) is defined as one third of the trace of the orthogonalized U^{ij} tensor.

	x	y	z	U(eq)
N	7338(3)	3655(4)	11854(2)	43(1)
O(1)	6469(3)	6346(4)	10689(2)	68(1)
C(1)	7566(4)	4581(7)	13058(3)	59(1)
O(2)	8808(2)	5015(3)	9330(2)	35(1)
C(2)	8053(4)	3240(7)	13991(4)	69(1)
O(3)	8658(3)	-995(3)	8979(2)	43(1)
C(3)	8150(4)	1417(7)	13377(3)	59(1)
C(4)	7706(3)	1697(5)	12076(3)	46(1)
C(5)	6788(3)	4658(5)	10667(3)	44(1)
C(6)	6668(3)	3495(5)	9420(3)	38(1)
C(7)	8128(3)	3164(3)	9236(3)	27(1)
C(8)	8124(3)	2118(4)	7951(2)	28(1)
C(9)	7631(3)	-15(4)	7983(2)	32(1)
C(10)	7345(3)	-1002(4)	6666(3)	40(1)
C(11)	6025(4)	-387(7)	5700(3)	66(1)
C(12)	8194(5)	-2319(6)	6386(4)	63(1)
C(13)	5688(3)	4576(7)	8271(3)	55(1)
C(14)	9544(3)	2235(5)	7675(3)	36(1)

Table 13. Bond lengths [\AA] and angles [$^\circ$] for **84**

N-C(4)	1.389(5)
N-C(1)	1.391(4)
N-C(5)	1.411(4)
O(1)-C(5)	1.197(4)
C(1)-C(2)	1.341(6)
C(1)-H(1A)	0.9400
O(2)-C(7)	1.425(3)
O(2)-H(2O)	0.86(4)
C(2)-C(3)	1.421(6)
C(2)-H(2A)	0.9400
O(3)-C(9)	1.429(3)
O(3)-H(3O)	0.81(6)
C(3)-C(4)	1.348(5)
C(3)-H(3A)	0.9400
C(4)-H(4A)	0.9400
C(5)-C(6)	1.521(4)
C(6)-C(13)	1.535(4)
C(6)-C(7)	1.543(4)
C(6)-H(6A)	0.9900
C(7)-C(8)	1.540(3)
C(7)-H(7A)	0.9900
C(8)-C(14)	1.528(4)
C(8)-C(9)	1.540(4)
C(8)-H(8A)	0.9900
C(9)-C(10)	1.510(4)
C(9)-H(9A)	0.9900
C(10)-C(12)	1.325(5)
C(10)-C(11)	1.499(5)
C(11)-H(11A)	0.9700
C(11)-H(11B)	0.9700
C(11)-H(11C)	0.9700
C(12)-H(12A)	0.9400
C(12)-H(12B)	0.9400

C(13)-H(13A)	0.9700
C(13)-H(13B)	0.9700
C(13)-H(13C)	0.9700
C(14)-H(14A)	0.9700
C(14)-H(14B)	0.9700
C(14)-H(14C)	0.9700
C(4)-N-C(1)	108.0(3)
C(4)-N-C(5)	129.8(3)
C(1)-N-C(5)	122.1(3)
C(2)-C(1)-N	108.0(4)
C(2)-C(1)-H(1A)	126.0
N-C(1)-H(1A)	126.0
C(7)-O(2)-H(2O)	103(3)
C(1)-C(2)-C(3)	108.3(3)
C(1)-C(2)-H(2A)	125.9
C(3)-C(2)-H(2A)	125.9
C(9)-O(3)-H(3O)	108(3)
C(4)-C(3)-C(2)	107.6(4)
C(4)-C(3)-H(3A)	126.2
C(2)-C(3)-H(3A)	126.2
C(3)-C(4)-N	108.1(3)
C(3)-C(4)-H(4A)	126.0
N-C(4)-H(4A)	126.0
O(1)-C(5)-N	119.4(3)
O(1)-C(5)-C(6)	124.1(3)
N-C(5)-C(6)	116.5(3)
C(5)-C(6)-C(13)	109.1(3)
C(5)-C(6)-C(7)	109.3(2)
C(13)-C(6)-C(7)	113.2(2)
C(5)-C(6)-H(6A)	108.4
C(13)-C(6)-H(6A)	108.4
C(7)-C(6)-H(6A)	108.4
O(2)-C(7)-C(8)	111.1(2)
O(2)-C(7)-C(6)	108.2(2)
C(8)-C(7)-C(6)	113.8(2)

O(2)-C(7)-H(7A)	107.9
C(8)-C(7)-H(7A)	107.9
C(6)-C(7)-H(7A)	107.9
C(14)-C(8)-C(7)	111.4(2)
C(14)-C(8)-C(9)	111.9(2)
C(7)-C(8)-C(9)	110.1(2)
C(14)-C(8)-H(8A)	107.8
C(7)-C(8)-H(8A)	107.8
C(9)-C(8)-H(8A)	107.8
O(3)-C(9)-C(10)	113.5(3)
O(3)-C(9)-C(8)	106.7(2)
C(10)-C(9)-C(8)	112.5(2)
O(3)-C(9)-H(9A)	108.0
C(10)-C(9)-H(9A)	108.0
C(8)-C(9)-H(9A)	108.0
C(12)-C(10)-C(11)	122.4(3)
C(12)-C(10)-C(9)	122.5(3)
C(11)-C(10)-C(9)	115.1(3)
C(10)-C(11)-H(11A)	109.5
C(10)-C(11)-H(11B)	109.5
H(11A)-C(11)-H(11B)	109.5
C(10)-C(11)-H(11C)	109.5
H(11A)-C(11)-H(11C)	109.5
H(11B)-C(11)-H(11C)	109.5
C(10)-C(12)-H(12A)	120.0
C(10)-C(12)-H(12B)	120.0
H(12A)-C(12)-H(12B)	120.0
C(6)-C(13)-H(13A)	109.5
C(6)-C(13)-H(13B)	109.5
H(13A)-C(13)-H(13B)	109.5
C(6)-C(13)-H(13C)	109.5
H(13A)-C(13)-H(13C)	109.5
H(13B)-C(13)-H(13C)	109.5
C(8)-C(14)-H(14A)	109.5
C(8)-C(14)-H(14B)	109.5
H(14A)-C(14)-H(14B)	109.5

C(8)-C(14)-H(14C) 109.5

H(14A)-C(14)-H(14C) 109.5

H(14B)-C(14)-H(14C) 109.5

Symmetry transformations used to generate equivalent atoms:

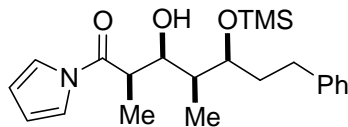
Table 14. Anisotropic displacement parameters ($\text{\AA}^2 \times 10^3$) for **84**

The anisotropic displacement factor exponent takes the form: $-2\pi^2 [h^2 a^{*2} U^{11} + \dots + 2 h k a^* b^* U^{12}]$

	U^{11}	U^{22}	U^{33}	U^{23}	U^{13}	U^{12}
N	44(1)	49(2)	38(1)	-7(1)	16(1)	1(1)
O(1)	83(2)	52(2)	66(2)	-9(1)	18(1)	29(2)
C(1)	65(2)	70(3)	48(2)	-15(2)	25(2)	-2(2)
O(2)	36(1)	21(1)	44(1)	1(1)	2(1)	-1(1)
C(2)	74(3)	97(4)	40(2)	-7(2)	21(2)	-1(3)
O(3)	56(1)	21(1)	40(1)	4(1)	-9(1)	-4(1)
C(3)	59(2)	75(3)	48(2)	14(2)	20(2)	1(2)
C(4)	44(2)	53(2)	45(2)	2(2)	20(1)	-4(2)
C(5)	38(2)	49(2)	46(2)	-3(2)	14(1)	10(2)
C(6)	32(1)	41(2)	38(2)	-3(1)	6(1)	2(1)
C(7)	28(1)	19(1)	30(1)	3(1)	2(1)	1(1)
C(8)	32(1)	22(1)	27(1)	2(1)	3(1)	-1(1)
C(9)	37(1)	25(1)	29(1)	0(1)	2(1)	-4(1)
C(10)	53(2)	28(1)	32(1)	-4(1)	2(1)	-9(1)
C(11)	65(2)	66(3)	48(2)	-10(2)	-17(2)	-8(2)
C(12)	96(3)	44(2)	46(2)	-11(2)	15(2)	7(2)
C(13)	37(2)	71(3)	54(2)	2(2)	4(1)	16(2)
C(14)	40(1)	33(2)	36(2)	3(1)	13(1)	-2(1)

Table 15. Hydrogen coordinates ($\times 10^4$) and isotropic displacement parameters ($\text{\AA}^2 \times 10^3$) for**84**

	x	y	z	U(eq)
H(1A)	7407	5912	13194	71
H(2O)	9620(40)	4780(70)	9840(40)	59(11)
H(2A)	8289	3468	14896	83
H(3O)	8490(50)	-2150(90)	8920(40)	86(16)
H(3A)	8466	229	13801	71
H(4A)	7654	735	11431	55
H(6A)	6257	2202	9515	45
H(7A)	8654	2337	9967	32
H(8A)	7449	2801	7233	33
H(9A)	6757	2	8250	38
H(11A)	5921	-1100	4890	98
H(11B)	6056	1009	5535	98
H(11C)	5245	-671	6050	98
H(12A)	7978	-2906	5556	75
H(12B)	9012	-2668	7018	75
H(13A)	4833	4896	8490	83
H(13B)	5483	3742	7504	83
H(13C)	6128	5772	8092	83
H(14A)	9738	3582	7494	53
H(14B)	9545	1424	6926	53
H(14C)	10251	1771	8431	53



68

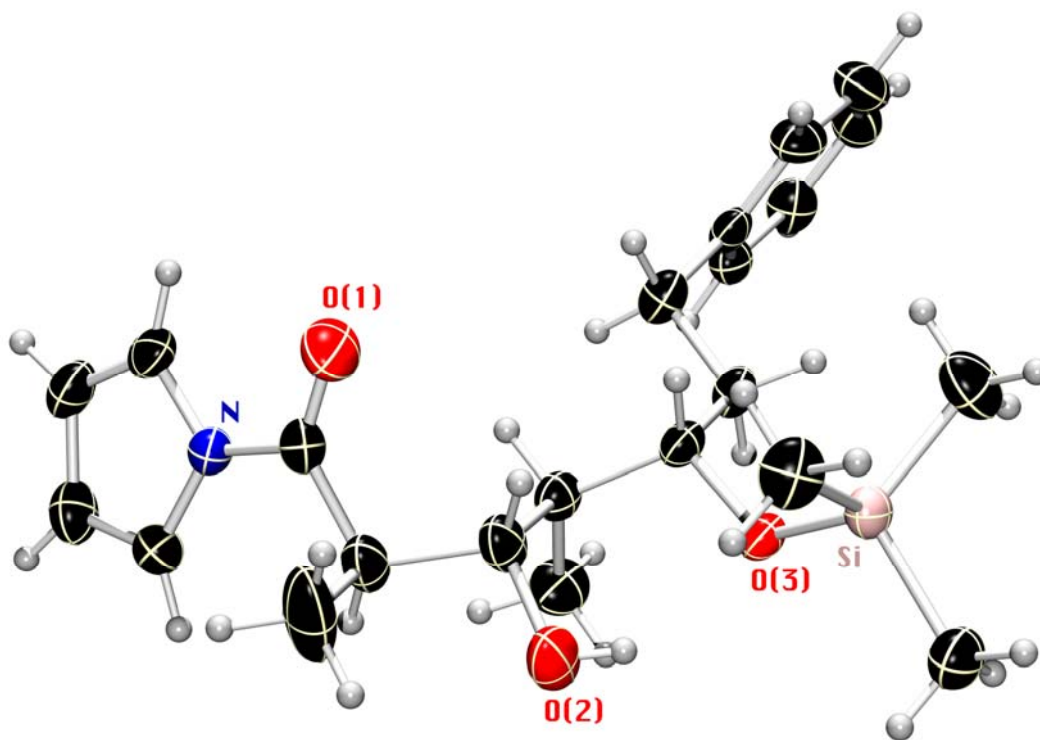


Table 16. Crystal data and structure refinement for **68**

Identification code	df2s	
Empirical formula	C ₁₅ H ₂₀ O ₃	
Formula weight	248.31	
Temperature	173(2) K	
Wavelength	0.71073 Å	
Crystal system	Orthorhombic	
Space group	P2(1)2(1)2(1)	
Unit cell dimensions	a = 7.3606(11) Å	α = 90°.
	b = 7.5782(12) Å	β = 90°.
	c = 24.352(4) Å	γ = 90°.
Volume	1358.4(4) Å ³	

Z	4
Density (calculated)	1.214 Mg/m ³
Absorption coefficient	0.083 mm ⁻¹
F(000)	536
Crystal size	0.45 x 0.40 x 0.02 mm ³
Theta range for data collection	1.67 to 28.35°.
Index ranges	-9<=h<=9, -10<=k<=10, -32<=l<=32
Reflections collected	13924
Independent reflections	3380 [R(int) = 0.0652]
Completeness to theta = 28.35°	99.7 %
Absorption correction	multi-scan (SADABS)
Max. and min. transmission	0.9983 and 0.9635
Refinement method	Full-matrix least-squares on F ²
Data / restraints / parameters	3380 / 0 / 243
Goodness-of-fit on F ²	1.123
Final R indices [I>2sigma(I)]	R1 = 0.0715, wR2 = 0.1442
R indices (all data)	R1 = 0.1097, wR2 = 0.1605
Largest diff. peak and hole	0.579 and -0.197 e.Å ⁻³

Table 17. Atomic coordinates ($\times 10^4$) and equivalent isotropic displacement parameters $(\text{\AA}^2 \times 10^3)$ for **68**U(eq) is defined as one third of the trace of the orthogonalized U^{ij} tensor.

	x	y	z	U(eq)
O(1)	4908(3)	5279(3)	7123(1)	48(1)
O(2)	-1419(3)	4503(3)	7181(1)	53(1)
O(3)	46(2)	4285(3)	7952(1)	38(1)
C(1)	1732(4)	4065(4)	8269(1)	33(1)
C(2)	3296(4)	5053(4)	8008(1)	33(1)
C(3)	3465(4)	4441(4)	7414(1)	38(1)
C(4)	1756(4)	4792(5)	7093(1)	45(1)
C(5)	27(4)	4463(4)	7411(1)	36(1)
C(6)	1249(4)	4607(4)	8846(1)	36(1)
C(7)	-341(5)	3594(5)	9100(1)	44(1)
C(8)	-2069(4)	5672(4)	9711(1)	43(1)
C(9)	-2515(5)	6343(5)	10217(1)	54(1)
C(10)	-1774(5)	5658(5)	10683(1)	55(1)
C(11)	-579(5)	4286(5)	10640(1)	54(1)
C(12)	-117(4)	3597(4)	10133(1)	47(1)
C(13)	-857(3)	4289(4)	9656(1)	35(1)
C(14)	5056(4)	4740(5)	8323(1)	42(1)
C(15)	1711(5)	3873(5)	6543(1)	46(1)

Table 18. lengths [\AA] and angles [$^\circ$] for **68**

O(1)-C(3)	1.425(3)
O(1)-H(10)	1.12(5)
O(2)-C(5)	1.203(3)
O(3)-C(5)	1.323(3)
O(3)-C(1)	1.472(3)
C(1)-C(6)	1.507(4)
C(1)-C(2)	1.514(4)
C(1)-H(1)	0.98(3)
C(2)-C(14)	1.524(4)
C(2)-C(3)	1.525(4)
C(2)-H(2)	0.95(3)
C(3)-C(4)	1.505(4)
C(3)-H(3)	1.05(3)
C(4)-C(15)	1.510(4)
C(4)-C(5)	1.511(4)
C(4)-H(4)	1.17(4)
C(6)-C(7)	1.530(4)
C(6)-H(6A)	0.94(3)
C(6)-H(6B)	1.00(3)
C(7)-C(13)	1.501(4)
C(7)-H(7B)	1.01(3)
C(7)-H(7A)	0.86(3)
C(8)-C(9)	1.373(4)
C(8)-C(13)	1.383(4)
C(8)-H(8)	0.96(3)
C(9)-C(10)	1.362(5)
C(9)-H(9)	0.88(3)
C(10)-C(11)	1.366(5)
C(10)-H(10)	0.89(3)
C(11)-C(12)	1.383(5)
C(11)-H(11)	0.89(3)
C(12)-C(13)	1.386(4)
C(12)-H(12)	0.91(3)

C(14)-H(14A)	0.98(3)
C(14)-H(14B)	0.93(3)
C(14)-H(14C)	0.94(4)
C(15)-H(15A)	0.92(4)
C(15)-H(15B)	1.04(4)
C(15)-H(15C)	0.93(4)

C(3)-O(1)-H(10)	99(2)
C(5)-O(3)-C(1)	122.9(2)
O(3)-C(1)-C(6)	105.1(2)
O(3)-C(1)-C(2)	111.3(2)
C(6)-C(1)-C(2)	115.9(2)
O(3)-C(1)-H(1)	104.6(16)
C(6)-C(1)-H(1)	110.2(16)
C(2)-C(1)-H(1)	109.0(17)
C(1)-C(2)-C(14)	110.9(2)
C(1)-C(2)-C(3)	108.1(2)
C(14)-C(2)-C(3)	111.2(2)
C(1)-C(2)-H(2)	105.5(16)
C(14)-C(2)-H(2)	107.0(16)
C(3)-C(2)-H(2)	114.1(15)
O(1)-C(3)-C(4)	106.7(2)
O(1)-C(3)-C(2)	113.3(2)
C(4)-C(3)-C(2)	111.8(2)
O(1)-C(3)-H(3)	111.0(14)
C(4)-C(3)-H(3)	101.2(14)
C(2)-C(3)-H(3)	112.1(13)
C(3)-C(4)-C(15)	113.4(3)
C(3)-C(4)-C(5)	114.1(3)
C(15)-C(4)-C(5)	111.2(3)
C(3)-C(4)-H(4)	99.7(19)
C(15)-C(4)-H(4)	111.1(18)
C(5)-C(4)-H(4)	106.6(19)
O(2)-C(5)-O(3)	118.4(2)
O(2)-C(5)-C(4)	120.1(3)
O(3)-C(5)-C(4)	121.2(2)

C(1)-C(6)-C(7)	114.9(2)
C(1)-C(6)-H(6A)	106.9(15)
C(7)-C(6)-H(6A)	107.1(16)
C(1)-C(6)-H(6B)	109.6(17)
C(7)-C(6)-H(6B)	107.5(17)
H(6A)-C(6)-H(6B)	111(2)
C(13)-C(7)-C(6)	112.5(2)
C(13)-C(7)-H(7B)	111.4(17)
C(6)-C(7)-H(7B)	106.8(19)
C(13)-C(7)-H(7A)	114(2)
C(6)-C(7)-H(7A)	112(2)
H(7B)-C(7)-H(7A)	100(3)
C(9)-C(8)-C(13)	121.4(3)
C(9)-C(8)-H(8)	120.2(18)
C(13)-C(8)-H(8)	118.4(18)
C(10)-C(9)-C(8)	120.7(3)
C(10)-C(9)-H(9)	123(2)
C(8)-C(9)-H(9)	117(2)
C(9)-C(10)-C(11)	119.0(3)
C(9)-C(10)-H(10)	122(2)
C(11)-C(10)-H(10)	119(2)
C(10)-C(11)-C(12)	120.9(3)
C(10)-C(11)-H(11)	125(2)
C(12)-C(11)-H(11)	114(2)
C(11)-C(12)-C(13)	120.6(3)
C(11)-C(12)-H(12)	120(2)
C(13)-C(12)-H(12)	120(2)
C(8)-C(13)-C(12)	117.4(3)
C(8)-C(13)-C(7)	121.0(3)
C(12)-C(13)-C(7)	121.6(3)
C(2)-C(14)-H(14A)	106.2(17)
C(2)-C(14)-H(14B)	111.1(16)
H(14A)-C(14)-H(14B)	113(2)
C(2)-C(14)-H(14C)	110(2)
H(14A)-C(14)-H(14C)	105(3)
H(14B)-C(14)-H(14C)	111(3)

C(4)-C(15)-H(15A) 110(2)
C(4)-C(15)-H(15B) 110.3(19)
H(15A)-C(15)-H(15B) 118(3)
C(4)-C(15)-H(15C) 115(3)
H(15A)-C(15)-H(15C) 106(3)
H(15B)-C(15)-H(15C) 98(3)

Symmetry transformations used to generate equivalent atoms:

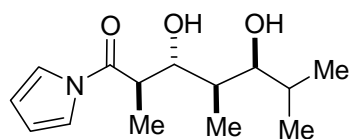
Table 19. Anisotropic displacement parameters ($\text{\AA}^2 \times 10^3$) for **68**

The anisotropic displacement factor exponent takes the form: $-2\pi^2 [h^2 a^{*2} U^{11} + \dots + 2 h k a^* b^* U^{12}]$

U^{11}	U^{22}	U^{33}	U^{23}	U^{13}	U^{12}
O(1)33(1)	57(1)	53(1)	7(1)	1(1)	-4(1)
O(2)25(1)	81(2)	54(1)	6(1)	-3(1)	-2(1)
O(3)24(1)	52(1)	40(1)	-3(1)	0(1)	-2(1)
C(1)26(1)	34(2)	40(2)	-2(1)	-2(1)	-2(1)
C(2)25(1)	33(1)	41(2)	0(1)	-3(1)	-4(1)
C(3)31(1)	40(2)	43(2)	1(1)	1(1)	-3(1)
C(4)31(1)	58(2)	45(2)	-6(2)	3(1)	-3(2)
C(5)27(1)	40(1)	43(2)	-1(1)	-2(1)	0(1)
C(6)30(1)	37(2)	40(2)	-4(1)	1(1)	0(1)
C(7)43(2)	45(2)	44(2)	-10(2)	5(2)	-6(2)
C(8)43(2)	48(2)	38(2)	0(2)	-5(1)	4(1)
C(9)49(2)	58(2)	55(2)	-10(2)	5(2)	10(2)
C(10)63(2)	62(2)	39(2)	-10(2)	10(2)	-8(2)
C(11)64(2)	61(2)	38(2)	15(2)	-12(2)	-11(2)
C(12)41(2)	41(2)	59(2)	5(2)	-8(2)	1(2)
C(13)30(1)	37(2)	37(2)	-1(1)	2(1)	-6(1)
C(14)26(1)	54(2)	45(2)	4(2)	-2(1)	-7(2)
C(15)36(2)	61(2)	41(2)	2(2)	1(2)	-6(2)

Table 20. Hydrogen coordinates ($\times 10^4$) and isotropic displacement parameters ($\text{\AA}^2 \times 10^3$) for**68**

	x	y	z	U(eq)
H(1O)	6060(70)	4460(70)	7280(17)	115(16)
H(1)	1980(40)	2800(40)	8255(10)	33(7)
H(2)	3010(30)	6270(40)	8046(10)	24(7)
H(3)	3560(30)	3070(30)	7383(9)	20(6)
H(4)	1880(50)	6330(50)	7039(14)	77(11)
H(6A)	910(30)	5800(30)	8832(10)	24(7)
H(6B)	2330(40)	4440(40)	9093(12)	45(8)
H(7B)	40(40)	2320(40)	9120(12)	51(9)
H(7A)	-1240(50)	3500(40)	8875(13)	52(10)
H(8)	-2590(40)	6170(40)	9383(12)	41(8)
H(9)	-3340(50)	7180(40)	10222(13)	60(11)
H(10)	-2090(40)	6030(40)	11017(13)	46(9)
H(11)	-60(50)	3740(40)	10924(14)	62(10)
H(12)	750(40)	2740(50)	10112(13)	51(9)
H(14A)	4870(40)	5250(40)	8688(12)	36(7)
H(14B)	6050(40)	5240(40)	8140(11)	30(7)
H(14C)	5240(50)	3530(50)	8382(14)	66(11)
H(15A)	2730(50)	4160(50)	6346(14)	69(11)
H(15B)	1400(50)	2550(50)	6592(14)	74(11)
H(15C)	730(60)	4170(60)	6320(16)	80(13)



81

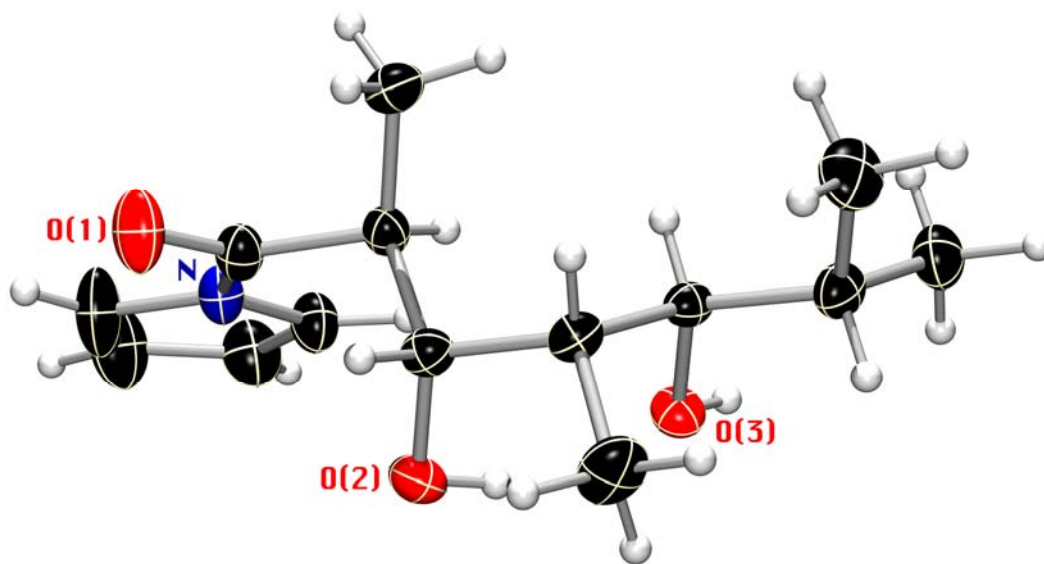


Table 21. Crystal data and structure refinement for **81**

Identification code	dfu226s	
Empirical formula	C ₁₄ H ₂₃ N O ₃	
Formula weight	253.33	
Temperature	173(2) K	
Wavelength	0.71073 Å	
Crystal system	Orthorhombic	
Space group	P2(1)2(1)2(1)	
Unit cell dimensions	a = 7.563(2) Å	α = 90°.
	b = 9.182(2) Å	β = 90°.
	c = 20.472(5) Å	γ = 90°.

Volume	1421.5(6) Å ³
Z	4
Density (calculated)	1.184 Mg/m ³
Absorption coefficient	0.082 mm ⁻¹
F(000)	552
Crystal size	0.30 x 0.25 x 0.14 mm ³
Theta range for data collection	1.99 to 32.62°.
Index ranges	-11<=h<=10, -13<=k<=13, -30<=l<=30
Reflections collected	17492
Independent reflections	2912 [R(int) = 0.0432]
Completeness to theta = 32.62°	98.8 %
Absorption correction	None
Max. and min. transmission	0.9886 and 0.9757
Refinement method	Full-matrix least-squares on F ²
Data / restraints / parameters	2912 / 0 / 255
Goodness-of-fit on F ²	1.023
Final R indices [I>2sigma(I)]	R1 = 0.0471, wR2 = 0.1131
R indices (all data)	R1 = 0.0616, wR2 = 0.1212
Absolute structure parameter	-1.2(11)
Largest diff. peak and hole	0.345 and -0.175 e.Å ⁻³

Table 22. Atomic coordinates ($\times 10^4$) and equivalent isotropic displacement parameters $(\text{\AA}^2 \times 10^3)$ for **81**U(eq) is defined as one third of the trace of the orthogonalized U_{ij} tensor.

	x	y	z	U(eq)
N	9901(2)	1942(1)	3424(1)	29(1)
O(1)	11255(2)	368(1)	2745(1)	44(1)
C(1)	10827(3)	1518(2)	3979(1)	49(1)
O(2)	6517(2)	610(1)	2601(1)	33(1)
C(2)	10271(4)	2334(3)	4486(1)	53(1)
O(3)	4825(2)	2847(1)	2027(1)	28(1)
C(3)	8961(3)	3289(2)	4252(1)	43(1)
C(4)	8742(2)	3039(2)	3605(1)	34(1)
C(5)	10173(2)	1329(2)	2808(1)	28(1)
C(6)	9124(2)	1927(2)	2236(1)	24(1)
C(7)	7686(2)	816(2)	2055(1)	25(1)
C(8)	6657(2)	1199(2)	1432(1)	25(1)
C(9)	5887(2)	2755(2)	1447(1)	22(1)
C(10)	4822(2)	3150(2)	835(1)	28(1)
C(11)	4128(3)	4703(2)	866(1)	37(1)
C(12)	5935(3)	2951(3)	224(1)	43(1)
C(13)	10419(2)	2209(2)	1675(1)	35(1)
C(14)	5250(3)	37(2)	1305(1)	40(1)

Table 23. Bond lengths [\AA] and angles [$^\circ$] for **81**

N-C(4)	1.385(2)
N-C(1)	1.389(2)
N-C(5)	1.398(2)
O(1)-C(5)	1.210(2)
C(1)-C(2)	1.347(3)
C(1)-H(1)	0.90(3)
O(2)-C(7)	1.4378(19)
O(2)-H(2O)	0.84(3)
C(2)-C(3)	1.408(3)
C(2)-H(2)	0.99(3)
O(3)-C(9)	1.4366(17)
O(3)-H(3O)	0.86(3)
C(3)-C(4)	1.354(3)
C(3)-H(3)	0.91(3)
C(4)-H(4)	0.98(2)
C(5)-C(6)	1.517(2)
C(6)-C(13)	1.532(2)
C(6)-C(7)	1.537(2)
C(6)-H(6)	0.91(2)
C(7)-C(8)	1.534(2)
C(7)-H(7)	0.95(2)
C(8)-C(14)	1.529(2)
C(8)-C(9)	1.543(2)
C(8)-H(8)	0.932(19)
C(9)-C(10)	1.533(2)
C(9)-H(9)	0.964(19)
C(10)-C(12)	1.519(2)
C(10)-C(11)	1.521(3)
C(10)-H(10)	0.92(2)
C(11)-H(11C)	0.98(2)
C(11)-H(11A)	1.02(2)
C(11)-H(11B)	0.95(3)
C(12)-H(12B)	0.98(2)

C(12)-H(12C)	1.00(3)
C(12)-H(12A)	0.96(2)
C(13)-H(13B)	0.96(2)
C(13)-H(13C)	0.92(3)
C(13)-H(13A)	0.95(3)
C(14)-H(14C)	0.96(2)
C(14)-H(14A)	0.98(3)
C(14)-H(14B)	0.99(3)
C(4)-N-C(1)	107.75(14)
C(4)-N-C(5)	128.83(13)
C(1)-N-C(5)	123.42(15)
C(2)-C(1)-N	108.43(18)
C(2)-C(1)-H(1)	134.0(16)
N-C(1)-H(1)	117.3(16)
C(7)-O(2)-H(2O)	102.3(17)
C(1)-C(2)-C(3)	107.70(18)
C(1)-C(2)-H(2)	125(2)
C(3)-C(2)-H(2)	127(2)
C(9)-O(3)-H(3O)	114.0(16)
C(4)-C(3)-C(2)	108.24(18)
C(4)-C(3)-H(3)	126.2(17)
C(2)-C(3)-H(3)	125.6(17)
C(3)-C(4)-N	107.88(16)
C(3)-C(4)-H(4)	132.4(13)
N-C(4)-H(4)	119.6(13)
O(1)-C(5)-N	119.26(14)
O(1)-C(5)-C(6)	122.43(14)
N-C(5)-C(6)	118.30(14)
C(5)-C(6)-C(13)	107.80(14)
C(5)-C(6)-C(7)	108.44(12)
C(13)-C(6)-C(7)	112.54(13)
C(5)-C(6)-H(6)	112.2(11)
C(13)-C(6)-H(6)	107.3(11)
C(7)-C(6)-H(6)	108.6(12)
O(2)-C(7)-C(8)	111.33(13)

O(2)-C(7)-C(6)	109.54(12)
C(8)-C(7)-C(6)	114.06(12)
O(2)-C(7)-H(7)	106.6(11)
C(8)-C(7)-H(7)	107.0(11)
C(6)-C(7)-H(7)	108.0(11)
C(14)-C(8)-C(7)	109.58(14)
C(14)-C(8)-C(9)	112.76(13)
C(7)-C(8)-C(9)	112.81(12)
C(14)-C(8)-H(8)	108.1(12)
C(7)-C(8)-H(8)	105.4(11)
C(9)-C(8)-H(8)	107.8(13)
O(3)-C(9)-C(10)	111.57(12)
O(3)-C(9)-C(8)	106.32(11)
C(10)-C(9)-C(8)	113.67(12)
O(3)-C(9)-H(9)	107.3(10)
C(10)-C(9)-H(9)	108.3(10)
C(8)-C(9)-H(9)	109.5(11)
C(12)-C(10)-C(11)	109.73(16)
C(12)-C(10)-C(9)	110.69(14)
C(11)-C(10)-C(9)	111.69(13)
C(12)-C(10)-H(10)	109.3(14)
C(11)-C(10)-H(10)	107.8(14)
C(9)-C(10)-H(10)	107.5(13)
C(10)-C(11)-H(11C)	112.7(15)
C(10)-C(11)-H(11A)	108.7(15)
H(11C)-C(11)-H(11A)	107.5(18)
C(10)-C(11)-H(11B)	109.7(14)
H(11C)-C(11)-H(11B)	109.2(19)
H(11A)-C(11)-H(11B)	109.0(19)
C(10)-C(12)-H(12B)	114.2(14)
C(10)-C(12)-H(12C)	113.0(16)
H(12B)-C(12)-H(12C)	102(2)
C(10)-C(12)-H(12A)	112.4(13)
H(12B)-C(12)-H(12A)	107.0(19)
H(12C)-C(12)-H(12A)	108(2)
C(6)-C(13)-H(13B)	112.8(14)

C(6)-C(13)-H(13C) 108.5(15)
H(13B)-C(13)-H(13C) 110(2)
C(6)-C(13)-H(13A) 110.4(17)
H(13B)-C(13)-H(13A) 107(2)
H(13C)-C(13)-H(13A) 108(2)
C(8)-C(14)-H(14C) 112.9(16)
C(8)-C(14)-H(14A) 108.7(15)
H(14C)-C(14)-H(14A) 104(2)
C(8)-C(14)-H(14B) 106.1(15)
H(14C)-C(14)-H(14B) 113(2)
H(14A)-C(14)-H(14B) 112(2)

Symmetry transformations used to generate equivalent atoms:

Table 24. Anisotropic displacement parameters ($\text{\AA}^2 \times 10^3$) for **81**

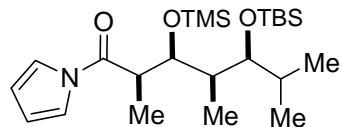
The anisotropic displacement factor exponent takes the form: $-2 \left[h^2 a^{*2} U^{11} + \dots + 2 \right]$

$h \ k \ a^* \ b^* \ U^{12} \]$

	U^{11}	U^{22}	U^{33}	U^{23}	U^{13}	U^{12}
N 33(1)	26(1)	28(1)	-1(1)	-7(1)	5(1)	
O(1)53(1)	34(1)	44(1)	-7(1)	-12(1)	19(1)	
C(1)60(1)	47(1)	40(1)	-6(1)	-23(1)	23(1)	
O(2)34(1)	31(1)	33(1)	8(1)	5(1)	-3(1)	
C(2)72(2)	56(1)	33(1)	-6(1)	-16(1)	14(1)	
O(3)31(1)	29(1)	23(1)	-1(1)	5(1)	2(1)	
C(3)51(1)	45(1)	32(1)	-5(1)	1(1)	9(1)	
C(4)36(1)	34(1)	32(1)	1(1)	-1(1)	10(1)	
C(5)30(1)	22(1)	33(1)	-2(1)	-6(1)	1(1)	
C(6)25(1)	21(1)	27(1)	1(1)	-3(1)	-1(1)	
C(7)25(1)	22(1)	29(1)	-2(1)	1(1)	-2(1)	
C(8)23(1)	25(1)	26(1)	-5(1)	1(1)	-1(1)	
C(9)21(1)	26(1)	20(1)	-1(1)	1(1)	-3(1)	
C(10)26(1)	35(1)	23(1)	-2(1)	-3(1)	-1(1)	
C(11)38(1)	41(1)	31(1)	4(1)	-5(1)	5(1)	
C(12)45(1)	60(1)	23(1)	0(1)	3(1)	8(1)	
C(13)24(1)	44(1)	37(1)	6(1)	1(1)	-5(1)	
C(14)37(1)	30(1)	54(1)	-11(1)	-9(1)	-8(1)	

Table 25. Hydrogen coordinates ($\times 10^4$) and isotropic displacement parameters ($\text{\AA}^2 \times 10^3$) for**81**

	x	y	z	U(eq)
H(1)	11690(40)	850(30)	3926(12)	53(7)
H(2O)	5760(30)	1270(40)	2543(12)	57(8)
H(2)	10720(40)	2250(40)	4938(16)	92(10)
H(3O)	4420(30)	3700(30)	2105(11)	48(7)
H(3)	8380(30)	3980(30)	4495(13)	59(7)
H(4)	7940(30)	3460(30)	3277(10)	41(6)
H(6)	8590(20)	2790(20)	2333(9)	19(4)
H(7)	8250(20)	-90(20)	1978(9)	23(4)
H(8)	7480(30)	1160(20)	1095(9)	28(5)
H(9)	6840(20)	3450(20)	1493(8)	18(4)
H(10)	3860(30)	2530(20)	817(10)	35(5)
H(11C)	3310(30)	4860(30)	1228(11)	42(6)
H(11A)	3460(30)	4920(30)	443(11)	49(6)
H(11B)	5090(30)	5360(30)	906(10)	42(6)
H(12B)	5360(30)	3270(30)	-179(11)	50(6)
H(12C)	6190(40)	1910(40)	124(13)	71(8)
H(12A)	7050(30)	3460(30)	250(10)	42(6)
H(13B)	9890(30)	2750(20)	1321(11)	40(5)
H(13C)	11380(40)	2700(30)	1837(12)	53(7)
H(13A)	10830(40)	1320(30)	1499(12)	58(7)
H(14C)	4720(40)	120(30)	882(12)	50(7)
H(14A)	4270(30)	190(30)	1608(12)	54(7)
H(14B)	5840(30)	-910(30)	1376(12)	49(6)



78

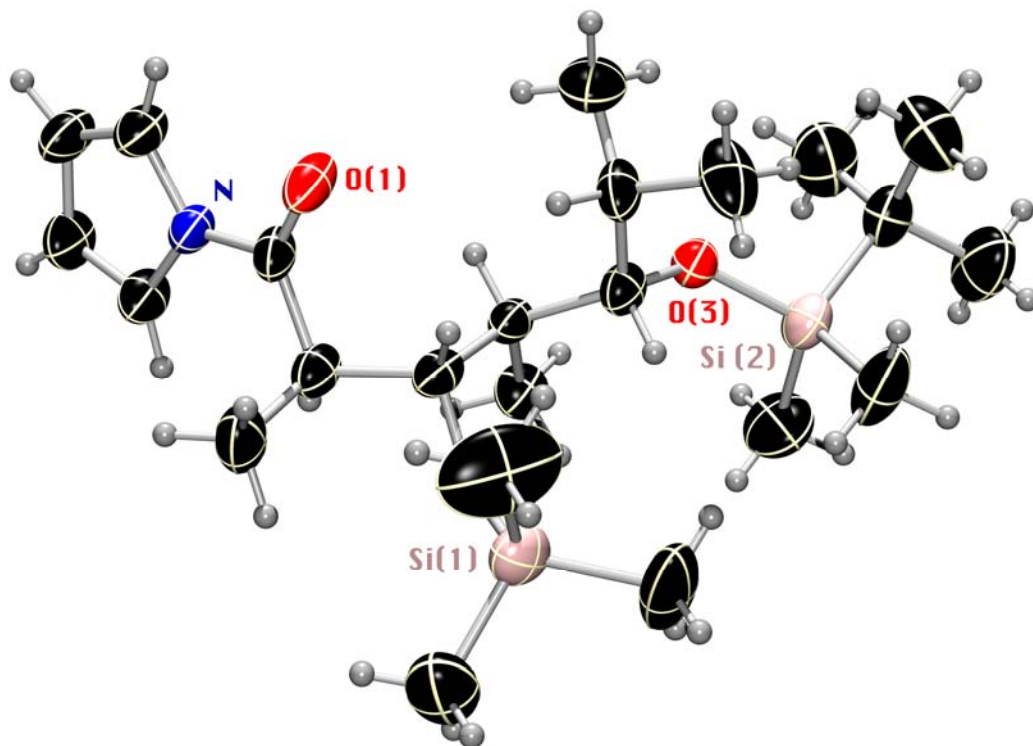


Table 26. Crystal data and structure refinement for **78**

Identification code	dfu917s	
Empirical formula	C ₂₃ H ₄₅ N O ₃ Si ₂	
Formula weight	439.78	
Temperature	203(2) K	
Wavelength	0.71073 Å	
Crystal system	Monoclinic	
Space group	P2(1)	
Unit cell dimensions	a = 8.5435(18) Å	α = 90°.
	b = 11.216(3) Å	β = 105.368(5)°.
	c = 15.340(3) Å	γ = 90°.
Volume	1417.3(5) Å ³	

Z	2
Density (calculated)	1.031 Mg/m ³
Absorption coefficient	0.145 mm ⁻¹
F(000)	484
Crystal size	0.27 x 0.23 x 0.18 mm ³
Theta range for data collection	2.28 to 25.00°.
Index ranges	-10<=h<=10, -13<=k<=13, -18<=l<=18
Reflections collected	11307
Independent reflections	4973 [R(int) = 0.0749]
Completeness to theta = 25.00°	100.0 %
Absorption correction	None
Max. and min. transmission	0.9743 and 0.9618
Refinement method	Full-matrix least-squares on F ²
Data / restraints / parameters	4973 / 1 / 263
Goodness-of-fit on F ²	0.895
Final R indices [I>2sigma(I)]	R1 = 0.0660, wR2 = 0.1399
R indices (all data)	R1 = 0.1159, wR2 = 0.1637
Absolute structure parameter	0.0(2)
Largest diff. peak and hole	0.207 and -0.232 e.Å ⁻³

Table 27. Atomic coordinates ($\times 10^4$) and equivalent isotropic displacement parameters $(\text{\AA}^2 \times 10^3)$ for **78**.U(eq) is defined as one third of the trace of the orthogonalized U_{ij} tensor.

	x	y	z	U(eq)
Si(1)	13969(2)	9803(1)	8491(1)	56(1)
Si(2)	8185(2)	9671(1)	5562(1)	51(1)
O(1)	9698(5)	11989(3)	9791(2)	59(1)
O(2)	12225(3)	9495(3)	8699(2)	44(1)
O(3)	8140(4)	10350(2)	6511(2)	43(1)
N	8882(5)	10655(3)	10680(2)	41(1)
C(1)	8806(6)	9550(4)	11076(3)	49(1)
C(2)	7835(6)	9662(5)	11636(3)	57(1)
C(3)	7307(7)	10868(4)	11602(3)	57(1)
C(4)	7970(6)	11450(5)	11025(3)	49(1)
C(5)	9766(6)	10976(4)	10071(3)	43(1)
C(6)	10836(5)	10033(4)	9817(3)	45(1)
C(7)	12482(6)	10064(6)	10535(3)	64(2)
C(8)	11001(5)	10271(4)	8864(3)	40(1)
C(9)	14517(11)	11389(7)	8738(7)	134(3)
C(10)	15499(7)	8848(7)	9203(4)	85(2)
C(11)	13870(7)	9461(10)	7314(4)	123(4)
C(12)	9413(6)	10078(4)	8128(3)	38(1)
C(13)	9005(6)	8764(4)	7966(3)	49(1)
C(14)	9446(6)	10724(4)	7247(3)	40(1)
C(15)	9385(7)	12087(4)	7326(3)	51(1)
C(16)	9879(8)	12691(5)	6556(3)	73(2)
C(17)	7739(8)	12535(5)	7383(4)	79(2)
C(18)	8151(9)	8023(6)	5697(4)	90(2)
C(19)	10051(7)	10043(7)	5222(4)	82(2)
C(20)	6321(6)	10174(5)	4686(3)	58(1)
C(21)	4801(7)	9995(7)	5016(4)	88(2)
C(22)	6119(7)	9454(7)	3811(4)	92(2)

C(23)

6430(8)

11487(6)

4456(4)

91(2)

Table 28. Bond lengths [\AA] and angles [$^\circ$] for **78**

Si(1)-O(2)	1.641(3)
Si(1)-C(10)	1.814(6)
Si(1)-C(11)	1.824(6)
Si(1)-C(9)	1.854(8)
Si(2)-O(3)	1.653(3)
Si(2)-C(19)	1.852(5)
Si(2)-C(18)	1.861(7)
Si(2)-C(20)	1.878(6)
O(1)-C(5)	1.210(5)
O(2)-C(8)	1.434(5)
O(3)-C(14)	1.424(5)
N-C(4)	1.379(6)
N-C(1)	1.389(6)
N-C(5)	1.396(5)
C(1)-C(2)	1.349(6)
C(1)-H(1A)	0.9400
C(2)-C(3)	1.422(7)
C(2)-H(2A)	0.9400
C(3)-C(4)	1.339(6)
C(3)-H(3A)	0.9400
C(4)-H(4A)	0.9400
C(5)-C(6)	1.516(6)
C(6)-C(8)	1.529(6)
C(6)-C(7)	1.540(6)
C(6)-H(6A)	0.9900
C(7)-H(7A)	0.9700
C(7)-H(7B)	0.9700
C(7)-H(7C)	0.9700
C(8)-C(12)	1.532(6)
C(8)-H(8A)	0.9900
C(9)-H(9A)	0.9700
C(9)-H(9B)	0.9700
C(9)-H(9C)	0.9700

C(10)-H(10A)	0.9700
C(10)-H(10B)	0.9700
C(10)-H(10C)	0.9700
C(11)-H(11A)	0.9700
C(11)-H(11B)	0.9700
C(11)-H(11C)	0.9700
C(12)-C(13)	1.519(6)
C(12)-C(14)	1.540(6)
C(12)-H(12A)	0.9900
C(13)-H(13A)	0.9700
C(13)-H(13B)	0.9700
C(13)-H(13C)	0.9700
C(14)-C(15)	1.535(6)
C(14)-H(14A)	0.9900
C(15)-C(16)	1.516(7)
C(15)-C(17)	1.518(8)
C(15)-H(15A)	0.9900
C(16)-H(16A)	0.9700
C(16)-H(16B)	0.9700
C(16)-H(16C)	0.9700
C(17)-H(17A)	0.9700
C(17)-H(17B)	0.9700
C(17)-H(17C)	0.9700
C(18)-H(18A)	0.9700
C(18)-H(18B)	0.9700
C(18)-H(18C)	0.9700
C(19)-H(19A)	0.9700
C(19)-H(19B)	0.9700
C(19)-H(19C)	0.9700
C(20)-C(23)	1.523(8)
C(20)-C(21)	1.526(7)
C(20)-C(22)	1.536(7)
C(21)-H(21A)	0.9700
C(21)-H(21B)	0.9700
C(21)-H(21C)	0.9700
C(22)-H(22A)	0.9700

C(22)-H(22B)	0.9700
C(22)-H(22C)	0.9700
C(23)-H(23A)	0.9700
C(23)-H(23B)	0.9700
C(23)-H(23C)	0.9700
O(2)-Si(1)-C(10)	107.8(2)
O(2)-Si(1)-C(11)	110.0(3)
C(10)-Si(1)-C(11)	108.0(3)
O(2)-Si(1)-C(9)	110.8(3)
C(10)-Si(1)-C(9)	109.9(5)
C(11)-Si(1)-C(9)	110.3(5)
O(3)-Si(2)-C(19)	111.6(2)
O(3)-Si(2)-C(18)	110.8(2)
C(19)-Si(2)-C(18)	107.2(3)
O(3)-Si(2)-C(20)	106.2(2)
C(19)-Si(2)-C(20)	111.1(3)
C(18)-Si(2)-C(20)	110.0(3)
C(8)-O(2)-Si(1)	130.5(3)
C(14)-O(3)-Si(2)	129.6(3)
C(4)-N-C(1)	108.2(4)
C(4)-N-C(5)	123.5(4)
C(1)-N-C(5)	128.2(4)
C(2)-C(1)-N	107.7(4)
C(2)-C(1)-H(1A)	126.2
N-C(1)-H(1A)	126.2
C(1)-C(2)-C(3)	107.9(4)
C(1)-C(2)-H(2A)	126.1
C(3)-C(2)-H(2A)	126.1
C(4)-C(3)-C(2)	107.6(4)
C(4)-C(3)-H(3A)	126.2
C(2)-C(3)-H(3A)	126.2
C(3)-C(4)-N	108.6(4)
C(3)-C(4)-H(4A)	125.7
N-C(4)-H(4A)	125.7
O(1)-C(5)-N	119.8(4)

O(1)-C(5)-C(6)	122.6(4)
N-C(5)-C(6)	117.6(4)
C(5)-C(6)-C(8)	109.8(4)
C(5)-C(6)-C(7)	107.4(4)
C(8)-C(6)-C(7)	112.5(4)
C(5)-C(6)-H(6A)	109.0
C(8)-C(6)-H(6A)	109.0
C(7)-C(6)-H(6A)	109.0
C(6)-C(7)-H(7A)	109.5
C(6)-C(7)-H(7B)	109.5
H(7A)-C(7)-H(7B)	109.5
C(6)-C(7)-H(7C)	109.5
H(7A)-C(7)-H(7C)	109.5
H(7B)-C(7)-H(7C)	109.5
O(2)-C(8)-C(6)	108.6(3)
O(2)-C(8)-C(12)	109.3(3)
C(6)-C(8)-C(12)	113.1(4)
O(2)-C(8)-H(8A)	108.6
C(6)-C(8)-H(8A)	108.6
C(12)-C(8)-H(8A)	108.6
Si(1)-C(9)-H(9A)	109.5
Si(1)-C(9)-H(9B)	109.5
H(9A)-C(9)-H(9B)	109.5
Si(1)-C(9)-H(9C)	109.5
H(9A)-C(9)-H(9C)	109.5
H(9B)-C(9)-H(9C)	109.5
Si(1)-C(10)-H(10A)	109.5
Si(1)-C(10)-H(10B)	109.5
H(10A)-C(10)-H(10B)	109.5
Si(1)-C(10)-H(10C)	109.5
H(10A)-C(10)-H(10C)	109.5
H(10B)-C(10)-H(10C)	109.5
Si(1)-C(11)-H(11A)	109.5
Si(1)-C(11)-H(11B)	109.5
H(11A)-C(11)-H(11B)	109.5
Si(1)-C(11)-H(11C)	109.5

H(11A)-C(11)-H(11C) 109.5
H(11B)-C(11)-H(11C) 109.5
C(13)-C(12)-C(8) 112.2(4)
C(13)-C(12)-C(14) 111.7(4)
C(8)-C(12)-C(14) 111.2(3)
C(13)-C(12)-H(12A) 107.2
C(8)-C(12)-H(12A) 107.2
C(14)-C(12)-H(12A) 107.2
C(12)-C(13)-H(13A) 109.5
C(12)-C(13)-H(13B) 109.5
H(13A)-C(13)-H(13B) 109.5
C(12)-C(13)-H(13C) 109.5
H(13A)-C(13)-H(13C) 109.5
H(13B)-C(13)-H(13C) 109.5
O(3)-C(14)-C(15) 108.6(4)
O(3)-C(14)-C(12) 111.4(3)
C(15)-C(14)-C(12) 113.0(4)
O(3)-C(14)-H(14A) 107.9
C(15)-C(14)-H(14A) 107.9
C(12)-C(14)-H(14A) 107.9
C(16)-C(15)-C(17) 110.5(5)
C(16)-C(15)-C(14) 111.2(4)
C(17)-C(15)-C(14) 112.7(4)
C(16)-C(15)-H(15A) 107.4
C(17)-C(15)-H(15A) 107.4
C(14)-C(15)-H(15A) 107.4
C(15)-C(16)-H(16A) 109.5
C(15)-C(16)-H(16B) 109.5
H(16A)-C(16)-H(16B) 109.5
C(15)-C(16)-H(16C) 109.5
H(16A)-C(16)-H(16C) 109.5
H(16B)-C(16)-H(16C) 109.5
C(15)-C(17)-H(17A) 109.5
C(15)-C(17)-H(17B) 109.5
H(17A)-C(17)-H(17B) 109.5
C(15)-C(17)-H(17C) 109.5

H(17A)-C(17)-H(17C) 109.5
H(17B)-C(17)-H(17C) 109.5
Si(2)-C(18)-H(18A) 109.5
Si(2)-C(18)-H(18B) 109.5
H(18A)-C(18)-H(18B) 109.5
Si(2)-C(18)-H(18C) 109.5
H(18A)-C(18)-H(18C) 109.5
H(18B)-C(18)-H(18C) 109.5
Si(2)-C(19)-H(19A) 109.5
Si(2)-C(19)-H(19B) 109.5
H(19A)-C(19)-H(19B) 109.5
Si(2)-C(19)-H(19C) 109.5
H(19A)-C(19)-H(19C) 109.5
H(19B)-C(19)-H(19C) 109.5
C(23)-C(20)-C(21) 108.3(5)
C(23)-C(20)-C(22) 107.8(5)
C(21)-C(20)-C(22) 108.2(5)
C(23)-C(20)-Si(2) 111.4(4)
C(21)-C(20)-Si(2) 111.0(4)
C(22)-C(20)-Si(2) 110.2(4)
C(20)-C(21)-H(21A) 109.5
C(20)-C(21)-H(21B) 109.5
H(21A)-C(21)-H(21B) 109.5
C(20)-C(21)-H(21C) 109.5
H(21A)-C(21)-H(21C) 109.5
H(21B)-C(21)-H(21C) 109.5
C(20)-C(22)-H(22A) 109.5
C(20)-C(22)-H(22B) 109.5
H(22A)-C(22)-H(22B) 109.5
C(20)-C(22)-H(22C) 109.5
H(22A)-C(22)-H(22C) 109.5
H(22B)-C(22)-H(22C) 109.5
C(20)-C(23)-H(23A) 109.5
C(20)-C(23)-H(23B) 109.5
H(23A)-C(23)-H(23B) 109.5
C(20)-C(23)-H(23C) 109.5

H(23A)-C(23)-H(23C) 109.5

H(23B)-C(23)-H(23C) 109.5

Symmetry transformations used to generate equivalent atoms:

Table 29. Anisotropic displacement parameters ($\text{\AA}^2 \times 10^3$) for **78**

The anisotropic displacement factor exponent takes the form: $-2 \sum [h^2 a^{*2} U^{11} + \dots + 2$

$h k a^* b^* U^{12}]$

U^{11}	U^{22}	U^{33}	U^{23}	U^{13}	U^{12}
Si(1)51(1)	65(1)	62(1)	4(1)	29(1)	0(1)
Si(2)59(1)	51(1)	45(1)	-11(1)	18(1)	-2(1)
O(1)104(3)	32(2)	55(2)	1(2)	49(2)	0(2)
O(2)44(2)	43(2)	53(2)	-1(2)	24(1)	0(2)
O(3)50(2)	43(2)	39(2)	-1(1)	16(2)	4(1)
N 55(3)	35(2)	38(2)	-2(2)	22(2)	3(2)
C(1)74(3)	32(3)	50(3)	4(2)	31(2)	-3(3)
C(2)80(3)	50(3)	51(3)	12(3)	36(3)	1(3)
C(3)77(4)	50(3)	58(3)	0(3)	41(3)	9(3)
C(4)62(3)	41(3)	51(3)	-4(3)	26(3)	2(2)
C(5)66(3)	35(3)	31(2)	0(2)	20(2)	-2(2)
C(6)61(3)	37(3)	44(3)	1(2)	27(2)	-2(2)
C(7)67(4)	88(4)	42(3)	5(3)	22(3)	4(3)
C(8)47(3)	34(2)	46(3)	-2(2)	23(2)	0(2)
C(9)110(6)	88(5)	237(11)	8(6)	107(7)	-29(5)
C(10)54(4)	123(6)	80(4)	16(4)	19(3)	12(4)
C(11)70(4)	251(11)	56(4)	-1(6)	31(3)	43(6)
C(12)48(3)	34(3)	38(2)	2(2)	21(2)	5(2)
C(13)55(3)	41(3)	53(3)	3(3)	21(3)	-8(2)
C(14)49(3)	38(3)	39(3)	1(2)	21(2)	-4(2)
C(15)86(4)	36(3)	33(3)	2(2)	20(3)	-5(3)
C(16)118(5)	45(3)	51(3)	6(3)	15(3)	-23(3)
C(17)120(5)	46(3)	76(4)	8(3)	36(4)	25(3)
C(18)126(6)	61(4)	81(4)	-26(4)	21(4)	12(4)
C(19)68(4)	129(6)	57(3)	-29(4)	29(3)	-8(4)
C(20)62(3)	68(4)	48(3)	-4(3)	24(3)	-4(3)
C(21)65(4)	120(6)	81(4)	9(4)	23(3)	-4(4)

C(22)83(4)	127(6)	58(4)	-30(4)	6(3)	6(4)
C(23)101(5)	87(5)	73(4)	18(4)	6(4)	-2(4)

Table 30. Hydrogen coordinates ($\times 10^4$) and isotropic displacement parameters ($\text{\AA}^2 \times 10^3$) for**78**

	x	y	z	U(eq)
H(1A)	9335	8851	10972	59
H(2A)	7558	9051	11987	68
H(3A)	6618	11196	11925	69
H(4A)	7836	12265	10881	59
H(6A)	10332	9241	9829	54
H(7A)	12318	9906	11126	96
H(7B)	12972	10845	10536	96
H(7C)	13194	9462	10395	96
H(8A)	11355	11106	8832	48
H(9A)	14568	11559	9365	200
H(9B)	13704	11894	8348	200
H(9C)	15567	11545	8630	200
H(10A)	15199	8020	9075	128
H(10B)	15578	9017	9833	128
H(10C)	16540	8998	9081	128
H(11A)	13581	8630	7194	184
H(11B)	14920	9611	7204	184
H(11C)	13057	9962	6920	184
H(12A)	8534	10444	8347	46
H(13A)	8997	8386	8533	73
H(13B)	9814	8385	7719	73
H(13C)	7944	8684	7542	73
H(14A)	10473	10512	7102	48
H(15A)	10188	12317	7894	61
H(16A)	9833	13549	6623	109
H(16B)	9143	12454	5985	109
H(16C)	10977	12456	6566	109
H(17A)	7765	13397	7434	118

H(17B)	7482	12192	7908	118
H(17C)	6917	12303	6841	118
H(18A)	9119	7771	6149	136
H(18B)	8117	7643	5125	136
H(18C)	7197	7796	5889	136
H(19A)	10994	9774	5685	123
H(19B)	10113	10899	5148	123
H(19C)	10025	9650	4655	123
H(21A)	3856	10260	4553	132
H(21B)	4897	10455	5563	132
H(21C)	4685	9157	5141	132
H(22A)	5151	9719	3365	138
H(22B)	6020	8614	3936	138
H(22C)	7060	9576	3581	138
H(23A)	5451	11721	4004	136
H(23B)	7364	11612	4219	136
H(23C)	6544	11964	4996	136

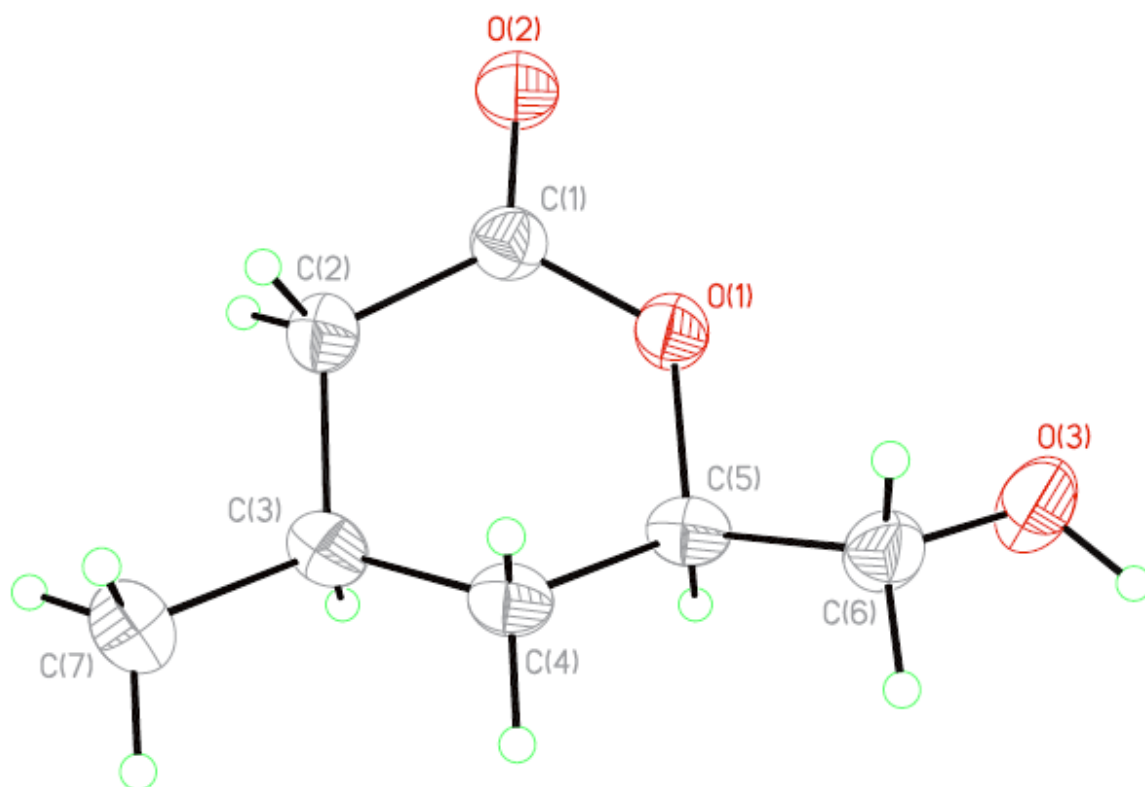
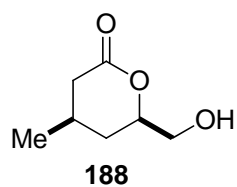


Table 31. Crystal data and structure refinement for **188**

Identification code	df1022s	
Empirical formula	C ₇ H ₁₂ O ₃	
Formula weight	144.17	
Temperature	223(2) K	
Wavelength	0.71073 Å	
Crystal system	Orthorhombic	
Space group	P 21 21 21	
Unit cell dimensions	a = 7.024(7) Å	$\alpha = 90^\circ$.
	b = 8.140(8) Å	$\beta = 90^\circ$.

	$c = 13.034(12) \text{ \AA}$	$\gamma = 90^\circ$.
Volume	$745.2(12) \text{ \AA}^3$	
Z	4	
Density (calculated)	1.285 Mg/m^3	
Absorption coefficient	0.100 mm^{-1}	
F(000)	312	
Crystal size	$0.42 \times 0.22 \times 0.03 \text{ mm}^3$	
Theta range for data collection	2.95 to 28.45° .	
Index ranges	$-9 \leq h \leq 9$, $-10 \leq k \leq 10$, $-17 \leq l \leq 17$	
Reflections collected	7441	
Independent reflections	1104 [R(int) = 0.0581]	
Completeness to theta = 28.45°	99.1 %	
Absorption correction	Semi-empirical from equivalents	
Max. and min. transmission	0.9970 and 0.9594	
Refinement method	Full-matrix least-squares on F^2	
Data / restraints / parameters	1104 / 0 / 139	
Goodness-of-fit on F^2	1.025	
Final R indices [I > 2sigma(I)]	R1 = 0.0479, wR2 = 0.1165	
R indices (all data)	R1 = 0.0764, wR2 = 0.1336	
Absolute structure parameter	?	
Largest diff. peak and hole	0.258 and $-0.180 \text{ e.\AA}^{-3}$	

Table 32. Atomic coordinates ($\times 10^4$) and equivalent isotropic displacement parameters $(\text{\AA}^2 \times 10^3)$ for **188**U(eq) is defined as one third of the trace of the orthogonalized U^{ij} tensor.

	x	y	z	U(eq)
O(1)	9702(4)	8388(2)	6014(1)	47(1)
C(1)	9700(5)	7749(3)	5079(2)	43(1)
O(2)	9730(4)	6267(3)	5018(2)	58(1)
C(2)	9726(5)	8824(4)	4152(2)	46(1)
O(3)	9956(5)	9637(3)	8024(2)	62(1)
C(3)	9307(4)	10636(4)	4331(2)	43(1)
C(4)	10286(5)	11142(4)	5312(2)	42(1)
C(5)	9589(5)	10157(3)	6215(2)	42(1)
C(6)	10745(5)	10458(4)	7163(2)	48(1)
C(7)	9903(6)	11667(5)	3420(3)	56(1)

Table 33. Bond lengths [Å] and angles [°] for **188**

O(1)-C(1)	1.325(4)
O(1)-C(5)	1.466(3)
C(1)-O(2)	1.210(4)
C(1)-C(2)	1.492(4)
C(2)-C(3)	1.522(5)
C(2)-H(2B)	0.98(3)
C(2)-H(2A)	0.94(4)
O(3)-C(6)	1.419(4)
O(3)-H(3O)	0.86(3)
C(3)-C(4)	1.509(4)
C(3)-C(7)	1.513(4)
C(3)-H(3)	0.99(4)
C(4)-C(5)	1.506(4)
C(4)-H(4A)	0.97(3)
C(4)-H(4B)	0.94(4)
C(5)-C(6)	1.499(5)
C(5)-H(5)	0.98(3)
C(6)-H(6A)	0.89(3)
C(6)-H(6B)	1.07(4)
C(7)-H(7A)	1.03(4)
C(7)-H(7B)	1.00(4)
C(7)-H(7C)	1.02(4)
C(1)-O(1)-C(5)	123.3(2)
O(2)-C(1)-O(1)	116.9(3)
O(2)-C(1)-C(2)	122.1(3)
O(1)-C(1)-C(2)	121.0(2)
C(1)-C(2)-C(3)	116.2(2)
C(1)-C(2)-H(2B)	106(2)
C(3)-C(2)-H(2B)	113.3(19)
C(1)-C(2)-H(2A)	102(2)
C(3)-C(2)-H(2A)	110(2)
H(2B)-C(2)-H(2A)	108(3)

C(6)-O(3)-H(3O)	110(2)
C(4)-C(3)-C(7)	112.8(3)
C(4)-C(3)-C(2)	107.8(3)
C(7)-C(3)-C(2)	111.4(3)
C(4)-C(3)-H(3)	107.6(19)
C(7)-C(3)-H(3)	112.2(19)
C(2)-C(3)-H(3)	105(2)
C(5)-C(4)-C(3)	111.6(3)
C(5)-C(4)-H(4A)	106.7(17)
C(3)-C(4)-H(4A)	111.9(18)
C(5)-C(4)-H(4B)	113(2)
C(3)-C(4)-H(4B)	107(2)
H(4A)-C(4)-H(4B)	107(3)
O(1)-C(5)-C(6)	106.2(2)
O(1)-C(5)-C(4)	111.5(2)
C(6)-C(5)-C(4)	112.4(3)
O(1)-C(5)-H(5)	103.1(18)
C(6)-C(5)-H(5)	113.2(18)
C(4)-C(5)-H(5)	110.0(18)
O(3)-C(6)-C(5)	111.3(3)
O(3)-C(6)-H(6A)	113(2)
C(5)-C(6)-H(6A)	108(2)
O(3)-C(6)-H(6B)	110.4(17)
C(5)-C(6)-H(6B)	106.3(18)
H(6A)-C(6)-H(6B)	108(3)
C(3)-C(7)-H(7A)	110.9(19)
C(3)-C(7)-H(7B)	109(2)
H(7A)-C(7)-H(7B)	117(3)
C(3)-C(7)-H(7C)	112(2)
H(7A)-C(7)-H(7C)	104(3)
H(7B)-C(7)-H(7C)	103(3)

Symmetry transformations used to generate equivalent atoms:

Table 34. Aisotropic displacement parameters ($\text{\AA}^2 \times 10^3$) for **188**

The anisotropic displacement factor exponent takes the form: $-2\pi^2 [h^2 a^{*2}U^{11} + \dots + 2 h k a^* b^* U^{12}]$

U^{11}	U^{22}	U^{33}	U^{23}	U^{13}	U^{12}
O(1)63(1)	37(1)	40(1)	2(1)	-1(1)	-6(1)
C(1)43(2)	41(2)	45(2)	-1(1)	-2(2)	0(1)
O(2)83(2)	37(1)	54(1)	-1(1)	-2(1)	-2(1)
C(2)53(2)	47(2)	38(1)	-1(1)	-3(2)	1(2)
O(3)95(2)	52(1)	41(1)	-6(1)	8(1)	-21(2)
C(3)40(2)	41(2)	50(2)	7(1)	0(1)	2(1)
C(4)43(2)	35(1)	49(2)	1(1)	1(1)	-1(1)
C(5)40(2)	35(1)	51(2)	1(1)	3(2)	1(1)
C(6)63(2)	38(2)	43(2)	-2(1)	2(2)	-8(1)
C(7)61(2)	54(2)	53(2)	12(2)	-3(2)	-2(2)

Table 35. Hydrogen coordinates ($\times 10^4$) and isotropic displacement parameters ($\text{\AA}^2 \times 10^3$) for

188

	x	y	z	U(eq)
H(2B)	8870(50)	8310(40)	3650(30)	49(9)
H(2A)	10980(50)	8690(50)	3910(30)	60(10)
H(3O)	9990(50)	10270(40)	8560(20)	49(9)
H(3)	7910(50)	10690(40)	4450(20)	58(9)
H(4A)	10060(50)	12290(40)	5480(20)	42(8)
H(4B)	11610(60)	11030(50)	5200(20)	56(9)
H(5)	8230(50)	10340(40)	6320(20)	45(8)
H(6A)	10830(40)	11530(40)	7260(20)	50(9)
H(6B)	12140(60)	10000(40)	7000(20)	62(10)
H(7A)	9320(50)	11210(50)	2750(30)	60(10)
H(7B)	9670(60)	12850(50)	3580(30)	83(12)
H(7C)	11340(60)	11630(40)	3300(30)	62(11)

BIBLIOGRAPHY

- (1) Mahrwald, R.; Editor *Modern Aldol Reactions, Vol. 1: Enolates, Organocatalysis, Biocatalysis and Natural Product Synthesis*, 2004.
- (2) Mukaiyama, T. *Org. React.* **1982**, 28, 203-331.
- (3) Schetter, B.; Mahrwald, R. *Angew. Chem. Int. Ed.* **2006**, 45, 7506-7525.
- (4) Nelson, S. G. *Tetrahedron: Asymm.* **1998**, 9, 357-389.
- (5) Mahrwald, R. *Chem. Rev.* **1999**, 99, 1095-1120.
- (6) Zimmerman, H. E.; Traxler, M. D. *J. Am. Chem. Soc.* **1957**, 79, 1920-1923.
- (7) Gijzen, H. J. M.; Wong, C. H. *J. Am. Chem. Soc.* **1995**, 117, 2947-2948.
- (8) Northrup, A. B.; MacMillan, D. W. C. *Science* **2004**, 305, 1752-1755.
- (9) Casas, J.; Engqvist, M.; Ibrahim, I.; Kaynak, B.; Cordova, A. *Angew. Chem. Int. Ed.* **2005**, 44, 1343-1345.
- (10) Crimmins, M. T.; King, B. W.; Tabet, E. A.; Chaudhary, K. *J. Org. Chem.* **2001**, 66, 894-902.
- (11) Evans, D. A.; Urpi, F.; Somers, T. C.; Clark, J. S.; Bilodeau, M. T. *J. Am. Chem. Soc.* **1990**, 112, 8215-8216.
- (12) Peng, Z. H.; Woerpel, K. A. *J. Am. Chem. Soc.* **2003**, 125, 6018-6019.
- (13) Shen, X. Q.; Wasmuth, A. S.; Zhao, J. P.; Zhu, C.; Nelson, S. G. *J. Am. Chem. Soc.* **2006**, 128, 7438-7439.

- (14) Zhu, C.; Shen, X. Q.; Nelson, S. G. *J. Am. Chem. Soc.* **2004**, *126*, 5352-5353.
- (15) Evans, D. A.; Dart, M. J.; Duffy, J. L.; Yang, M. G. *J. Am. Chem. Soc.* **1996**, *118*, 4322-4343.
- (16) Evans, D. A.; Yang, M. G.; Dart, M. J.; Duffy, J. L. *Tetrahedron Lett.* **1996**, *37*, 1957-1960.
- (17) Noyori, R.; Yokoyama, K.; Sakata, J.; Kuwajima, I.; Nakamura, E.; Shimizu, M. *J. Am. Chem. Soc.* **1977**, *99*, 1265-1267.
- (18) Miura, K.; Nakagawa, T.; Hosomi, A. *J. Am. Chem. Soc.* **2002**, *124*, 536-537.
- (19) Denmark, S. E.; Stavenger, R. A. *Acc. Chem. Res.* **2000**, *33*, 432-440.
- (20) Song, J. J.; Tan, Z. L.; Reeves, J. T.; Yee, N. K.; Senanayake, C. H. *Org. Lett.* **2007**, *9*, 1013-1016.
- (21) Nakagawa, T.; Fujisawa, H.; Nagata, Y.; Mukaiyama, T. *Bull. Chem. Soc. Jpn.* **2004**, *77*, 1555-1567.
- (22) Fujisawa, H.; Nagata, Y.; Sato, Y.; Mukaiyama, T. *Chem. Lett.* **2005**, *34*, 842-843.
- (23) Nakagawa, T.; Fujisawa, H.; Nagata, Y.; Mukaiyama, T. *Bull. Chem. Soc. Jpn.* **2005**, *78*, 236-246.
- (24) Myers, A. G.; Widdowson, K. L. *J. Am. Chem. Soc.* **1990**, *112*, 9672-9674.
- (25) Creger, P. L. *Tetrahedron Lett.* **1972**, 79-80.
- (26) Loh, T. P.; Feng, L. C.; Wei, L. L. *Tetrahedron* **2000**, *56*, 7309-7312.
- (27) Genisson, Y.; Gorrichon, L. *Tetrahedron Lett.* **2000**, *41*, 4881-4884.
- (28) McGuire, J. M.; Bunch, R. L.; Anderson, R. C.; Boaz, H. E.; Flynn, E. H.; Powell, H. M.; Smith, J. W. *Schweiz Med Wochenschr* **1952**, *82*, 1064-1065.

- (29) Corey, E. J. H., P. B.; Kim, S.; Yoo, S.; Nambiar, K. B.; Falck, J. R. *J. Am. Chem. Soc.* **1979**, *101*, 131-132.
- (30) Muri, D.; Lohse-Fraefel, N.; Carreira, E. M. *Angew. Chem. Int. Ed.* **2005**, *44*, 4036-4038.
- (31) Mulzer, J. K., H. M.; Buschmann, J.; Lehmann, C.; Luger, P. *J. Am. Chem. Soc.* **1991**, *113*, 910-923.
- (32) Corey, E. J. T., E. J.; Melvin, L. S.; Nicolaou, K. C.; Secrest, J. R.; Lett, R.; Sheldrake, P. W.; Falck, J. R.; Brunelle, D. J.; Haslanger, M. F.; Kim, S.; Yoo, S. *J. Am. Chem. Soc.* **1978**, *100*, 4618-4619.
- (33) Kochetkov, N. K. S., A. F.; Ermolenko, M. S.; Yashunsky, D. V.; Borodkin, V. S. *Tetrahedron Lett.* **1987**, *28*, 3835-3849.
- (34) Evans, D. A.; Yang, M. G.; Dart, M. J.; Duffy, J. L.; Kim, A. S. *J. Am. Chem. Soc.* **1995**, *117*, 9598-9599.
- (35) Buncel, E.; Hoz, S. *Tetrahedron Lett.* **1983**, *24*, 4777-4780.
- (36) Still, W. C. K., M.; Mitra, A. *J. Org. Chem.* **1978**, *43*, 2923-2925.
- (37) Evans, D. A.; Johnson, D. S. *Org. Lett.* **1999**, *1*, 595-598.
- (38) Evans, D. A.; Scheidt, K. A.; Johnston, J. N.; Willis, M. C. *J. Am. Chem. Soc.* **2001**, *123*, 4480-4491.
- (39) Gennari, C.; Bernardi, A.; Cardani, S.; Scolastico, C. *Tetrahedron Lett.* **1985**, *26*, 797-800.
- (40) Sheng, X. PhD. Dissertation. University of Pittsburgh, 2007.
- (41) Chandra, B. PhD. Dissertation, University of Pittsburgh, 2010
- (42) Chandra, B.; Fu, D. Z.; Nelson, S. G. *Angew. Chem. Int. Ed.* **2010**, *49*, 2591-2594.

- (43) Kobayashi, J. *J. Antibiot.* **2008**, *61*, 271-284.
- (44) Kobayashi, J.; Shigemori, H.; Ishibashi, M.; Yamasu, T.; Hirota, H.; Sasaki, T. *J. Org. Chem.* **1991**, *56*, 5221-5224.
- (45) Kobayashi, J.; Shimbo, K.; Sato, M.; Shiro, M.; Tsuda, M. *Org. Lett.* **2000**, *2*, 2805-2807.
- (46) Kobayashi, J.; Tsuda, M. *Nat. Prod. Rep.* **2004**, *21*, 77-93.
- (47) Li, H. M.; Wu, J. L.; Luo, J. L.; Dai, W. M. *Chem. Eur. J.* **2010**, *16*, 11530-11534.
- (48) Hangyou, M.; Ishiyama, H.; Takahashi, Y.; Kobayashi, J. *Org. Lett.* **2009**, *11*, 5046-5049.
- (49) Furstner, A.; Flugge, S.; Larionov, O.; Takahashi, Y.; Kubota, T.; Kobayashi, J. *Chem. Eur. J.* **2009**, *15*, 4011-4029.
- (50) Ko, H. M.; Lee, C. W.; Kwon, H. K.; Chung, H. S.; Choi, S. Y.; Chung, Y. K.; Lee, E. *Angew. Chem. Int. Ed.* **2009**, *48*, 2364-2366.
- (51) Rodriguez-Esrich, C.; Urpi, F.; Vilarrasa, J. *Org. Lett.* **2008**, *10*, 5191-5194.
- (52) Barbazanges, M.; Meyer, C.; Cossy, J. *Org. Lett.* **2008**, *10*, 4489-4492.
- (53) Liang, L.; Wei, Z.; Carter, R. G. *J. Am. Chem. Soc.* **2008**, *130*, 11834-11834.
- (54) Dai, W. M.; Chen, Y. L.; Jin, J.; Wu, J. L.; Lou, J. S.; He, Q. J. *Synlett* **2008**, 1737-1741.
- (55) Lu, L.; Zhang, W.; Carter, R. G. *J. Am. Chem. Soc.* **2008**, *130*, 7253-7254.
- (56) Va, P.; Roush, W. R. *Tetrahedron* **2007**, *63*, 5768-5796.
- (57) Jin, J.; Chen, Y. L.; Li, Y. N.; Wu, J. L.; Dai, W. M. *Org. Lett.* **2007**, *9*, 2585-2588.

- (58) Kim, C. H.; An, H. J.; Shin, W. K.; Yu, W.; Woo, S. K.; Jung, S. K.; Lee, E. *Angew. Chem. Int. Ed.* **2006**, *45*, 8019-8021.
- (59) Trost, B. M.; Harrington, P. E.; Chisholm, J. D.; Wroblewski, S. T. *J. Am. Chem. Soc.* **2005**, *127*, 13598-13610.
- (60) Lepage, O.; Kattnig, E.; Furstner, A. *J. Am. Chem. Soc.* **2004**, *126*, 15970-15971.
- (61) Trost, B. M.; Harrington, P. E. *J. Am. Chem. Soc.* **2004**, *126*, 5028-5029.
- (62) Ghosh, A. K.; Gong, G. *J. Am. Chem. Soc.* **2004**, *126*, 3704-3705.
- (63) Ghosh, A. K.; Liu, C. F. *J. Am. Chem. Soc.* **2003**, *125*, 2374-2375.
- (64) Furstner, A.; Aissa, C.; Riveiros, R.; Ragot, J. *Angew. Chem. Int. Ed.* **2002**, *41*, 4763-4766.
- (65) Chakraborty, T. K.; Das, S. *Tetrahedron Lett.* **2001**, *42*, 3387-3390.
- (66) Williams, D. R.; Myers, B. J.; Mi, L. *Org. Lett.* **2000**, *2*, 945-948.
- (67) Williams, D. R.; Kissel, W. S. *J. Am. Chem. Soc.* **1998**, *120*, 11198-11199.
- (68) Kobayashi, J.; Shimbo, K.; Sato, M.; Tsuda, M. *J. Org. Chem.* **2002**, *67*, 6585-6592.
- (69) Karas, M.; Bachmann, D.; Hillenkamp, F. *Anal. Chem.* **1985**, *57*, 2935-2939.
- (70) Saito, S. Y.; Feng, J.; Kira, A.; Kobayashi, J.; Ohizumi, Y. *Biochem. Biophys. Res. Commun.* **2004**, *320*, 961-965.
- (71) Usui, T.; Kazami, S.; Dohmae, N.; Mashimo, Y.; Kondo, H.; Tsuda, M.; Terasaki, A. G.; Ohashi, K.; Kobayashi, J.; Osada, H. *Chem. Biol.* **2004**, *11*, 1269-1277.
- (72) Chakraborty, T. K.; Suresh, V. R. *Tetrahedron Lett.* **1998**, *39*, 9109-9112.
- (73) Liesener, F. P.; Janssen, U.; Kalesse, M. *Synthesis* **2006**, 2590-2602.
- (74) Liesener, F. P.; Kalesse, M. *Synlett* **2005**, 2236-2238.

- (75) Formentin, P.; Murga, J.; Carda, M.; Marco, J. A. *Tetrahedron: Asymm.* **2006**, *17*, 2938-2942.
- (76) Petri, A. F.; Schneekloth, J. S.; Mandal, A. K.; Crews, C. M. *Org. Lett.* **2007**, *9*, 3001-3004.
- (77) Deng, L. S.; Huang, X. P.; Zhao, G. *J. Org. Chem.* **2006**, *71*, 4625-4635.
- (78) Deng, L. S.; Ma, Z. X.; Zhao, G. *Synlett* **2008**, 728-732.
- (79) Furstner, A.; Bouchez, L. C.; Funel, J. A.; Liepins, V.; Poree, F. H.; Gilmour, R.; Beaufils, F.; Laurich, D.; Tamiya, M. *Angew. Chem. Int. Ed.* **2007**, *46*, 9265-9270.
- (80) Nelson, S. G.; Peelen, T. J.; Wan, Z. H. *J. Am. Chem. Soc.* **1999**, *121*, 9742-9743.
- (81) Nelson, S. G.; Zhu, C.; Shen, X. Q. *J. Am. Chem. Soc.* **2004**, *126*, 14-15.
- (82) Vargo, T. R.; Hale, J. S.; Nelson, S. G. *Angew. Chem. Int. Ed.* **2010**, *49*, 8678-8681.
- (83) Nelson, S. G.; Cheung, W. S.; Kassick, A. J.; Hilfiker, M. A. *J. Am. Chem. Soc.* **2002**, *124*, 13654-13655.
- (84) Nelson, S. G.; Wan, Z. H.; Stan, M. A. *J. Org. Chem.* **2002**, *67*, 4680-4683.
- (85) Nelson, S. G.; Spencer, K. L. *Angew. Chem. Int. Ed.* **2000**, *39*, 1323-1325.
- (86) Miller, D. J.; Moody, C. J. *Tetrahedron* **1995**, *51*, 10811-10843.
- (87) Ronan, B.; Bacque, E.; Barriere, J. C. *Tetrahedron* **2004**, *60*, 3819-3824.
- (88) Nagai, K.; Sunazuka, T.; Omura, S. *Tetrahedron Lett.* **2004**, *45*, 2507-2509.
- (89) Morilla, M. E.; Molina, M. J.; Diaz-Requejo, M. M.; Belderrain, T. R.; Nicasio, M. C.; Trofimenko, S.; Perez, P. J. *Organometallics* **2003**, *22*, 2914-2918.
- (90) Doyle, M. P.; Yan, M. *Tetrahedron Lett.* **2002**, *43*, 5929-5931.

- (91) Moody, C. J.; Morfitt, C. N.; Slawin, A. M. Z. *Tetrahedron: Asymm.* **2001**, *12*, 1657-1661.
- (92) Nelson, T. D.; Song, Z. J.; Thompson, A. S.; Zhao, M. Z.; DeMarco, A.; Reamer, R. A.; Huntington, M. F.; Grabowski, E. J. J.; Reider, P. J. *Tetrahedron Lett.* **2000**, *41*, 1877-1881.
- (93) Maier, T. C.; Fu, G. C. *J. Am. Chem. Soc.* **2006**, *128*, 4594-4595.
- (94) Chen, C.; Zhu, S. F.; Liu, B.; Wang, L. X.; Zhou, Q. L. *J. Am. Chem. Soc.* **2007**, *129*, 12616-12617.
- (95) Zhu, S. T.; Chen, C.; Cai, Y.; Zhou, Q. L. *Angew. Chem. Int. Ed.* **2008**, *47*, 932-934.
- (96) Robles, O.; McDonald, F. E. *Org. Lett.* **2008**, *10*, 1811-1814.
- (97) Barton, D. H. R.; McCombie, S. W. *J. Chem. Soc., Perkin Trans. I* **1975**, 1574-1585.
- (98) Davis, F. A.; Kumar, A. *J. Org. Chem.* **1992**, *57*, 3337-3339.
- (99) Mahoney, W. S.; Brestensky, D. M.; Stryker, J. M. *J. Am. Chem. Soc.* **1988**, *110*, 291-293.
- (100) Gopalarathnam, A.; Nelson, S. G. *Org. Lett.* **2006**, *8*, 7-10.
- (101) Dess, D. B.; Martin, J. C. *J. Org. Chem.* **1983**, *48*, 4155-4156.
- (102) Cram, D. J.; Elhafez, F. A. A. *J. Am. Chem. Soc.* **1952**, *74*, 5828-5835.